

PB84-193747

SEISMIC RESPONSE FOR MULTICOMPONENT  
EARTHQUAKES

by

Mohsen Ghafory-Ashtiany

and

Mahendra P. Singh

Technical Report of the Research Supported by  
The National Science Foundation Under  
Grant No. CEE-8214070

Department of Engineering Science & Mechanics  
Virginia Polytechnic Institute & State University  
Blacksburg, VA 24061

April 1984

REPRODUCED BY  
NATIONAL TECHNICAL  
INFORMATION SERVICE  
U.S. DEPARTMENT OF COMMERCE  
SPRINGFIELD, VA. 22161



BIBLIOGRAPHIC DATA SHEET	1. Report No. VPI-E-84-17	2.	3. Recipient's Accession No. 193747		
4. Title and Subtitle SEISMIC RESPONSE FOR MULTICOMPONENT EARTHQUAKES		5. Report Date April 1984			
7. Author(s) Mohsen Ghafory-Ashtiany and Mahendra P. Singh		8. Performing Organization Report No.			
9. Performing Organization Name and Address Department of Engineering Science & Mechanics Virginia Polytechnic Institute & State University Blacksburg, VA 24061		10. Project/Task/Work Unit No.			
		11. Contract/Grant No. CEE-8214070			
12. Sponsoring Organization Name and Address National Science Foundation Washington, D.C. 20550		13. Type of Report & Period Covered Technical			
		14.			
15. Supplementary Notes					
16. Abstracts <p>The earthquake induced ground motions, in general, have six components: three translational and three rotational. These components are also correlated in general. In this study, the response spectrum methods have been developed to obtain the structural design response for such correlated components. The forces induced in a structure depend upon the orientation of the structure with respect to the impinging seismic waves. An approach has also been developed to obtain the maximum or the worst-case response which could possibly be induced in the structure when it is oriented in a particular direction. The numerical results demonstrating the application of these approaches are presented for the proportionally as well as the nonproportionally damped structures. The results indicate that a systematic approach, as given in the report, should be used to obtain the worst-case response to avoid an unconservative structural design. Also, the rotational components of a ground input should not be customarily disregarded as inconsequential, especially if the structure is large or tall.</p>					
17. Key Words and Document Analysis: 17a. Descriptors <table border="0" style="width: 100%;"> <tr> <td style="vertical-align: top;"> EARTHQUAKES  STRUCTURAL DESIGN  STRUCTURAL RESPONSE  GROUND MOTION  RESPONSE SPECTRA  DYNAMIC ANALYSIS </td> <td style="vertical-align: top;"> MULTI-COMPONENT EARTHQUAKE  ROTATIONAL EARTHQUAKE INPUTS  CORRELATED INPUT  STRUCTURAL DYNAMICS  PROPORTIONAL DAMPING  NONPROPORTIONAL DAMPING </td> </tr> </table> 17b. Identifiers/Open-Ended Terms  17c. COSATI Field Group				EARTHQUAKES STRUCTURAL DESIGN STRUCTURAL RESPONSE GROUND MOTION RESPONSE SPECTRA DYNAMIC ANALYSIS	MULTI-COMPONENT EARTHQUAKE ROTATIONAL EARTHQUAKE INPUTS CORRELATED INPUT STRUCTURAL DYNAMICS PROPORTIONAL DAMPING NONPROPORTIONAL DAMPING
EARTHQUAKES STRUCTURAL DESIGN STRUCTURAL RESPONSE GROUND MOTION RESPONSE SPECTRA DYNAMIC ANALYSIS	MULTI-COMPONENT EARTHQUAKE ROTATIONAL EARTHQUAKE INPUTS CORRELATED INPUT STRUCTURAL DYNAMICS PROPORTIONAL DAMPING NONPROPORTIONAL DAMPING				
18. Availability Statement Distribution Unlimited		19. Security Class (This Report) UNCLASSIFIED 20. Security Class (This Page) UNCLASSIFIED	21. No. of Pages 205 22. Price		



## ACKNOWLEDGEMENTS

This report is based on the dissertation of Mohsen Ghafory-Ashtiany which was completed under the supervision of M. P. Singh as his Major Thesis Advisor. The dissertation was submitted to Virginia Polytechnic Institute and State University in April 1984 in partial fulfillment of the requirements of the degree of Doctor of Philosophy in Engineering Mechanics.

This work is funded by the National Science Foundation Grant No. CEE-8214070 with Dr. John E. Goldberg and Dr. S. C. Liu as its Program Directors. This support is gratefully acknowledged. Any opinion, findings and conclusions or recommendations expressed in this report are those of the writers and do not necessarily reflect the views of the National Science Foundation.

Preceding page blank

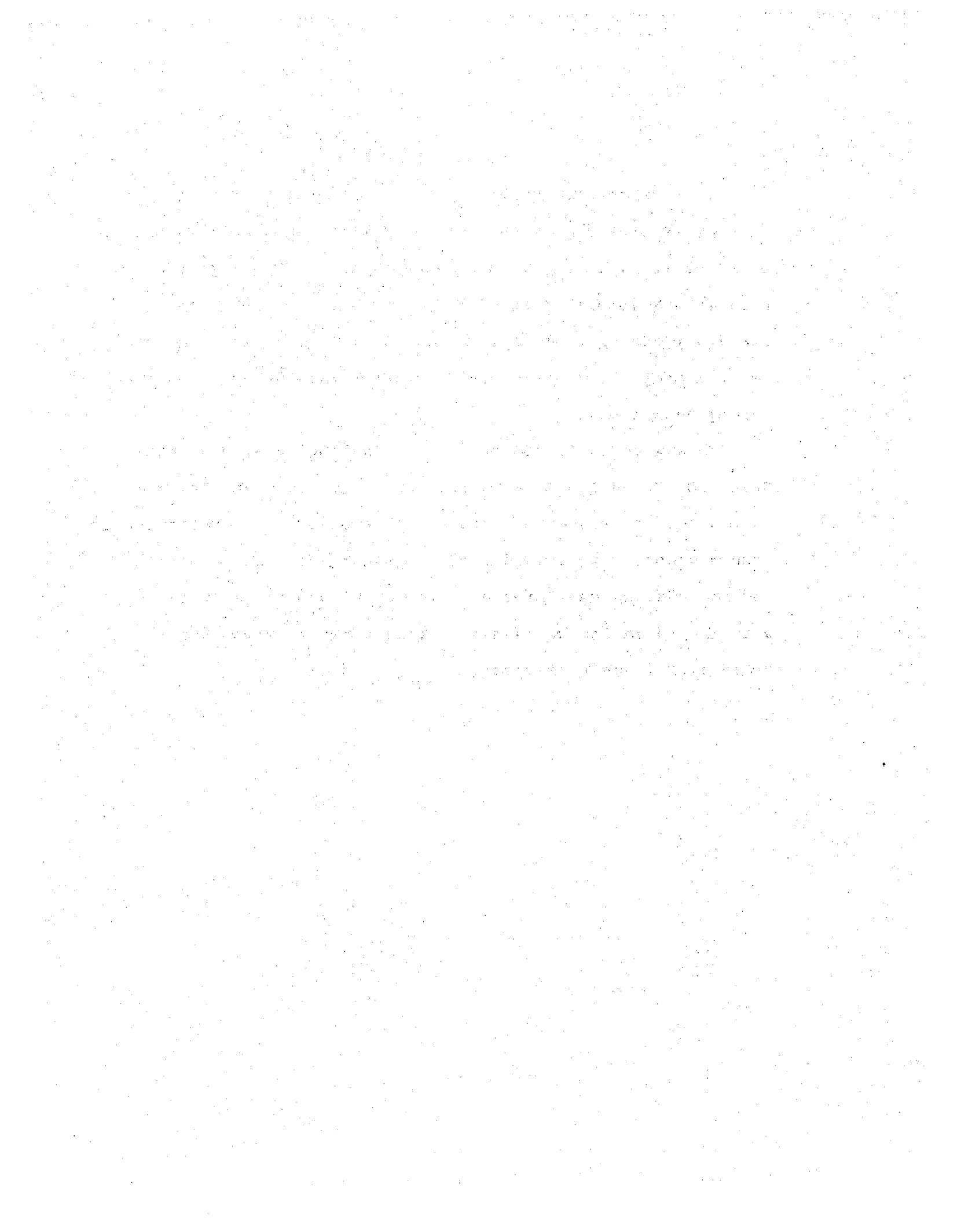


## TABLE OF CONTENTS

	<u>Page</u>
BIBLIOGRAPHIC DATA SHEET .....	i
ACKNOWLEDGEMENTS .....	iii
TABLE OF CONTENTS .....	iv
 <u>Chapter</u>	
1. INTRODUCTION .....	1
1.1 BACKGROUND AND SCOPE .....	1
1.2 REPORT ORGANIZATION .....	4
2. RESPONSE FOR THREE UNCORRELATED EARTHQUAKE COMPONENTS .....	6
2.1 INTRODUCTION .....	6
2.2 ANALYTICAL BACKGROUND .....	8
2.3 CLASSICALLY DAMPED STRUCTURES .....	9
2.3.1 AUTOCORRELATION OF RESPONSE .....	11
2.3.2 DESIGN RESPONSE .....	13
2.4 NONCLASSICALLY DAMPED STRUCTURES .....	22
2.4.1 RESPONSE AUTOCORRELATION .....	25
2.4.2 DESIGN RESPONSE .....	28
2.5 EVALUATION OF MODAL AND RESPONSE PEAK FACTORS .....	33
2.6 SIMULATION STUDY .....	38
2.7 TIME HISTORY ANALYSIS OF STRUCTURES .....	42
2.7.1 TIME INTEGRATION OF NONCLASSICALLY DAMPED STRUCTURES .....	45
2.7.2 DISPLACEMENT AND MEMBER RESPONSE OF NONCLASSICALLY DAMPED STRUCTURES .....	51
2.8 NUMERICAL RESULTS .....	52
3. RESPONSE FOR SIX CORRELATED EARTHQUAKE COMPONENTS BY MODE DISPLACEMENT APPROACH .....	59
3.1 INTRODUCTION .....	59
3.2 CORRELATED AND UNCORRELATED EARTHQUAKE COMPONENTS .....	61
3.3 CORRELATION MATRIX OF EXCITATIONS .....	67
3.4 STRUCTURAL RESPONSE .....	69
3.4.1 CLASSICALLY DAMPED STRUCTURES .....	70
3.4.2 NONCLASSICALLY DAMPED STRUCTURES ..	74
3.5 MAXIMUM DESIGN RESPONSE .....	79
3.6 NUMERICAL RESULTS .....	85
3.6.1 TORSIONAL STRUCTURE .....	86
3.6.2 SPACE FRAME STRUCTURE .....	90

4.	RESPONSE FOR SIX CORRELATED EARTHQUAKE COMPONENTS BY MODE ACCELERATION APPROACH .....	93
4.1	INTRODUCTION .....	93
4.2	ANALYTICAL FORMULATION .....	94
4.2.1	MEAN SQUARE AND DESIGN RESPONSE ...	95
4.2.2	PSUEDO-STATIC RESPONSE .....	101
4.3	THE WORST-CASE MEAN SQUARE RESPONSE .....	108
4.4	NUMERICAL RESULTS .....	109
5.	SUMMARY AND CONCLUSIONS .....	113
	REFERENCES .....	118
	TABLES .....	123
	FIGURES .....	163
APPENDIX A.	TIME HISTORY ANALYSIS OF NONCLASSICALLY DAMPED SYSTEMS .....	177
APPENDIX B.	CORRELATION TERMS IN EQUATION 4.3 .....	185
APPENDIX C.	COEFFICIENTS OF PARTIAL FRACTIONS .....	190
	CLASSICAL DAMPED SYSTEMS .....	190
	NONCLASSICAL DAMPING SYSTEM .....	194
APPENDIX D.	RESPONSE COMBINATIONS .....	197

## CHAPTER 1

### INTRODUCTION

#### 1.1 BACKGROUND AND SCOPE

The earthquake induced ground motions, as felt by structures, will, in general, have six components: three translational and three rotational. However, for the seismic design of structures, it is a common practice to consider only the three translational components. In practice, a structure is analyzed for these components applied along the structural axes. The responses obtained for the three components are then combined by the square-root-of-the-sum-of-the-squares procedures [1,35] to obtain the total response. This assumes that the three excitation components are uncorrelated.

In general, however, this assumption is not true. Penzien and his colleagues have studied the correlative character of the translational components in a series of papers [26,27]. The correlation between the components considered along any three arbitrarily selected structural axes can be shown to depend upon the orientation of the axes with respect to the impinging seismic wave. In this study, this correlation between the translational as well as the rotational components has been considered.

The rotational components are customarily neglected "as being of minor consequence" in seismic structural analyses. Only a few researchers, notably Newmark [23], Rosenblueth [28,29], Tso and Hsu [40] and Nathan and Mackenzie [22],

have considered the rotational components in their work. Here, the Newmark's approach [23] is utilized in describing the rotational components. This is based on a simple representation of the ground motion components as traveling waves. (Earlier, the idea of ground motion as a traveling wave was also considered by Bogdanoff, Goldberg and Schiff [4] to evaluate the effect of transmission time on the response of long structures.) With this representation, the rotational components are related to the jerks of the translational components and the shear wave velocity of propagation. Here, the methods to obtain the design response for such correlated excitations are developed.

For the purpose of describing the seismic design input for the calculation of the design response for an earthquake component, the smoothed elastic response spectra are now commonly used [13,24,41]. For linear structures, the method of the square-root-of-the-sum-of-squares of the modal responses, commonly abbreviated as SRSS, and its several modifications are used. Several investigators [2,9,29,33, 35] have established the theoretical bases for the SRSS and its modifications. However, most of these studies have so far been directed to the classically damped structural systems where the damping matrix of the structure can be uncoupled by the undamped normal modes. Recently, Singh [33] has extended the application of the response spectrum approach to the nonclassically damped systems also. The theoretical basis of this approach was established by the

stationary random vibration theory. However, no numerical validation of this approach by simulation is available. In this study a numerical validation of this response spectrum approach is provided for its application to the nonclassically damped structures subjected to uncorrelated translational components. As a by-product, the validation results for the classically damped systems are also obtained.

After validating the response spectrum methods for the calculation of design response for uncorrelated components, here similar response spectrum approaches have been developed for the correlated six component inputs. These approaches, developed for the correlated components, can employ the component response spectra directly in their methodology.

The response of a structure is shown to depend upon the orientation of the structure with respect to the impinging seismic waves. For a particular orientation, the induced response could be the maximum. Here, this maximum response is being referred to as the worst-case response. A direct methodology is developed to obtain the worst-case response, irrespective of the orientation of the structure. The numerical results demonstrating the application of this methodology are presented. The rotational components have also been considered in this approach and it is shown that the effects of these can be significant for tall and large structures.

The currently used seismic response evaluation procedures are usually based on the method of mode displacement of structural dynamics. However, some specific advantages can be realized by employing the method of mode acceleration. Here, therefore, an alternative response analysis approach, based on the method of mode acceleration, has also been developed for the proportionally damped structural systems. This is a generalization of the approach proposed by Singh and Mehta [38], which is now applicable to the correlated six component inputs. This approach is computationally more efficient than the mode displacement approach in as much as it requires only first few modes for a sufficiently accurate evaluation of the response; the effect of the omission of the high frequency modes in this approach is rather inconsequential, even for the stiff structural systems. The numerical results demonstrating the effectiveness of this alternative approach are also presented.

## 1.2 REPORT ORGANIZATION

In Chapter 2, the development of the response spectrum approach for the classically as well as the nonclassically damped structures, subjected to three uncorrelated components, is described. Some of the formulation in Chapter 2 may be available elsewhere, but it is given here for the sake of completeness, and also because it is needed in the subsequent chapters. A new modal superposition approach, developed for the time history analysis of the nonclassi-

cally damped structures, is also presented in this chapter. The numerical results obtained for the validation of the response spectrum approaches for the nonclassically as well as classically damped structures are presented.

Chapter 3 describes the development of the mode displacement procedures used with the correlated excitation components. The relationships between the rotational and translational components are developed here. The correlation matrix of the correlated six components is defined in terms of the autocorrelations and spectral density functions of the uncorrelated principal excitation components. The analytical development for the identification of the "worst case" response are given. The numerical results for the classically and nonclassically damped structures, employing the methodology developed in this chapter, are presented.

In Chapter 4, the analytical formulation of the response spectrum approach employing the method of mode acceleration and the numerical results obtained with this approach are given.

The summary and general conclusions are given in Chapter 5. More detailed and specific conclusions are given in various chapters themselves where the numerical results pertaining to the topic of the chapter are presented.

The appendices provide the details of some analytical developments and expressions used in the main text.

## Chapter II

### RESPONSE FOR THREE UNCORRELATED EARTHQUAKE COMPONENTS

#### 2.1 INTRODUCTION

For the calculation of structural design response for earthquake loads prescribed in terms of response spectra, the method of SRSS is most commonly used in practice. In its simplest form, the method consists of obtaining the maximum modal responses using response spectra and then their combination by the simple square-root-of-the-sum-of-the-squares (SRSS) procedure. Several modifications to this mode response combination rule have been suggested which especially account for the correlation between modal responses. This method and its modifications are applicable to the structures for which the energy dissipation can be defined in terms of modal damping ratios. Mathematically speaking it means that the damping matrix of the system is proportional or classical [5].

Herein, the SRSS method as used in practice and its modification are reformulated and refined to obtain more accurate numerical results for structures subjected to multi-component earthquakes. Three translational components of

excitation are considered and assumed uncorrelated. The correlated components are considered in the next two chapters. A comprehensive numerical simulation study is conducted to verify the SRSS procedures.

The cases where the damping matrix of a system is non-proportional or nonclassical, a response spectrum procedure similar to the SRSS can still be used (see Singh[33]). Here, this procedure is formulated such that the effect of peak factors can be included in the calculation of design response. Again, the formulation is developed for three uncorrelated earthquake components. A comprehensive study of correlation between modal responses of a nonproportionally damped structure is also conducted.

The verification of this response spectrum procedure for nonclassically damped systems is also done by a comprehensive simulation study. To obtain numerical results for nonclassically damped systems by the modal analysis procedure for ground acceleration defined in digitized time history form, a new step-by-step time history analysis approach has been developed. This new approach has been used to obtain results for two ensembles of time histories. These results are discussed in the later part of this chapter.

## 2.2 ANALYTICAL BACKGROUND

The equations of motion of a multi-degree-of-freedom structure subjected to earthquake induced ground motion along its geometric axes can be written as:

$$[M]\{\ddot{u}\} + [C]\{\dot{u}\} + [K]\{u\} = - [M][r]\{E\} \quad (2.1)$$

where  $[M]$  = mass matrix;  $[C]$  = damping matrix;  $[K]$  = stiffness matrix;  $\{u\}$  = relative displacement vector;  $\{E\}$  = the acceleration vector of the ground motion components;  $[r]$  = the matrix of the ground displacement influence coefficients, the columns of which are the influence coefficient vectors  $\{r_{\ell}\}$  for each excitation component. In general, the earthquake motions as felt by a structure will have six components, and thus  $[r]$  will be a  $N \times 6$  matrix where  $N$  is the number of degrees-of-freedom. In this chapter, only three translational components of excitations are considered and are assumed to be uncorrelated. The more general case of six correlated excitation components is considered in the next two chapters.

As mentioned earlier, the SRSS procedure is most commonly used for the evaluation of design response for design inputs defined in terms of response spectra. This requires that a modal analysis approach be used. Thus here the solution of Eq. 2.1 by a modal analysis approach is sought.

The classical normal mode approach can only be used for a very special form of damping matrix [C]. Such damping matrices are often called proportional, Rayleigh or classical. A proportional damping matrix is a linear combination of the mass and stiffness matrices. Such matrices can be decoupled by the normal modes of the system. Another form of damping matrix which also possesses a similar property was defined by Caughey [5]. For classical [C], the solution of Eq. 2.1 can be obtained by the normal mode approach. However if [C] is not classical, that is it can not be diagonalized by the undamped modes of the system, a complex or damped mode approach is used. In the following sections, both types of structural systems, i.e., systems with classical as well as nonclassical damping matrices, will be considered.

### 2.3 CLASSICALLY DAMPED STRUCTURES

If the damping matrix [C] is classical, then Eq. 2.1 can be decoupled into its modal equations by standard transformation [7]. One such decoupled modal equation is:

$$\ddot{V}_j + 2\beta_j\omega_j \dot{V}_j + \omega_j^2 V_j = -\{\chi_j\}^T \{E(t)\} \quad (2.2)$$

where  $V_j$  = the  $j^{\text{th}}$  principal coordinate or the modal displacement;  $\omega_j$  =  $j^{\text{th}}$  natural frequency;  $\beta_j$  =  $\{\phi_j\}^T [C] \{\phi_j\} / 2\omega_j m_j$  is  $j^{\text{th}}$  modal damping ratio;  $\{\phi_j\}$  = rela-

tive displacement mode shape;  $m_j = \{\phi_j\}^T [M] \{\phi_j\}$  is the  $j^{\text{th}}$  modal mass ;  $\{\gamma_j\}$  = the vector of participation factors with its elements as the participation factors for the excitation components, defined as  $\gamma_{\ell j} = \{\phi_j\}^T [M] \{r_\ell\} / m_j$   $\ell=1,2,3$ . The superscript 'T' represents the transpose of a matrix or vector, and dot over a time varying quantity represents its time derivative.

A response quantity of design interest, like displacement, member forces and moments which are linearly related to displacement, can be written in terms of modal quantities as follows:

$$S(t) = -\sum_{j=1}^N \xi_j \{\gamma_j\}^T \int_0^t \{E(t)\} h_j(t-\tau) d\tau \quad (2.3)$$

where  $\xi_j = j^{\text{th}}$  normal mode shape of the response quantity  $S(t)$  which can be obtained by linear transformation from the  $j^{\text{th}}$  eigenvector  $\{\phi_j\}$ , and  $h_j(t)$  is the impulse response function of Eq. 2.2.

We are interested in the calculation of design response. It is a high value such that it is not likely to be exceeded very often when earthquakes occur. To obtain this, the ensemble of earthquake motions which can occur at the site should be considered. Thus the components  $\ddot{X}_\ell(t)$  should be modeled by random processes to obtain the design res-

ponse. The design response then may be considered to be a value which will have a small probability of exceedance. The magnitude of such response depends upon the root mean square (RMS) value of response, probability of exceedance, correlation character of the response random process, etc. In practice, however, this design response usually can be obtained as a factor times the maximum RMS response. This factor is called the "peak factor" [42]. Herein, this simplified approach is used to define the design response. A brief development of the RMS expressions and peak factors are given in the following sections.

### 2.3.1 AUTOCORRELATION OF RESPONSE

Using Eq. 2.3, the autocorrelation function of the response can be written as:

$$\begin{aligned} \text{Ex}\{S(t_1)S(t_2)\} = & \\ & \sum_{j=1}^N \sum_{k=1}^N \xi_j \xi_k \{x_j\}^T \left( \int_0^{t_1} \int_0^{t_2} [\text{Ex}\{\{E(t_1)\}\{E(t_2)\}^T\}] \right. \\ & \left. h_j(t_1-\tau_1) h_k(t_2-\tau_2) d\tau_1 d\tau_2 \right) \{x_k\} \end{aligned} \quad (2.4)$$

where  $\text{Ex}\{.\}$  denotes the expected value of  $\{.\}$ . For a given correlation matrix,  $\text{Ex}\{\{E(t_1)\}\{E(t_2)\}^T\}$ , of the excitation, Eq. 2.4 can be evaluated at least theoretically. If the excitation components are stochastically nonstationary, then

the definition of autocorrelation matrix and evaluation of Eq. 2.4 are very cumbersome. Therefore, often with the main purpose of simplifying the analysis, the earthquake motions are assumed to be stationary random processes. With this assumption, the motion components can be characterized by the auto- and cross- spectral density functions. Furthermore, in this chapter only uncorrelated components are considered. Thus the cross-spectral density functions are zero. Also, only stationary response situations are considered. (The effect of these simplifying assumptions on the calculation of design response is evaluated by a simulation study, described later.) Employing standard analytical manipulations of random vibration for stationary input and response, the autocorrelation function in Eq. 2.4 can be shown to be:

$$\begin{aligned} \text{Ex}[S(t_1)S(t_2)] &= \sum_{\ell=1}^3 \sum_{j=1}^N \sum_{k=1}^N \xi_j \xi_k^* \gamma_{\ell j} \gamma_{\ell k} \\ &\int_{-\infty}^{+\infty} \phi_{\ell}(\omega) e^{i\omega(t_1-t_2)} H_j(\omega) H_k^*(\omega) d\omega \end{aligned} \quad (2.5)$$

where  $\phi_{\ell}(\omega)$  is the spectral density function (SDF) of the  $\ell^{\text{th}}$  excitation component and  $H_j(\omega)$  is the well-known complex frequency response function defined as:

$$H_j(\omega) = 1 / (\omega_j^2 - \omega^2 + 2i\beta_j \omega_j \omega) \quad (2.6)$$

The stationary value of the mean square response can be obtained from Eq. 2.5 by setting  $t_1=t_2=t$ .

### 2.3.2 DESIGN RESPONSE

To obtain the design response,  $S_d$ , the root mean square value is to be multiplied by the response peak factor. Let this factor be  $C$ , then

$$S_d^2 = C^2 \text{Ex}[S^2(t)] \quad (2.7)$$

For earthquake motions defined by a spectral density function, Eq. 2.7 can be used to obtain the design response. However, a direct prescription of the spectral density function for earthquake motion has not been possible so far. The main difficulty being that earthquake motions are inherently nonstationary random processes and thus they can not be modeled by spectral density function which, strictly speaking, exist only for a stationary random process. In practice, seismic design input is often characterized by smoothed ground response spectrum curves [13,24]. As it is often convenient to use spectral density function in an analysis, such as in Eq. 2.5, numerical methods have been developed [11] to obtain this from smoothed ground spectra.

A response spectrum value represents the maximum response of an oscillator. This maximum response value is also equal to the RMS response times the peak factor. For exam-

ple, if the psuedo acceleration response spectrum value for the  $\ell^{\text{th}}$  component of excitation at frequency  $\omega_j$  and damping  $\beta_j$  is  $R_{\ell a}(\omega_j)$ , and the peak factor relating the maximum response to the root mean square relative displacement response is  $C_{\ell dj}$ , then, using Eq. 2.7

$$C_{\ell dj}^2 \int_{-\infty}^{+\infty} \Phi_{\ell}(\omega) |H_j(\omega)|^2 d\omega = R_{\ell d}^2(\omega_j) = R_{\ell a}^2(\omega_j) / \omega_j^4 \quad (2.8)$$

in which the division of  $R_{\ell a}(\omega_j)$  by  $\omega_j^2$  converts it into the corresponding spectral displacement value,  $R_{\ell d}(\omega_j)$ . The peak factor,  $C_{\ell dj}$ , depends upon the central frequency, band width and duration of the motion and can be obtained by procedures such as developed by Vanmarcke [44] and Mason [20].

Eq. 2.8 defines the relationship between a response spectrum curve and the spectral density function of ground motion. To obtain the spectral density function from this equation, the method described by Vanmarcke [42] and Gasparini and Vanmarcke [11] can be used. This will define the spectral density function at discrete frequencies  $\omega_j$ . Such numerically obtained spectral density functions can be used in Eq. 2.5 and 2.7 to obtain the RMS and the maximum response. If the variation of spectral density function between discrete frequencies is assumed linear, then the frequency integral in Eq. 2.5 can also be obtained in closed form.

Although all the curves of a set of prescribed design spectra, such as in References 24 and 41, supposedly belong to the same ground motion, the spectral density functions obtained by the above procedure for individual response spectrum curves of different damping ratios may not be the same. This internal inconsistency in the prescribed motion has been observed quite often, and is due to several reasons: (1) the process of development of a design spectrum [11], (2) the assumption of stationarity for nonstationary earthquake motions, and (3) approximations involved in the calculation of peak factors. With the current state-of-the-art of random vibration analysis for earthquake motions, this inconsistency can not be resolved, or at least has not been resolved rationally yet.

Thus, realizing that this internal inconsistency in the definition of spectral density functions from a prescribed spectrum can not be resolved with the current state-of-the-art, the explicit use of  $\phi_g(\omega)$  in response calculations has been avoided herein. This can be accomplished if Eq. 2.8 can be directly used in Eq. 2.5 to obtain the mean square response. This, indeed, can be done, as is shown by Singh and Chu [35]. For this,  $Ex[S^2(t)]$  in Eq. 2.7 is expanded into terms with  $j=k$  (called the single summation terms) and  $j \neq k$  (called the double summation terms or also cross terms) as follows:

$$\begin{aligned}
S_d^2 = C^2 \sum_{\ell=1}^3 \left\{ \sum_{j=1}^N \xi_j^2 \gamma_{\ell j}^2 \int_{-\infty}^{+\infty} \phi_{\ell}(\omega) |H_j(\omega)|^2 d\omega \right. \\
+ 2 \sum_{j=1}^N \sum_{k=j+1}^N \xi_j \xi_k \gamma_{\ell j} \gamma_{\ell k} \\
\left. \int_{-\infty}^{+\infty} \phi_{\ell}(\omega) N(\omega) |H_j(\omega)|^2 |H_k(\omega)|^2 d\omega \right\} \quad (2.9)
\end{aligned}$$

where  $N(\omega)$  is defined as:

$$N(\omega) = \omega^4 - \omega^2(\omega_j^2 + \omega_k^2 - 4\beta_j \beta_k \omega_j \omega_k) + \omega_j^2 \omega_k^2 \quad (2.10)$$

The integral in the double summation term can be further split into partial fractions, leading to

$$\begin{aligned}
S_d^2 = C^2 \sum_{\ell=1}^3 \left\{ \sum_{j=1}^N \xi_j^2 \gamma_{\ell j}^2 I_{0\ell}(\omega_j) \right. \\
+ 2 \sum_{j=1}^N \sum_{k=j+1}^N \xi_j \xi_k \gamma_{\ell j} \gamma_{\ell k} [A_1 I_{0\ell}(\omega_j) + A_2 I_{1\ell}(\omega_j) \\
\left. + A_3 I_{0\ell}(\omega_k) + A_4 I_{1\ell}(\omega_k)] \right\} \quad (2.11)
\end{aligned}$$

where  $I_{0\ell}(\omega_j)$  and  $I_{1\ell}(\omega_j)$  are the frequency integrals defined as:

$$I_{0\ell}(\omega_j) = \int_{-\infty}^{+\infty} \phi_{\ell}(\omega) |H_j(\omega)|^2 d\omega \quad (2.12)$$

$$I_{1\ell}(\omega_j) = \int_{-\infty}^{+\infty} \phi_{\ell}(\omega) \omega^2 |H_j(\omega)|^2 d\omega \quad (2.13)$$

and the coefficients of the partial fractions  $A_1$ ,  $A_2$ ,  $A_3$  and  $A_4$  are defined in Appendix C.

It is seen that the frequency integral  $I_{0\ell}(\omega_j)$  in Eq. 2.12 can be defined in terms of the psuedo acceleration spectrum and peak factor according to Eq. 2.8. To define the integral  $I_{1\ell}(\omega_j)$  in Eq. 2.13 we need to have a relationship similar to Eq. 2.8. This relationship is defined in terms of the relative velocity spectrum value as follows:

$$C_{\ell Vj}^2 \int_{-\infty}^{+\infty} \ddot{\phi}_{\ell}(\omega) \omega^2 |H_j(\omega)|^2 d\omega = R_{\ell V}^2(\omega_j) \quad (2.14)$$

where  $R_{\ell V}(\omega_j)$  = relative velocity response spectrum value for the  $\ell^{\text{th}}$  component of excitation at frequency  $\omega_j$  and damping  $\beta_j$ , and  $C_{\ell Vj}$  = the peak factor for the relative velocity response of the oscillator.  $C_{\ell Vj}$  depends upon the duration of motion, the band width and effective central frequency of the relative velocity response.

The use of relative velocity spectra is rather uncommon and these are rarely prescribed for designs in smooth spectra form. In the absence of such availability these can, however, be obtained by making simplifying assumptions. See Reference 32. For example, for the oscillator frequencies within the range of excitation frequencies, the relative

velocity spectrum is almost the same as the psuedo velocity spectrum. For higher oscillator frequencies, however, relative velocity decreases faster than psuedo velocity. Thus for frequency values higher than the so-called zero period acceleration (ZPA) frequency, relative velocity spectrum may be assumed to be zero. For the in-between frequencies, a log-log linear variation to achieve a value equal to the psuedo velocity spectrum value at some earlier frequency may be assumed [32]. However, these are approximations, and certainly a more appropriate approach would be to obtain the smoothed relative velocity spectra for design in the same way as the psuedo acceleration spectra were obtained [24]. In the simulation study, to be described later, these relative velocity spectra were obtained for the ensembles of earthquake motions.

Employing Eqs. 2.8 and 2.14 in Eq. 2.11, the design response in terms of response spectrum values can be written as:

$$\begin{aligned}
 S_d^2 = & C^2 \sum_{\ell=1}^3 \left\{ \sum_{j=1}^N \xi_j^2 \gamma_{\ell j}^2 (R_{\ell d}(\omega_j)/C_{\ell dj})^2 \right. \\
 & + 2 \sum_{j=1}^N \sum_{k=j+1}^N \xi_j \xi_k \gamma_{\ell j} \gamma_{\ell k} [ A_1 (R_{\ell d}(\omega_j)/C_{\ell dj})^2 \\
 & \left. + A_2 (R_{\ell v}(\omega_j)/C_{\ell vj})^2 + A_3 (R_{\ell d}(\omega_k)/C_{\ell dk})^2 + A_4 (R_{\ell v}(\omega_k)/C_{\ell vk})^2 \right\} \\
 & \qquad \qquad \qquad (2.15)
 \end{aligned}$$

To obtain the peak factors required in this equation, the Vanmarcke's approach [42] is used. A brief outline of this approach is given in section 2.5.

Eq. 2.15 defines a response spectrum approach which also incorporates the effect of modal peak factors in the calculation of design response. Often, however, the peak factors involved in Eq. 2.15 are assumed to be the same. With this assumption, the design response can be rewritten as:

$$S_d^2 = \sum_{\ell=1}^3 S_{\ell}^2 \quad (2.16)$$

where  $S_{\ell}$  is the response for the  $\ell^{\text{th}}$  component of excitation defined as:

$$S_{\ell}^2 = \sum_{j=1}^N S_{\ell j}^2 + 2 \sum_{j=1}^N \sum_{k=j+1}^N S_{\ell jk} \quad (2.17)$$

where

$$S_{\ell j} = \xi_j \gamma_{\ell j} R_{\ell d}(\omega_j) \quad (2.18)$$

$$S_{\ell jk} = \xi_j \xi_k \gamma_{\ell j} \gamma_{\ell k} [ A_1 R_{\ell d}^2(\omega_j) + A_2 R_{\ell v}^2(\omega_j) + A_3 R_{\ell d}^2(\omega_k) + A_4 R_{\ell v}^2(\omega_k) ] \quad (2.19)$$

It is seen that the total response for three uncorrelated components is equal to the square root of the sum of the squares of the responses of the individual components.

See also the work of Chu, Amin and Singh [8]. Eq. 2.17 is the same expression as developed by Singh and Chu [35] for one excitation component. The single summation term in Eq. 2.17 is the same as the conventional SRSS approach. The double summation terms which represent the effect of correlation between modes are important in certain cases. The numerical results for Eqs. 2.15, 2.16 and 2.17 are presented and compared with the time history results later in Section 2.8.

The modal correlation coefficient for one component, say the  $\ell^{\text{th}}$  component, can be defined as follows [2]:

$$P_{\ell j k} = S_{\ell j k} / S_{\ell j} S_{\ell k} \quad (2.20)$$

Whereas this correlation coefficient considering all the excitation components can be written as:

$$P_{j k} = \frac{\sum_{\ell=1}^3 S_{\ell j k}}{\sqrt{(\sum_{\ell=1}^3 S_{\ell j}^2)(\sum_{\ell=1}^3 S_{\ell k}^2)}} \quad (2.21)$$

These two coefficients can have different values. However, the coefficient in Eq. 2.20 is a more important indicator of the importance of the double summation terms.

It is seen that the correlation coefficients defined by Eqs. 2.20 and 2.21 do not depend on  $\xi_j$ . That is, they remain the same for all response quantities. However, they are

affected by the closeness of modal frequencies (a well known fact), damping values and frequency characteristics of the input. The correlation is also high when the modal frequencies are higher than the highest frequency of the input, see Reference 38.

Here, the numerical values of the modal correlation coefficients are presented for the structure shown in Fig. 2.1. For this structure, the mass and stiffness properties as well as the eccentricity between mass and stiffness centers, represented by the  $e/r$  parameter (eccentricity divided by the radius of gyration of a floor slab), can be easily adjusted to create closely spaced frequencies. Tables 2.1 and 2.2 show the modal frequencies, damping ratios and participation factors for the structures with the  $e/r$  values of .0 and .05. It is seen that when the  $e/r$  value is small the frequencies are closely spaced.

Tables 2.3a and 2.4a show the modal correlation coefficient defined by Eq. 2.20 for these values of  $e/r$ . It is seen that the correlation is strong among the nearby modes when  $e/r$  is small. In such cases it becomes essential to consider the double summation terms in the calculation of design response [30,31].

Tables 2.3b and 2.4b show the modal correlation coefficient as defined by Eq. 2.21, when two excitation components

are considered. These values are quite different from those in Tables 2.3a and 2.4a. In fact, the high correlation between modes 1 and 2 for one component becomes small when two components are considered. This is because the double summation terms of two components in Eq. 2.19 tend to cancel each other out to give a small value of  $\rho_{jk}$ .

#### 2.4 NONCLASSICALLY DAMPED STRUCTURES

In this section, the evaluation of design response for nonclassically damped structures is described. For nonclassically damped structures, the normal mode approach can not be used, and the 2N-dimension state vector approach [10,21] is required. With this approach, it is possible to develop an SRSS procedure as shown by Singh [33]. Here, a brief description of Singh's formulation is given as it is used in a later section of this report where a new modal time history analysis approach is developed, as well as in the following chapters where correlated seismic components of the input are considered. The development presented here is also different from that given by Singh [33] in as much as it considers three components and includes the peak factor in the evaluation of design response.

In the state vector approach, Eq. 2.1 is rewritten, with the help of an identity equation, in the following form:

$$[A]\{\dot{y}\} + [B]\{y\} = - \sum_{\ell=1}^3 \{D_{\ell}\} \ddot{X}_{\ell}(t) \quad (2.22)$$

where  $\ddot{X}_{\ell}(t)$  is the  $\ell^{\text{th}}$  component of ground acceleration vector  $\{E\}$  and

$$[A] = \begin{bmatrix} [O] & [M] \\ [M] & [C] \end{bmatrix}, \quad [B] = \begin{bmatrix} -[M] & [O] \\ [O] & [K] \end{bmatrix} \quad \text{and} \quad \{D_{\ell}\} = \begin{cases} \{O\} \\ [M]\{r_{\ell}\} \end{cases} \quad \ell=1,2,3 \quad (2.23)$$

and

$$\{y\} = \begin{Bmatrix} \{\dot{u}\} \\ \{u\} \end{Bmatrix} \quad (2.24)$$

is the 2N- dimension state vector of response.

Using the complex eigenvector matrix,  $[\phi]$ , of the following eigenvalue problem

$$p [A]\{\phi\} + [B]\{\phi\} = \{O\} \quad (2.25)$$

Eq. 2.22 can be decoupled. (In Eq. 2.25,  $p$  is the eigenvalue and  $\{\phi\}$  is the corresponding eigenvector.) For this the state vector  $\{y\}$  is expressed in terms of the eigenvector matrix  $[\phi]$  and the complex-valued principal coordinates  $\{Z\}$  as,

$$\{y\} = [\phi]\{Z\} \quad (2.26)$$

Substituting in Eq. 2.22 and invoking orthogonal properties of the eigenvectors, the following equation for the  $j^{\text{th}}$  principle coordinate is obtained:

$$\dot{Z}_j - p_j Z_j = \sum_{\ell=1}^3 F_{\ell j} \ddot{X}_{\ell}(t) \quad (2.27)$$

where  $Z_j = j^{\text{th}}$  principal coordinate,  $p_j =$  the complex  $j^{\text{th}}$  eigenvalue and

$$F_{\ell j} = -\{\phi_j\}^T [M] \{r_{\ell}\} / A_j^* \quad \ell=1,2,3 \quad (2.28)$$

in which  $\{\phi_j\} =$  the lower part of the  $j^{\text{th}}$  complex eigenvector of Eq. 2.25 and

$$A_j^* = \{\phi_j\}^T (2p_j [M] + [C]) \{\phi_j\} \quad (2.29)$$

The solution of Eq. 2.27 can be written as :

$$Z_j = \sum_{\ell=1}^3 \int_0^t F_{\ell j} \ddot{X}_{\ell}(\tau) e^{p_j(t-\tau)} d\tau \quad (2.30)$$

In terms of Eq. 2.30, a response quantity  $S(t)$  of design interest can now be written as follows:

$$S(t) = \sum_{\ell=1}^3 \left\{ \sum_{j=1}^{2N} q_{\ell j} \int_0^t \ddot{X}_{\ell}(\tau) e^{p_j(t-\tau)} d\tau \right\} \quad (2.31)$$

where

$$q_{\ell j} = g_j F_{\ell j} \quad (\ell=1,2,3) \quad (2.32)$$

in which  $g_j$  is the modal response of  $S(t)$ . This can be obtained in terms of  $\{\phi_j\}$  and a vector  $\{T\}$  which transforms the relative displacement into the response  $S(t)$  as follows:

$$g_j = \{T\}^T \{\phi_j\} \quad (2.33)$$

Here we are primarily interested in the calculation of the maximum value of  $S(t)$ , i.e., the design response. Thus as in the previous section, the excitation components  $\ddot{X}_1(\tau)$ ,  $\ddot{X}_2(\tau)$  and  $\ddot{X}_3(\tau)$  are considered as sample functions of random processes. Again, to simplify the analysis, the random processes are assumed to be stationary and the RMS value required to define the maximum response is obtained.

#### 2.4.1 RESPONSE AUTOCORRELATION

In Eq. 2.31 the complex and conjugate terms are paired and the autocorrelation function is defined as follows:

$$\text{Ex}[S(t_1)S(t_2)] =$$

$$\sum_{\ell=1}^3 \left\{ \sum_{j=1}^N \sum_{k=1}^N \int_0^{t_1} \int_0^{t_2} \text{Ex}[\ddot{X}_\ell(\tau_1)\ddot{X}_\ell(\tau_2)] \right. \\ \left. \left( [q_{\ell j} e^{p_j(t_1-\tau_1)} + q_{\ell j}^* e^{p_j^*(t_1-\tau_1)}] \right) \right. \\ \left. [q_{\ell k} e^{p_k(t_2-\tau_2)} + q_{\ell k}^* e^{p_k^*(t_2-\tau_2)}] \right) d\tau_1 d\tau_2 \quad (2.34)$$

where  $\text{Ex}[\ddot{X}_\ell(\tau_1)\ddot{X}_m(\tau_2)] = 0$  has been assumed for  $\ell \neq m$  since the accelerations in directions  $x_1$ ,  $x_2$  and  $x_3$  are assumed to be independent. Expressing  $\text{Ex}[\ddot{X}_\ell(\tau_1)\ddot{X}_\ell(\tau_2)]$  in terms of the spectral density function  $\phi_\ell(\omega)$ , and carrying out the standard algebraic manipulations of random vibration, Eq. 2.34 can be written as

$$\begin{aligned} \text{Ex}[S(t_1)S(t_2)] &= \sum_{\ell=1}^3 \left\{ \sum_{j=1}^N \sum_{k=1}^N \int_{-\infty}^{+\infty} \phi_\ell(\omega) \right. \\ &\quad \left. \left( \int_0^{t_1} e^{i\omega\tau_1} [q_{\ell j} e^{p_j(t_1-\tau_1)} + q_{\ell j}^* e^{p_j^*(t_1-\tau_1)}] d\tau_1 \right) \right. \\ &\quad \left. \left( \int_0^{t_2} e^{-i\omega\tau_2} [q_{\ell k} e^{p_k(t_2-\tau_2)} + q_{\ell k}^* e^{p_k^*(t_2-\tau_2)}] d\tau_2 \right) d\omega \right\} \end{aligned} \quad (2.35)$$

For large  $t_1$  and  $t_2$  the response becomes stationary. Considering such a situation, the integrals in the parentheses can be shown to be

$$\begin{aligned} \int_0^{t_1} e^{i\omega\tau_1} \{q_{\ell j} e^{p_j(t_1-\tau_1)} + q_{\ell j}^* e^{p_j^*(t_1-\tau_1)}\} d\tau_1 \\ = G_{\ell j}(\omega) H_j(\omega) e^{i\omega t_1} \end{aligned} \quad (2.36)$$

$$\begin{aligned} \int_0^{t_2} e^{-i\omega\tau_2} \{q_{\ell k} e^{p_k(t_2-\tau_2)} + q_{\ell k}^* e^{p_k^*(t_2-\tau_2)}\} d\tau_2 \\ = G_{\ell k}^*(\omega) H_k^*(\omega) e^{i\omega t_2} \end{aligned} \quad (2.37)$$

where

$$\begin{aligned}
 G_{\ell j}(\omega) &= 2[ \omega_j (a_{\ell j} \beta_j - b_{\ell j} \sqrt{1 - \beta_j^2}) + i \omega a_{\ell j} ] \\
 &= 2(A_{\ell j} + i \omega a_{\ell j})
 \end{aligned}
 \tag{2.38}$$

in which  $A_{\ell j}$  is half the real parts of  $G_{\ell j}$ ;  $a_{\ell j}$  and  $b_{\ell j}$  are the real and imaginary part of  $q_{\ell j}$ , respectively; and  $\omega_j$  and  $\beta_j$ , which are analogous to the modal frequency and damping ratio, are defined in terms of the real and imaginary parts of  $p_j$  as follows:

$$\omega_j = |p_j|, \quad \beta_j = -\text{Real}(p_j) / (\omega_j)
 \tag{2.39}$$

Substituting Eqs. 2.36 and 2.37 in Eq. 2.35, the autocorrelation function of the response is obtained. The mean square value of this response is obtained by setting  $t_1 = t_2 = t$  as:

$$\begin{aligned}
 \text{Ex}[S^2(t)] &= \sum_{\ell=1}^3 \left\{ \sum_{j=1}^N \sum_{k=1}^N \right. \\
 &\quad \left. \int_{-\infty}^{+\infty} [\Phi_{\ell}(\omega) G_{\ell j}(\omega) G_{\ell k}^*(\omega)] H_j(\omega) H_k^*(\omega) \right\} d\omega
 \end{aligned}
 \tag{2.40}$$

This expression of the mean square response is a little different from the one given by Singh [33]. Here the separation of modal terms is explicit; it can be of help in the study of modal correlations and their relevance to the res-

ponse evaluation procedures used with nonclassically damped structures.

#### 2.4.2 DESIGN RESPONSE

To calculate the design response  $S_d$ , the root mean square value is to be amplified by the peak factor,  $C$ , as:

$$S_d^2 = C^2 \sum_{\ell=1}^3 \left\{ \sum_{j=1}^N \sum_{k=1}^N \int_{-\infty}^{+\infty} [\Phi_{\ell}(\omega) G_{\ell j}(\omega) G_{\ell k}^*(\omega)] H_j(\omega) H_k^*(\omega) \right\} d\omega \quad (2.41)$$

As design inputs for earthquake analyses are defined in terms of smoothed response spectrum curves, we will develop Eq. 2.41 in terms of response spectrum values. For this, Eq. 2.41 is expanded into terms with  $j=k$  and  $j \neq k$  as:

$$S_d^2 = C^2 \sum_{\ell=1}^3 \left\{ \sum_{j=1}^N \int_{-\infty}^{+\infty} \Phi_{\ell}(\omega) |G_{\ell j}(\omega)|^2 |H_j(\omega)|^2 d\omega \right. \\ \left. + \sum_{\substack{j=1 \\ j \neq k}}^N \sum_{k=1}^N \int_{-\infty}^{+\infty} \Phi_{\ell}(\omega) G_{\ell j}(\omega) G_{\ell k}^*(\omega) H_j(\omega) H_k^*(\omega) d\omega \right\} \quad (2.42)$$

The terms with  $j \neq k$  can also be written as:

$$\sum_{\ell=1}^3 \left( 4 \sum_{j \neq k} \int_{-\infty}^{+\infty} \Phi_{\ell}(\omega) \right. \\ \left. [(U_{\ell jk} + \omega^2 V_{\ell jk}) \{H_j(\omega) H_k^*(\omega) + H_j^*(\omega) H_k(\omega)\} \right. \\ \left. + i\omega W_{\ell jk} \{H_j(\omega) H_k^*(\omega) - H_j^*(\omega) H_k(\omega)\}] d\omega \right) \quad (2.43)$$

where

$$U_{\ell jk} = A_{\ell j} A_{\ell k}, \quad V_{\ell jk} = a_{\ell j} a_{\ell k}, \quad W_{\ell jk} = (a_{\ell j} A_{\ell k} - a_{\ell k} A_{\ell j}) \quad (2.44)$$

Eq. 2.43, after simplification, can also be written as:

$$\sum_{\ell=1}^2 \sum_{j=1}^N \sum_{k=j+1}^N \Phi_{\ell}(\omega) N'_{\ell}(\omega) |H_j(\omega)|^2 |H_k(\omega)|^2 d\omega \quad (2.45)$$

where

$$\left. \begin{aligned} N'_{\ell}(\omega) &= w_{\ell 1} \omega^5 + w_{\ell 2} \omega^4 + w_{\ell 3} \omega^2 + w_{\ell 4} \\ w_{\ell 1} &= V_{\ell jk} \\ w_{\ell 2} &= U_{\ell jk} - (\omega_j^2 + \omega_k^2 - 4\beta_j \beta_k \omega_j \omega_k) V_{\ell jk} \\ &\quad - 2(\beta_k \omega_k - \beta_j \omega_j) W_{\ell jk} \\ w_{\ell 3} &= -(\omega_j^2 + \omega_k^2 - 4\beta_j \beta_k \omega_j \omega_k) U_{\ell jk} \\ &\quad - \omega_j^2 \omega_k^2 V_{\ell jk} + 2(\beta_j \omega_k - \beta_k \omega_j) \omega_j \omega_k W_{\ell jk} \\ w_{\ell 4} &= \omega_j^2 \omega_k^2 U_{\ell jk} \end{aligned} \right\} \quad (2.46)$$

The integrand of Eq. 2.45 can be further broken into partial fractions as follows:

$$\begin{aligned} N'_{\ell}(\omega) |H_j(\omega)|^2 |H_k(\omega)|^2 d\omega &= (A'_{1\ell} + A'_{2\ell} \omega^2) |H_j(\omega)|^2 \\ &\quad + (A'_{3\ell} + A'_{4\ell} \omega^2) |H_k(\omega)|^2 \end{aligned} \quad (2.47)$$

where  $A'_{1\ell}$ ,  $A'_{2\ell}$ ,  $A'_{3\ell}$  and  $A'_{4\ell}$  are defined in Appendix C.

With this division into partial fractions, Eq. 2.42 can now be written in terms of the frequency integrals  $I_{0\ell}(\omega_j)$  and  $I_{1\ell}(\omega_j)$ , defined by Eqs. 2.12 and 2.13, as follows:

$$\begin{aligned}
 S_d^2 = C^2 \sum_{\ell=1}^3 \{ & \sum_{j=1}^N 4 [A_{\ell j}^2 I_{0\ell}(\omega) + a_{\ell j}^2 I_{1\ell}(\omega)] \\
 & + 8 \sum_{j=1}^N \sum_{k=j+1}^N [A'_{1\ell} I_{0\ell}(\omega_j) + A'_{2\ell} I_{1\ell}(\omega_j) \\
 & + A'_{3\ell} I_{0\ell}(\omega_k) + A'_{4\ell} I_{1\ell}(\omega_k)] \} \quad (2.48)
 \end{aligned}$$

Employing Eqs. 2.8 and 2.14, the design response can now be written in terms of response spectrum values and peak factors as follows:

$$\begin{aligned}
 S_d^2 = C^2 \sum_{\ell=1}^3 \{ & \sum_{j=1}^N 4 [(A_{\ell j} R_{\ell d}(\omega_j)/C_{\ell d j})^2 \\
 & + (a_{\ell j} R_{\ell v}(\omega_j)/C_{\ell v j})^2] \\
 & + 8 \sum_{j=1}^N \sum_{k=j+1}^N [A'_{1\ell} (R_{\ell d}(\omega_j)/C_{\ell d j})^2 + A'_{2\ell} (R_{\ell v}(\omega_j)/C_{\ell v j})^2 \\
 & + A'_{3\ell} (R_{\ell d}(\omega_k)/C_{\ell d k})^2 + A'_{4\ell} (R_{\ell v}(\omega_k)/C_{\ell v k})^2] \} \quad (2.49)
 \end{aligned}$$

This equation defines the design response in terms of ground response spectrum values and modal response peak factors.

Here again, if the peak factors are assumed equal, Eq. 2.49 can be written as:

$$S_d^2 = \sum_{\ell=1}^3 S_{\ell}^2 \quad (2.50)$$

where  $S_{\ell}$  is defined as:

$$S_{\ell}^2 = \sum_{j=1}^N S_{\ell j}^2 + 2 \sum_{j=1}^N \sum_{k=j+1}^N S_{\ell jk} \quad (2.51)$$

in which

$$S_{\ell j}^2 = 4 [ \{A_{\ell j} R_{\ell d}(\omega_j)\}^2 + \{a_{\ell j} R_{\ell v}(\omega_j)\}^2 ] \quad (2.52)$$

$$S_{\ell jk} = 8 [ A'_{1\ell} R_{\ell d}^2(\omega_j) + A'_{2\ell} R_{\ell v}^2(\omega_j) + A'_{3\ell} R_{\ell d}^2(\omega_j) + A'_{4\ell} R_{\ell v}^2(\omega_j) ] \quad (2.53)$$

Eqs. 2.50-2.53 are similar to the Eqs. 2.16-2.19 for proportionally damped systems. Again the double summation terms in Eq. 2.51 represent the effect of correlation between modes. The correlation coefficient between two modes for the  $\ell^{\text{th}}$  excitation component is defined as follows:

$$\rho_{\ell jk} = S_{\ell jk} / S_{\ell j} S_{\ell k} \quad (2.54)$$

When more than one component is considered, this coefficient is defined as

$$\rho_{jk} = \frac{\sum_{\ell=1}^3 S_{\ell jk}}{\left(\sum_{\ell=1}^3 S_{\ell j}^2\right)^{1/2} \left(\sum_{\ell=1}^3 S_{\ell k}^2\right)^{1/2}} \quad (2.55)$$

where

$$S_{\ell j}^2 = A_{\ell j}^2 I_{0\ell}(\omega_j) + a_{\ell j}^2 I_{1\ell}(\omega_j) \quad (2.56)$$

$$S_{\ell jk} = A'_{1\ell} I_{0\ell}(\omega_j) + A'_{2\ell} I_{1\ell}(\omega_j) + A'_{3\ell} I_{0\ell}(\omega_k) + A'_{4\ell} I_{1\ell}(\omega_j) \quad (2.57)$$

Here, unlike the proportional systems, this correlation is seen to depend on the response quantity of interest. Thus, different response quantities could have different degrees of correlation in their modal responses.

Here again, the system shown in Fig. 2.1, but with non-proportional damping characteristics, was considered to obtain the modal correlation coefficients for the responses of story shear, torsional story moment and column bending moments. Results are presented in Tables 2.5 through 2.10. A scrutiny of these results shows that for low  $e/r$  values, the modal correlation is high. However, it changes drastically without any specific pattern when  $e/r$  becomes large. For example, see the values of the correlation coefficient bet-

ween modes 1 and 2 for story shear in the  $x_1$ - and  $x_2$ -directions for  $e/r=.05$ . Also, the values change, again not with any specific pattern, when two components of excitation are considered simultaneously. Thus modal correlation does not seem to hold the same significance in this case as it did for the proportionally damped systems. Thus a complete expression with all modes included in the summation should be used in Eq. 2.49 for the calculation of design response.

## 2.5 EVALUATION OF MODAL AND RESPONSE PEAK FACTORS

In the previous sections, response spectrum approaches for the calculation of design response of classically and nonclassically damped structures were described. These expressions, in general, require the peak factors  $C$ ,  $C_{\ell dj}$  and  $C_{\ell vj}$ . Here, the Vanmarcke's approach [42] used for the calculation of these factors is outlined.

In this approach, the peak factor  $C$  is obtained from the solution of the following equation:

$$\ln \left[ \frac{2n(1 - \exp(-\pi/2 \delta_e C))}{1 - \exp(-C^2/2)} \right] = \frac{C^2}{2} \quad (2.58)$$

where,

$$n = -\Omega s / (2\pi \ln(p)) \quad (2.59)$$

$$\delta_e = (1. - \Lambda_1^2 / \Lambda_0 \Lambda_2)^{0.6} = \delta^{1.2} \quad (2.60)$$

$$\Omega = \sqrt{\Lambda_2 / \Lambda_0} \quad (2.61)$$

in which  $s$  = duration of earthquake (equivalent stationary duration);  $p$  = probability that response will be less than the design response where the design response  $= C \sigma_0 = C \Lambda_0$ ; and  $\Lambda_m$  is the  $m^{\text{th}}$  spectral moment [43] defined as equal to

$$\Lambda_m = \int_{-\infty}^{+\infty} |\omega|^m \phi_R(\omega) d\omega \quad (2.62)$$

in which  $\phi_R(\omega)$  is the spectral density function of the response quantity for which the peak factor is being obtained.

The parameters  $\Omega$  and  $\delta$  are often referred to as the central frequency and band width parameters of the response, and these are defined in terms of the zero<sup>th</sup> (mean square value), 1<sup>st</sup> and 2<sup>nd</sup> moments of the response. However, if we want to use response spectra as input, it is not possible to define the 1<sup>st</sup> spectral moment. Thus here the bandwidth parameter is defined in terms of the 0<sup>th</sup>, 2<sup>nd</sup> and 4<sup>th</sup> moment as follows:

$$\delta = \sqrt{1. - \Lambda_2^2 / \Lambda_0 \Lambda_4} \quad (2.63)$$

This definition of bandwidth parameter was used by Longuet-Higgins [19]. This parameter has similar characteristics to the one defined by Vanmarcke, Eq. 2.60.

This approach requires that the spectral density function of the response quantity be known. If the spectral density function for the acceleration of the  $\ell^{\text{th}}$  component is  $\Phi_{\ell}(\omega)$ , then the spectral density functions for the relative displacement and relative velocity of an oscillator with frequency  $\omega_j$  and damping  $\beta_j$  can be written as:

$$\Phi_{\ell dj}(\omega) = \Phi_{\ell}(\omega) |H_j(\omega)|^2 \quad (2.64)$$

$$\Phi_{\ell vj}(\omega) = \omega^2 \Phi_{\ell}(\omega) |H_j(\omega)|^2 \quad (2.65)$$

where  $\Phi_{\ell dj}(\omega)$  and  $\Phi_{\ell vj}(\omega)$ , respectively, are the spectral density functions for relative displacement and relative velocity response. These density functions are used in the calculation of the  $C_{\ell dj}$  and  $C_{\ell vj}$  values by the approach described above.

To obtain  $C$ , the spectral density function of structural response is required. This density function can be easily identified from Eqs. 2.11 and 2.47, respectively, for the classically and nonclassically damped system as follows:

Classically Damped System:

$$\begin{aligned} \Phi_S(\omega) = & \sum_{\ell=1}^3 \left\{ \sum_{j=1}^N \xi_j^2 \gamma_{\ell j}^2 |H_j(\omega)|^2 \right. \\ & + 2 \sum_{j=1}^N \sum_{k=j+1}^N \xi_j \xi_k \gamma_{\ell j} \gamma_{\ell k} [(A_1 + \omega^2 A_2) |H_j(\omega)|^2 \\ & \left. + (A_3 + \omega^2 A_4) |H_k(\omega)|^2 \right] \} \Phi_{\ell}(\omega) \quad (2.66) \end{aligned}$$

Nonclassically Damped System:

$$\begin{aligned} \Phi_S(\omega) = & \sum_{\ell=1}^3 \left\{ \sum_{j=1}^N 4(A_{\ell j}^2 + \omega^2 a_{\ell j}^2) |H_j(\omega)|^2 \right. \\ & + 8 \sum_{j=1}^N \sum_{k=j+1}^N [(A'_{1\ell} + \omega^2 A'_{2\ell}) |H_j(\omega)|^2 \\ & \left. + (A'_{3\ell} + \omega^2 A'_{4\ell}) |H_k(\omega)|^2] \right\} \Phi_{\ell}(\omega) \quad (2.67) \end{aligned}$$

It is clearly seen that the spectral moments which are required in the calculation of  $C_{\ell dj}$  and  $C_{\ell vj}$  can be directly used to obtain the corresponding spectral moments for the response quantity  $S$  without explicitly knowing  $\Phi_S(\omega)$ . For example, the  $m^{\text{th}}$  spectral moment of response can be obtained from Eq. 2.62 as:

$$\Lambda_{sm} = \int_{-\infty}^{+\infty} |\omega|^m \Phi_S(\omega) d\omega \quad (2.68)$$

which, say, for a classically damped system can be written as:

$$\begin{aligned} \Lambda_{sm}(\omega) = & \sum_{\ell=1}^3 \left( \sum_{j=1}^N \xi_j^2 \gamma_{\ell j}^2 \Lambda_{\ell djm} \right. \\ & + 2 \sum_{j=1}^N \sum_{k=j+1}^N \xi_j \xi_k \gamma_{\ell j} \gamma_{\ell k} [A_1 \Lambda_{\ell djm} + A_2 \Lambda_{\ell vjm} \\ & \left. + A_3 \Lambda_{\ell dkm} + A_4 \Lambda_{\ell vkm}] \right) \quad (2.69) \end{aligned}$$

where  $\Lambda_{sm}$  is the  $m^{\text{th}}$  spectral moment of response  $S$ ; and  $\Lambda_{\ell djm}$  and  $\Lambda_{\ell vjm}$ , respectively, are the  $m^{\text{th}}$  spectral moments of displacement and velocity responses in the  $j^{\text{th}}$  mode for the  $\ell^{\text{th}}$  excitation component.

In actual practice, the spectral density function of the input motion will not be known. Thus, to obtain the peak factors some assumption about this will have to be made. To see how sensitive the response results are to this assumption, two different spectral density functions were employed for the calculation of peak factors. The Kanai-Tajimi [15,39] form, as defined by Eq. 2.73, and the easy-to-use white noise spectral density function with cut-off frequency of 30 cps. were used. An attempt was also made to use ground spectra in the calculation of peak factors. In this method the spectral moments of the modal responses were obtained in terms of response spectra. For example, the moments for the calculation of  $C_{\ell dj}$  were obtained as:

$$\Lambda_{\ell dj0} = k R_{\ell a}^2(\omega_j) \quad (2.70)$$

$$\Lambda_{\ell dj2} = k R_{\ell v}^2(\omega_j) \quad (2.71)$$

$$\Lambda_{\ell dj4} = k [A_g^2 - R_{\ell a}^2(\omega_j) + 2\omega_j^2(1-2\beta_j^2)R_{\ell v}^2(\omega_j)] \quad (2.72)$$

where  $A_g$  = maximum ground acceleration. Some problems were encountered in the evaluation of the moments of the relative

velocity in terms of response spectra. Here, thus,  $C_{\xi v_j}$  was assumed equal to  $C_{\xi d_j}$  in the numerical evaluation of the results. It is noted that the factor  $k$  appears both in the moments of response quantity  $S$  as well as in the moments of the modal responses. Thus it cancels out, and can be assumed equal to 1 without affecting the results.

For illustration purposes, the modal peak factor values obtained by this approach for the structure shown in Fig. 2.1 for the Kanai-Tajimi spectral density function, white noise spectral density function and smoothed response spectra, are shown in Table 2.11. It is seen that they are not drastically different from each other.

## 2.6 SIMULATION STUDY

In the development of the expressions for the design response, several simplifying assumptions were made. Probably the most questionable one is the assumption of stationarity of input and response. Also, the relationships between spectra and spectral density function and the procedure for the evaluation of peak factors have inherent assumptions. Thus, to verify the validity of these equations for the calculation of design response, a comprehensive simulation study has been conducted.

The simulation study consists of:

1. synthetic generation of an ensemble of earthquake motions with similar frequency content;
2. development of the mean and mean-plus-one-standard deviation values of the ground response spectra for the ensemble;
3. evaluation of the design response using the expression developed in previous sections for the seismic inputs defined by the spectra developed in step (2);
4. calculation of the maximum value of the structural response of interest by the step-by-step time history analysis method for the ensemble of time histories; and
5. calculation of mean and mean-plus-one-standard deviation values of the maximum response obtained in step (4).

The values obtained in step (3) with mean spectra as inputs are compared with the mean of the maximum value obtained in step (5); likewise the value with mean-plus-one-standard deviation spectra as input in step (3) are compared with the mean-plus-one-standard deviation values obtained in step (5). A good comparison of these values will verify the response evaluation procedure used in step (3), in spite of the assumption made in its derivation.

This comparison of the results has been made for structures with different properties, different input motion characteristic and different response quantities. The response quantities which have been considered in this study are the story shear, story torsional moment and column bending moments.

As broad-band response spectra [13,24,41] are used as seismic inputs for design purposes, the frequency content of the motions used in this study was also defined by a broad-band Kanai-Tajimi type of spectral density function of following form:

$$\ddot{\phi}(\omega) = \sum_{i=1}^3 s_i \left( \frac{\omega_i^4 + 4\beta_i^2 \omega_i^2 \omega^2}{(\omega_i^2 - \omega^2)^2 + 4\beta_i^2 \omega_i^2 \omega^2} \right) \quad -30 \leq \omega \leq 30 \text{ cps.} \quad (2.73)$$

The parameters,  $s_i$ ,  $\omega_i$  and  $\beta_i$  of this density function are given in Table 2.12. This density function has also been used in several earlier studies.

A sample function of ground motion with frequency characteristic defined by this density function can be generated as a summation of randomly phased harmonics according to the following expression[7]:

$$\ddot{X}'_g(t) = \sum_{k=1}^N s \left[ 4\phi_g(\omega_k) \Delta\omega \right]^{1/2} \text{Cos}(\omega_k t + \phi_k) \quad (2.74)$$

where  $N_s$  = number of harmonics,  $\omega_k = k \Delta\omega$ ,  $\Delta\omega$  = frequency interval size =  $\omega_c/N_s$ , and  $\phi_k$  are uniformly distributed random variables between 0 and  $2\pi$ .

Using Eq. 2.74, several independent sample function were obtained. To introduce nonstationarity, these time histories were modulated by an envelope function  $e(t)$  [1] as:

$$\ddot{X}_g(t) = e(t) \ddot{X}'_g(t) \quad (2.75)$$

Two different forms of  $e(t)$  were used and these are shown in Figs. 2.2. They essentially differ in the duration of their strong motion phase. Thus, this simulation study has been carried out for the two ensembles with their total and strong motion phase durations of (15,4) and (30,15) seconds. The first set has 75 time histories in its ensemble and is referred to as 15-sec. time history set. The second set had 39 time histories and is referred to as 30-sec. time history set. A typical sample function of the 15-sec. set is shown in Fig. 2.3. The mean and mean-plus-one-standard deviation psuedo-acceleration and relative velocity spectra for these sets are also shown in Figs. 2.4 through 2.11.

The step-by-step time history analysis methods used in step (4) of the simulation study for classically and non-classically damped systems are described in the following section.

## 2.7 TIME HISTORY ANALYSIS OF STRUCTURES

To solve Eq. 2.1, a numerical step-by-step integration procedure can always be used with any type of damping matrix [C]. The most commonly used step-by-step procedure is based on the assumption of linear variation of acceleration response between any two consecutive time steps of integration. The analysis becomes unstable and the solution blows up if the time step of integration is not small. Thus, the time step should be small enough so as not to cause any instability in the higher frequency or shorter period modes. Sometimes this can cause problems if the structure has many degrees of freedom and the highest frequency is very large. In such cases, unconditionally stable procedures like the Wilson- $\theta$  method [7] are most appropriate. These unconditionally stable procedures tend to damp out the higher modes completely, which may be desirable in some cases and undesirable in others. In most cases, however, these procedures can be successfully used. Yet, because they assume linear variation of acceleration response, these procedures are approximate.

For structures which behave linearly, another commonly used method is the mode superposition approach. The currently available approaches assume that the damping matrix [C] is classical; that is, it can be decoupled by the normal

modes. In such cases, each decoupled modal equation is solved either by the assumption of linear acceleration response as discussed in the previous paragraph or by the Duhamel's integral approach. The latter approach is exact in as much as no assumption such as the linear variation of response between two time steps is made. One such approach was proposed by Nigam and Jennings [25]. This approach has been used here for the time history analysis of proportionally damped systems. In this approach the recursive solution of the decoupled normal mode equation such as Eq. 2.2, defining the state vector at time step  $t_{i+1}$  in terms of the state vector at step  $t_i$ , for three excitation components can be written as follows:

$$\begin{pmatrix} V_j \\ \dot{V}_j \end{pmatrix}_{t_{i+1}} = \begin{bmatrix} A_{11} & A_{12} \\ A_{21} & A_{22} \end{bmatrix} \begin{pmatrix} V_j \\ \dot{V}_j \end{pmatrix}_{t_i} + \begin{bmatrix} B_{11} & B_{12} \\ B_{21} & B_{22} \end{bmatrix} \sum_{\ell=1}^3 \begin{pmatrix} \ddot{X}_\ell(t_i) \\ \ddot{X}_\ell(t_{i+1}) \end{pmatrix} \quad (2.76)$$

Where  $\ddot{X}_\ell(t) =$  acceleration at  $t_i$ ,  $\ddot{X}_\ell(t_{i+1}) =$  acceleration at  $t_{i+1}$  and the elements  $A_{11}$ ,  $B_{11}$ , etc. are defined in Reference 25.

Knowing the modal response time histories, the time histories of displacement  $\{u\}$  can be easily obtained by a simple mode superposition procedure. Other response quanti-

ties such as bending moment can also be obtained at each time step by simple linear transformation of  $\{u\}$ .

Often the modal superposition procedure is preferred, as it lends a greater flexibility and control over the step-by-step time history integration of each modal equation. If it is considered appropriate, costly numerical integration of higher mode equations with smaller time steps can be avoided if the higher modes are known to contribute insignificantly to the calculated response. Also, if the higher modes are to be included, then only their own equations need to be solved with shorter time steps and the other modal equations can still be integrated with larger time steps.

To take advantage of these attributes of the modal analysis approach, and also to obtain results which will be comparable to the design response results obtained from Eqs. 2.48 and 2.50, which necessarily employ the modal analysis techniques, here a new modal step-by-step time history integration approach has been developed for the calculation of the response of nonclassically damped systems. This approach as described in the following section, is mathematically exact as no assumption about the variation of response, like the linearity of acceleration response between two consecutive time steps, is made.

### 2.7.1 TIME INTEGRATION OF NONCLASSICALLY DAMPED STRUCTURES

For nonclassically damped systems, a numerical integration approach employing Fourier transforms was described by Itoh [14]. Another approach in which coupled equations are analyzed was presented by Clough and Mojtahedi [6]. Here a different modal time history integration scheme is described.

In this approach, Eq. 2.1 is first decoupled into 2N-modal equations such as Eq. 2.27. The complete solution of this equation will consist of the homogeneous solution plus a particular solution as:

$$Z_j = Z_{jh} + Z_{jp} \quad (2.77)$$

where  $Z_{jh}$  and  $Z_{jp}$  are the homogeneous and the particular solutions, respectively. The homogeneous solution of Eq. 2.27 can be written as:

$$Z_{jh} = c_j e^{p_j t} \quad (2.78)$$

where  $c_j$  = constant of integration. The particular solution,  $Z_{jp}$ , can be obtained by any standard integration technique. For example, the general form of the particular solution, using the variation of parameter technique, can be written as:

$$Z_{jp} = \sum_{\ell=1}^3 F_{\ell j} \int_0^t \ddot{X}_{\ell}(\tau) e^{p_j(t-\tau)} d\tau \quad (2.79)$$

However, for the digitized time history as shown in Fig. 2.12 with linear variation between two consecutive time steps, an alternative approach to obtain the particular solution may be algebraically more convenient. The acceleration  $\ddot{X}_\ell(t)$  for the  $i^{\text{th}}$  step between the  $i^{\text{th}}$  and  $(i+1)^{\text{th}}$  discrete points of the time history can be written as follows:

$$\ddot{X}_\ell(t) = \ddot{X}_\ell(t_i) + \frac{1}{h}[\ddot{X}_\ell(t_{i+1}) - \ddot{X}_\ell(t_i)] t \quad (2.80)$$

where  $t$  is measured from  $t_i$  and  $h$  is the size of the time step. Substituting Eq. 2.80 into Eq. 2.27, the modal equation becomes:

$$\dot{Z}_j - p_j Z_j = \sum_{\ell=1}^3 F_{\ell j} (a_\ell + b_\ell t) \quad (2.81)$$

where

$$a_\ell = \ddot{X}_\ell(t_i) \quad (2.82)$$

$$b_\ell = [\ddot{X}_\ell(t_{i+1}) - \ddot{X}_\ell(t_i)]/h \quad (2.83)$$

The particular solution corresponding to such a forcing function in the  $x_\ell$ -direction can be obtained by the method of undetermined coefficients as:

$$Z_{\ell j p} = F_{\ell j} \{ b_\ell + p_j(a_\ell + b_\ell t) \} / p_j^2 \quad (2.84)$$

The complete solution of Eq. 2.79 can thus be written as:

$$Z_j = c_j e^{p_j t} + \sum_{\ell=1}^3 [F_{\ell j} \{b_{\ell} + p_j (a_{\ell} + b_{\ell} t) / p_j^2\}] \quad (2.85)$$

To obtain  $c_j$ , the initial condition on  $Z_j$  at the beginning of the time step will be used. Thus at  $t=0$ , Eq. 2.85 gives:

$$c_j = Z_j(t=0) - \sum_{\ell=1}^3 F_{\ell j} (b_{\ell} + p_j a_{\ell}) / p_j^2 \quad (2.86)$$

where  $Z_j(t=0)$  is the same as  $Z_j$  at time step  $t_i$ , i.e.,  $Z_j(t_i)$ . Using Eqs. 2.85 and 2.86, the solution at the end of the time step  $t=h$ , that is  $(t_{i+1})$ , can be obtained as:

$$Z_j(t_{i+1}) = \{Z_j(t_i) - \sum_{\ell=1}^3 F_{\ell j} (b_{\ell} + p_j a_{\ell}) / p_j^2\} e^{p_j h} - \sum_{\ell=1}^3 F_{\ell j} \{b_{\ell} + p_j (a_{\ell} + b_{\ell} h)\} / p_j^2 \quad (2.87)$$

Thus, knowing the solution  $Z_j(t_i)$  at the beginning of a time step, the solution at  $Z_j(t_{i+1})$  at the end of the step can be obtained from Eq. 2.87. A complete solution of Eq. 2.81 at all discrete time points can be obtained for a digitized acceleration time history if the initial value of  $Z_j$  in the first step is known.

To obtain the initial value of  $Z_j$  in terms of the response  $\{u\}$  and  $\{\dot{u}\}$  of the system, Eq. 2.26 is used. For example, if the system was in motion with certain initial velocity and displacement at the start, i.e.,

$$\{y\}_{t=0} = \begin{Bmatrix} \{\dot{u}\} \\ \{u\} \end{Bmatrix}_{t=0} \quad (2.88)$$

the initial value of  $Z_j$  at  $t=0$  can be obtained from Eq. 2.25 as follows:

$$[\phi]\{Z\}_{t=0} = \{y\}_{t=0} \quad (2.89)$$

Premultiplying by  $[\phi]^T[A]$ , and using the orthogonality of complex modes with respect to  $[A]$ , we obtain:

$$Z_j(t=0) = \{\phi_j\}^T[A]\{y\}_{t=0} / A_j^* \quad (2.90)$$

The variables and constants in Eq. 2.87 are complex quantities. However, a recursive scheme to obtain real and imaginary parts of  $Z_j$  at any time step can also be devised.

Expressing the complex quantities in Eq. 2.87 in terms of their real and imaginary parts as

$$\left. \begin{aligned} Z_j(t_i) &= Z_{Rj}(t_i) + i Z_{Ij}(t_i) \\ Z_j(t_{i+1}) &= Z_{Rj}(t_{i+1}) + i Z_{Ij}(t_{i+1}) \\ p_j &= -\beta_j \omega_j + i \omega_j \sqrt{1 - \beta_j^2} = -\beta_j \omega_j + i \omega_{dj} \\ F_{\ell j}/p_j &= c_{\ell j} + i d_{\ell j} \\ F_{\ell j}/p_j^2 &= e_{\ell j} + i f_{\ell j} \end{aligned} \right\} \quad (2.91)$$

and substituting in Eq. 2.87, it can be written as:

$$\begin{aligned}
Z_{Rj}(t_{i+1}) + iZ_{Ij}(t_{i+1}) = & \\
e^{-\beta_j \omega_j h} [\cos(\omega_{dj} h) + i \sin(\omega_{dj} h)] [Z_{Rj}(t_i) + iZ_{Ij}(t_i)] & \\
+ \sum_{\ell=1}^3 \{ (e_{\ell j} + i f_{\ell j}) [\ddot{X}_{\ell}(t_{i+1}) - \ddot{X}_{\ell}(t_i)]/h + (c_{\ell j} + d_{\ell j}) \ddot{X}_{\ell}(t_i) \} & \\
- \sum_{\ell=1}^3 \{ (e_{\ell j} + i f_{\ell j}) [\ddot{X}_{\ell}(t_{i+1}) - \ddot{X}_{\ell}(t_i)]/h - (c_{\ell j} + d_{\ell j}) \ddot{X}_{\ell}(t_i) \} & \\
\end{aligned} \tag{2.92}$$

Comparing the real and imaginary parts in Eq. 2.92, two simultaneous equations are obtained to obtain  $Z_{Rj}$  and  $Z_{Ij}$  at  $t = t_{i+1}$ . These equations can be written in the following matrix form:

$$\begin{aligned}
\begin{Bmatrix} Z_{Rj} \\ Z_{Ij} \end{Bmatrix}_{t_{i+1}} = \begin{bmatrix} A_{11} & A_{12} \\ A_{21} & A_{22} \end{bmatrix} \begin{Bmatrix} Z_{Rj} \\ Z_{Ij} \end{Bmatrix}_{t_i} & \\
+ \sum_{\ell=1}^3 \begin{bmatrix} B_{11}^{(\ell)} & B_{12}^{(\ell)} \\ B_{21}^{(\ell)} & B_{22}^{(\ell)} \end{bmatrix} \begin{Bmatrix} \ddot{X}_{\ell}(t_i) \\ \ddot{X}_{\ell}(t_{i+1}) \end{Bmatrix} & \\
\end{aligned} \tag{2.93}$$

where the elements of the two matrices are defined as follows:

$$A_{11} = e^{-\beta_j \omega_j h} \text{Cos}(\omega_{dj} h) \quad (2.94)$$

$$A_{12} = -e^{-\beta_j \omega_j h} \text{Sin}(\omega_{dj} h) \quad (2.95)$$

$$A_{21} = e^{-\beta_j \omega_j h} \text{Sin}(\omega_{dj} h) \quad (2.96)$$

$$A_{22} = e^{-\beta_j \omega_j h} \text{Cos}(\omega_{dj} h) \quad (2.97)$$

$$B_{11}^{(\ell)} = e^{-\beta_j \omega_j h} [(c_{\ell j} - e_{\ell j}/h) \text{Cos}(\omega_{dj} h) - (d_{\ell j} - f_{\ell j}/h) \text{Sin}(\omega_{dj} h)] \\ + e_{\ell j}/h \quad (2.98)$$

$$B_{12}^{(\ell)} = e^{-\beta_j \omega_j h} [e_{\ell j} \text{Cos}(\omega_{dj} h) - f_{\ell j} \text{Sin}(\omega_{dj} h)]/h \\ - (c_{\ell j} + e_{\ell j}/h) \quad (2.99)$$

$$B_{21}^{(\ell)} = e^{-\beta_j \omega_j h} [(c_{\ell j} - e_{\ell j}/h) \text{Sin}(\omega_{dj} h) + (d_{\ell j} - f_{\ell j}/h) \text{Cos}(\omega_{dj} h)] \\ + f_{\ell j}/h \quad (2.100)$$

$$B_{22}^{(\ell)} = e^{-\beta_j \omega_j h} [e_{\ell j} \text{Sin}(\omega_{dj} h) + f_{\ell j} \text{Cos}(\omega_{dj} h)]/h \\ - (d_{\ell j} + f_{\ell j}/h) \quad (2.101)$$

Eqs. 2.93 define the recursive solution of Eq. 2.27. The solution marches from  $t=0$  to the last discretized time step.

### 2.7.2 DISPLACEMENT AND MEMBER RESPONSE OF NONCLASSICALLY DAMPED STRUCTURES

Eq. 2.93 defines the complex valued principal coordinates at discrete time steps. In terms of this solution the other response quantities like displacements  $\{u\}$  and member forces,  $S(t)$ , which are linearly related to  $\{u\}$  can also be obtained. For example, a response quantity can be written in terms of  $Z_j$  as:

$$S(t) = \sum_{j=1}^{2N} g_j Z_j \quad (2.102)$$

where  $g_j$  is the modal value of the response quantity defined by Eq. 2.33, with its real and imaginary parts as:

$$g_j = g_{Rj} + i g_{Ij} \quad (2.103)$$

Combining the complex and conjugate pairs

$$S(t) = \sum_{j=1}^N (g_j Z_j + g_j^* Z_j^*) \quad (2.104)$$

Substituting in terms of real and imaginary parts

$$S(t) = \sum_{j=1}^N (g_{Rj} + i g_{Ij})(Z_R + i Z_I) + (g_{Rj} - i g_{Ij})(Z_R - i Z_I) \quad (2.105)$$

$$S(t) = 2 \sum_{j=1}^N (g_{Rj} Z_{Rj} - g_{Ij} Z_{Ij}) \quad (2.106)$$

To verify the correctness of the formulation of this new procedure for nonclassically damped structural systems, a classically damped structure was analyzed by this method

and the Nigam and Jennings' approach, Eq. 2.76, discussed in the earlier part of the section. The two approaches provided exactly the same response values. This cross-validated the two approaches.

To further cross check the method numerically, another slightly different formulation which obtained the particular solution by Eq. 2.79 was developed. The details of this formulation are given in Appendix A. The numerical results obtained by these two methods for the same system again gave exactly the same results, thus further validating this new numerical integration scheme.

## 2.8 NUMERICAL RESULTS

For the verification of the response spectrum (RS) approaches presented in the previous sections, the numerical results have been obtained for a three-story torsional building and a stick model with 10 lumped masses.

The torsional building consists of three rigid floor slabs connected by four corner columns. The mass centers of the slabs and stiffness centers of the stiffness elements provided by the column have been displaced to cause a torsional moment. The damping is provided by the dampers in the  $x_1$ - and  $x_2$  directions. By adjusting the stiffness, eccentricity between mass and stiffness centers and damping

values, a variety of structural systems with different dynamic characteristics can be created. For example, by adjusting the lateral and torsional stiffnesses and eccentricity between the mass and stiffness centers, a structural system with well separated to closely spaced frequencies can be created. For closely spaced modal frequencies, modal correlation is high as was shown in Sections 2.3 and 2.4. Also, by adjusting the damping values in the  $x_1$ - and  $x_2$  directions a varying degree of nonproportional damping effect can be introduced in the damping matrix of the structure.

The system with three eccentricity ratio parameters has been considered:  $e/r=.01$ ,  $.05$  and  $.30$ . Here,  $e$  = eccentricity between the mass and stiffness centers and  $r$  = radius of gyration of the slab mass. The modal frequencies, damping ratios and participation factors for the proportionally damped system are shown in Tables 2.1 and 2.2 for two systems with  $e/r=.01$  and  $.05$  under the columns of normal modes. For nonproportionally damped systems, the frequencies and damping ratios are defined by Eqs. 2.39. These values are shown in the same tables under the columns of complex modes. It is seen that for  $e/r=.01$ , the modal frequencies are closely spaced.

The numerical values have been obtained for the base story shears in the  $x_1$ - and  $x_2$  directions, base story tor-

sional moment and column bending moment about the  $x_1$  and  $x_2$  axes in one of the columns of the base story. The results have been obtained for 15- and 30-sec. time history ensembles, with mean as well as mean-plus-one-standard deviation (mean+1 sdv) spectra of the ensembles. The results have also been obtained for excitation applied in one as well as in two directions.

The results are shown in Tables 2.13 through 2.34. The results obtained under the normal mode section employ undamped normal modes of the structure with modal damping values defined in section 2.3. Thus, here the off-diagonal terms of  $[\phi]^T[C][\phi]$  were ignored. The results in the time history analysis were obtained with these modal parameters, using the modal time history analysis approach described in section 2.6. These are shown in Column (2) of the tables. The results in Column (3) were obtained by the response spectrum (RS) approaches, Eq. 2.17, which assumes the peak factors to be equal. For the results in Columns (4), (5) and (6), Eq. 2.15 was used which includes the modal and response peak factors. To obtain the peak factors, three different forms of input were used: Kanai-Tajimi spectral density function, white noise spectral density function and the response spectra of the ensemble. The response results in Column (3) through (6) are shown in the ratio forms. That

is, they are the ratios of the results obtained by the Eq. 2.17 or Eq. 2.15 divided by the time history ensemble results.

The results shown in the section of the complex modes are obtained by the  $2N$ -dimensional state vector approach. For the results in Column (3), Eq. 2.51 without peak factors was used, whereas for the results in Columns (4), (5) and (6), Eq. 2.49 was used.

The lower part of each table, entitled percent error, shows the difference between the results obtained by the normal and complex mode approaches. It shows the effect of the assumption of proportionality of damping matrix when in fact it is not. The differences between the results for the the normal and complex mode approaches obtained by the time history analyses are, approximately, of the same magnitude as the results obtained by the response spectrum analyses. Also, in most cases this difference is larger when the frequencies are closely spaced as is seen from the results in the tables for  $e/r=.01$  and becomes small when the frequencies are well separated as in the tables for  $e/r=.30$ .

The results obtained for a simple stick model, which has well separated frequencies, are also obtained. This 10 story shear structure with 10 degrees-of-freedom is shown in Fig. 2.13. The frequencies and damping ratios are shown in Table 2.35. Tables 2.36 and 2.37 show comparative results

for the total shear force at each story obtained by time history analysis and by the normal modes approach.

Tables 2.13 through 2.26, 2.36 and 2.37 are for the mean of the maximum response and tables 2.27 through 2.34 are for the mean-plus-one-standard deviation of the maximum response. Also, the results for one as well as two excitation components are shown in the tables. Almost half of the tables are for 15-sec. time history ensemble inputs and the remaining ones are for the 30-sec. time histories inputs.

A general comparison of the results obtained by the time history analysis and response spectrum approaches shows a rather good agreement. The response spectrum approaches which consider peak factors seem to give better results for small and large eccentricities. For  $e/r=.05$ , the results obtained by the response spectrum are in general lower than time history results for the response quantities in the direction of the excitation (e.g.  $x_1$ - base shear, and bending moment along the  $x_1$ -direction). Whereas, the base shear in the direction orthogonal to the direction of excitation, as well as the torsional moment, are over estimated by the response spectrum approach (e.g., Tables 2.17 and 2.18). However, when two components of excitation are considered, the response spectrum approach gives a very good comparison with the time history results.

In most cases it was noticed that the comparison between the time history and response spectrum approaches improves when peak factors are included, although there are some cases where this is not necessarily true. For column bending moment response in the  $x_2$ -direction, some problems were encountered in the calculation of the peak factor value. These were the limiting cases for which Vanmarcke's approach is not applicable. The problem values are shown by '---' in the Tables.

These observations are in general true for the mean and mean-plus-one-standard deviation results. This means that the response spectrum approach will predict accurate design response for any percentile spectra used as seismic inputs. In practice the mean-plus-one-standard deviation spectra are usually prescribed as design inputs [24,41].

To see which input for peak factor evaluation provided better response, the mean and coefficient of variation of the ratios reported in Columns (4), (5) and (6) of the Tables 2.13-2.34 are obtained and shown in Table 2.38. It is seen that on an average all three inputs led to a good estimate of maximum response when compared with the time history ensemble results. Out of the three, the response spectrum and white noise inputs provided a little better comparison than the Kanai-Tajimi input. As white noise is quite easy to use, its use is recommended for the calculation of peak

factors in the evaluation of design response by the response spectrum approach.

## Chapter III

### RESPONSE FOR SIX CORRELATED EARTHQUAKE COMPONENTS BY MODE DISPLACEMENT APPROACH

#### 3.1 INTRODUCTION

In Chapter 2, the structural response for only uncorrelated translational earthquake components acting along the structural axes was considered. In reality, however, a structure will experience all six components: three translational and three rotational components of an earthquake. Also, these components will in general be correlated with each other. In this chapter, the methods are developed to obtain design response for such six correlated earthquake components.

Penzien, et al. [16,17,26,27] have investigated the correlative character of the translational ground motion components in a series of papers. They have opined that there exists a set of orthogonal directions along which the components are uncorrelated. These directions were called the principal directions of excitation. The direction corresponding to the most intense excitation was called the major principal excitation axis, and the other two directions were designated as intermediate and minor principal excitation axes. It was also observed that the epicentral direction

and the major principal axis tend to coincide, though this tendency was not very strong.

Here it is assumed that such principal excitation axes do exist and remain fixed during an earthquake. In general they will not be fixed as the contribution of different types of waves to an earthquake motion will change as the motion progresses with time. Consideration of such changing principal directions in the calculation of design response seems mathematically and practically impossible at this moment. We will, therefore, assume that the principal excitation axes are fixed.

For an arbitrary orientation of a structure with respect to the principal excitation axes, the motions components experienced along the structural axes will be correlated. Here the effect of this correlation is included in the calculation of response.

For design purposes, we are interested in the evaluation of maximum response, irrespective of the direction of impinging ground motions. Here, a method is developed to obtain this maximum response in terms of response spectra of principal components and structural properties.

In Section 3.2, the relationships between the principal components and the translational and rotational components as experienced by a structure are established. This is fol-

lowed by a development of the correlation matrix of the excitation components in Section 3.3. This correlation matrix is then used in Section 3.4 to define the mean square and design responses for a given orientation of the structure. Section 3.5 is devoted to the development of a method to obtain the maximum response, followed by Section 3.6, giving the numerical results for the structures subjected to two and three principal components. These results include the effect of the rotational components.

### 3.2 CORRELATED AND UNCORRELATED EARTHQUAKE COMPONENTS

Let the primed coordinate axes,  $x'_1$ ,  $x'_2$  and  $x'_3$ , be along the geometric axes of the structure, as shown in Fig. 3.1. The principal excitation axes are shown by the unprimed set  $x_1$ ,  $x_2$  and  $x_3$  along which the acceleration components  $\ddot{X}_1$ ,  $\ddot{X}_2$  and  $\ddot{X}_3$ , respectively, are uncorrelated. By a simple geometric transformation, the acceleration components  $\ddot{X}'_1$ ,  $\ddot{X}'_2$  and  $\ddot{X}'_3$  along the structural axes can be defined in terms of uncorrelated components as:

$$\{E'_1\} = [D]^T \{E\} \quad (3.1)$$

where  $\{E'_1\}$  = the vector of excitation components along the structural axes,  $\{E\}$  = the vector of uncorrelated or principal excitation components and  $[D]$  = the matrix of direction cosines, all defined as:

$$\{E'_1\} = \begin{Bmatrix} \ddot{X}'_1 \\ \ddot{X}'_2 \\ \ddot{X}'_3 \end{Bmatrix}; \quad \{E\} = \begin{Bmatrix} \ddot{X}_1 \\ \ddot{X}_2 \\ \ddot{X}_3 \end{Bmatrix} \quad \text{and} \quad [D] = \begin{bmatrix} d_{11} & d_{12} & d_{13} \\ d_{21} & d_{22} & d_{23} \\ d_{31} & d_{32} & d_{33} \end{bmatrix} \quad (3.2)$$

in which  $d_{mn}$  = the direction cosine of the  $m^{\text{th}}$  principal excitation axis with respect to the  $n^{\text{th}}$  structural axes.

Very few studies in earthquake engineering have considered the rotational components of ground excitations. We believe, Newmark [23] was the first person to consider the rotational effects of ground motions. He related the rotational excitation to the translational components and defined the ground spectrum for rotational components. Later on, Rosenblueth [28,29], Nathan and Mackenzie [22] and Tso and Hsu [40] have also considered the effects of the rotational components on buildings in their investigations. In this section, Newmark's approach [23] is used to define the three rotational components of excitation.

To define the instantaneous values of the rotational components of excitation, the following relationship between the translational and rotational deformations is used:

$$\Psi_k(t) = [\partial X'_j / \partial x'_i - \partial X'_i / \partial x'_j] / 2 \quad (i \neq j \neq k) \quad (3.3)$$

where  $i$ ,  $j$  and  $k$  denote the axes,  $\Psi_k(t)$  = the rotation about the  $k$ -axis, expressed in terms of the spatial derivatives of displacements  $X'_i$  and  $X'_j$ .

The earthquake motions occur due to propagation of waves through the earth's crust. Usually, there will be several types of waves mixed in a motion. However, we will assume that the motion at a site has only one predominant wave which propagates with the wave frequency  $\omega$ . The ground displacements along the coordinate axes can then be written as:

$$X_i' = A_i f\left(\sum_{j=1}^3 k_j x_j' - \omega t\right) \quad (3.4)$$

where  $k_j$  is the wave number or the number of wave lengths contained in  $2\pi$  radius associated with direction  $j$ . In earthquake structural engineering, Bogdanoff, Goldberg and Schiff [4] were the first ones to use the wave-form representation for the earthquake induced ground motions to study the travelling waves effect on long structures such as bridges.

Eq. 3.4 is used to define the spatial derivatives required in Eq. 3.3 as follows:

$$\partial X_i' / \partial x_j' = A_i k_j f' \quad (3.5)$$

where  $f'(u)$  denotes the functional derivative of  $f(u)$  with respect to  $u$ . This derivative, however, can also be defined alternatively in terms of the time derivative as follows:

$$dX_i' / dt = - A_i \omega f' \quad (3.6)$$

Thus, from Eq. 3.5

$$\partial X_i' / \partial x_j' = - \frac{k_j}{\omega} dX_i' / dt \quad (3.7)$$

Substituting for  $\omega/k_j = c_j =$  shear wave velocity in direction  $j$ , we obtain:

$$\partial X_i' / \partial x_j' = - \frac{1}{c_j} dX_i' / dt \quad (3.8)$$

The shear wave velocities could be different in different directions. For simplicity, however, we will assume that these velocities are the same in all directions and are equal to  $c$ . Substituting in Eq. 3.3 and differentiating with respect to time twice, we obtain the expression for the rotational acceleration as follows:

$$\ddot{\psi}_k(t) = - \frac{1}{2c} \frac{d}{dt} [\ddot{X}_j'(t) - \ddot{X}_i'(t)] \quad (3.9)$$

Thus, a rotational acceleration component is related to the jerks of displacement components in the plane of rotation. Using Eq. 3.9, the three components of rotational acceleration felt by a structure can be written as:

$$\ddot{\psi}_1(t) = - \frac{1}{2cdt} [\ddot{X}_3'(t) - \ddot{X}_2'(t)] \quad (3.10a)$$

$$\ddot{\psi}_2(t) = - \frac{1}{2cdt} [\ddot{X}_1'(t) - \ddot{X}_3'(t)] \quad (3.10b)$$

$$\ddot{\psi}_3(t) = - \frac{1}{2cdt} [\ddot{X}_2'(t) - \ddot{X}_1'(t)] \quad (3.10c)$$

or in matrix form:

$$\begin{Bmatrix} \ddot{\Psi}_1 \\ \ddot{\Psi}_2 \\ \ddot{\Psi}_3 \end{Bmatrix} = -\frac{1}{2c} \frac{d}{dt} \begin{bmatrix} 0 & -1 & 1 \\ 1 & 0 & -1 \\ -1 & 1 & 0 \end{bmatrix} \begin{Bmatrix} \ddot{X}_1' \\ \ddot{X}_2' \\ \ddot{X}_3' \end{Bmatrix} \quad (3.11)$$

Substituting for the excitation vector  $\{E_1\}$  from Eq. 3.1, we obtain,

$$\begin{Bmatrix} \ddot{\Psi}_1 \\ \ddot{\Psi}_2 \\ \ddot{\Psi}_3 \end{Bmatrix} = [G_1'] [D]^T \{E\} \quad (3.12)$$

where  $[G_1']$  denotes the 3x3 matrix in Eq. 3.11. Consolidating Eqs. 3.1 and 3.12, the matrix representation of the six components of the excitation, applied along the structural axes, in terms of principal components is as follows:

$$\{E'(t)\} = [T]^T [D]^T \{E(t)\} \quad (3.13)$$

where  $\{E'\} = \{\ddot{X}_1' \ \ddot{X}_2' \ \ddot{X}_3' \ \ddot{\Psi}_1 \ \ddot{\Psi}_2 \ \ddot{\Psi}_3\}^T$  is the vector of excitation components acting along the structural axes and  $[T]$  is the time derivative operator matrix defined as:

$$[T] = \begin{bmatrix} 1 & 0 & 0 & 0 & \frac{-1}{2c} \frac{\partial}{\partial t} & \frac{1}{2c} \frac{\partial}{\partial t} \\ 0 & 1 & 0 & \frac{1}{2c} \frac{\partial}{\partial t} & 0 & \frac{-1}{2c} \frac{\partial}{\partial t} \\ 0 & 0 & 1 & \frac{-1}{2c} \frac{\partial}{\partial t} & \frac{1}{2c} \frac{\partial}{\partial t} & 0 \end{bmatrix} \quad (3.14)$$

It is analytically expedient to decompose matrix [T] into two constant matrices as:

$$[T] = [G_1] + \frac{1}{2c} \frac{\partial}{\partial t} [G_2] \quad (3.15)$$

where [G<sub>1</sub>] and [G<sub>2</sub>] are the constant transformation matrices, defined as follows:

$$[G_1] = \begin{bmatrix} 1 & 0 & 0 & 0 & 0 & 0 \\ 0 & 1 & 0 & 0 & 0 & 0 \\ 0 & 0 & 1 & 0 & 0 & 0 \end{bmatrix} \quad (3.16a)$$

$$[G_2] = \begin{bmatrix} 0 & 0 & 0 & 0 & -1 & 1 \\ 0 & 0 & 0 & 1 & 0 & -1 \\ 0 & 0 & 0 & -1 & 1 & 0 \end{bmatrix} \quad (3.16b)$$

Using Eq. 3.15 in Eq. 3.13, we obtain

$$\{E'(T)\} = ([G_1]^T + \frac{1}{2c} \frac{\partial}{\partial t} [G_2]^T) [D]^T \{E(t)\} \quad (3.17)$$

This form of excitation will be used to evaluate the structural response.

### 3.3 CORRELATION MATRIX OF EXCITATIONS

In the evaluation of design response, we will need the autocorrelation and cross-correlation functions of the excitation components. These are developed in this section. Using Eq. 3.17, the correlation matrix of  $\{E'(t)\}$  can be written as:

$$\begin{aligned} \text{Ex}[\{E'(t_1)\}\{E'(t_2)\}^T] &= ([G_1]^T + \frac{1}{2c} \frac{\partial}{\partial t_1} [G_2]^T) [D]^T \\ \text{Ex}[\{E(t_1)\}\{E(t_2)\}^T] [D] &= ([G_1] + \frac{1}{2c} \frac{\partial}{\partial t_2} [G_2]) \end{aligned} \quad (3.18)$$

in which the correlation matrix of the principal excitation components is a diagonal matrix, as each component of the excitation is a zero mean random process and is uncorrelated with the other components. As discussed in Chapter 2, we will assume that these components can be represented by stationary random processes. Thus, the correlation matrix of principal excitation components can be written in terms of their spectral density functions as follows:

$$\text{Ex}[\{E(t_1)\}\{E(t_2)\}^T] = \int_{-\infty}^{+\infty} [\Phi] e^{i\omega(t_1-t_2)} d\omega \quad (3.19)$$

where  $[\Phi]$  is a diagonal matrix of the spectral density functions, defined as:

$$[\Phi] = \begin{bmatrix} \Phi_1(\omega) & 0 & 0 \\ 0 & \Phi_2(\omega) & 0 \\ 0 & 0 & \Phi_3(\omega) \end{bmatrix} \quad (3.20)$$

$\phi_\ell(\omega)$  is the spectral density function of the  $\ell^{\text{th}}$  principal excitation component. Substituting Eq. 3.19 into Eq. 3.18, we obtain:

$$\begin{aligned} \text{Ex}[\{E'(t_1)\}\{E'(t_2)\}^T] &= \int_{-\infty}^{+\infty} e^{i\omega(t_1-t_2)} \\ &([G_1]^T + \frac{1}{2c\partial t_1} [G_2]^T) [D]^T [\Phi] [D] ([G_1] + \frac{1}{2c\partial t_2} [G_2]) d\omega \end{aligned} \quad (3.21)$$

It is seen that since  $[\Phi]$  is a diagonal matrix, the matrix product  $[D]^T [\Phi] [D]$  in Eq. 3.21 can be written as:

$$\begin{aligned} [D]^T [\Phi] [D] &= \\ &\begin{bmatrix} \{d_1\} & \{d_2\} & \{d_3\} \end{bmatrix} \begin{bmatrix} \phi_1(\omega) & 0 & 0 \\ 0 & \phi_2(\omega) & 0 \\ 0 & 0 & \phi_3(\omega) \end{bmatrix} \begin{bmatrix} \{d_1\}^T & \{d_2\}^T & \{d_3\}^T \end{bmatrix} \\ &= \sum_{\ell=1}^3 \{d_\ell\} \phi_\ell(\omega) \{d_\ell\}^T \end{aligned} \quad (3.22)$$

where  $\{d_\ell\} = \ell^{\text{th}}$  row of the coordinate transformation matrix  $[D]$  which consists of the direction cosines of the  $\ell^{\text{th}}$  principal excitation axes in the primed coordinates. Substituting Eq. 3.22 back into Eq. 3.21, and taking the proper time derivative, the correlation matrix for the six excitation components can be written as:

$$\begin{aligned}
\text{Ex}[\{E'(t_1)\}\{E'(t_2)\}^T] &= \sum_{\ell=1}^3 \int_{-\infty}^{+\infty} \Phi_{\ell}(\omega) e^{i\omega(t_1-t_2)} \\
&\{ [G_1]^T \{d_{\ell}\} \{d_{\ell}\}^T [G_1] + \frac{\omega^2}{4c^2} [G_2]^T \{d_{\ell}\} \{d_{\ell}\}^T [G_2] \\
&- \frac{i\omega}{2c} ([G_1]^T \{d_{\ell}\} \{d_{\ell}\}^T [G_2] - [G_2]^T \{d_{\ell}\} \{d_{\ell}\}^T [G_1]) \} d\omega
\end{aligned} \tag{3.23}$$

The first and second terms in the above equation are the autocorrelation functions of the translational and rotational components, respectively. The third term, associated with the imaginary quantity, represents the cross-correlation between translational and rotational components. Eq. 3.23 is used in the calculation of the design response.

### 3.4 STRUCTURAL RESPONSE

The equations of motion of a multi degrees-of-freedom structural system, subjected to an input defined by Eq. 3.17 as follows:

$$[M]\{\ddot{u}\} + [C]\{\dot{u}\} + [K]\{u\} = - [M][r]\{E'(t)\} \tag{3.24}$$

Here,  $[r]$  is the influence coefficient matrix of order  $N \times 6$ , with its  $\ell^{\text{th}}$  column,  $\{r_{\ell}\}$ , being the ground displacement influence vector for the  $\ell^{\text{th}}$  component.

As we are primarily interested in the evaluation of design response for seismic inputs prescribed in terms of

ground response spectra, it is necessary to use the modal analysis approach. The following formulations are, therefore, developed in terms of the modal responses.

### 3.4.1 CLASSICALLY DAMPED STRUCTURES

As in Eq. 2.3, a response quantity of design interest,  $S(t)$ , can be written in terms of the modal quantities as:

$$S(t) = \sum_{j=1}^N \xi_j \{\gamma_j\}^T \int_0^t \{E'(\tau)\} h_j(t-\tau) d\tau \quad (3.25)$$

where  $\xi_j$ ,  $\{\gamma_j\}$  and  $h_j(t)$  are the same as defined in Chapter 2. The autocorrelation function of  $S(t)$  can be written as:

$$\text{Ex}[S(t_1)S(t_2)] =$$

$$\sum_{j=1}^N \sum_{k=1}^N (\xi_j \xi_k) \int_0^{t_1} \int_0^{t_2} h_j(t_1-\tau_1) h_k(t_2-\tau_2) \{\gamma_j\}^T \text{Ex}[\{E'(\tau_1)\}\{E'(\tau_2)\}^T] \{\gamma_k\} d\tau_1 d\tau_2 \quad (3.26)$$

Substituting for  $\text{Ex}[\{E'(\tau_1)\}\{E'(\tau_2)\}^T]$  from Eq. 3.23 into Eq. 3.26, the stationary autocorrelation function of  $S(t)$  can be written as follows:

$$\text{Ex}[S(t_1)S(t_2)] = \sum_{\ell=1}^3 \left\{ \sum_{j=1}^N \sum_{k=1}^N \xi_j \xi_k \int_{-\infty}^{+\infty} \Phi_{\ell}(\omega) H_j(\omega) H_k^*(\omega) e^{i\omega(t_1-t_2)} [\{\gamma_j\}^T [G_1]^T \{d_{\ell}\} \{d_{\ell}\}^T [G_1] \{\gamma_k\}] \right.$$

$$\begin{aligned}
& + \frac{\omega^2}{4c^2} \{x_j\}^T [G_2]^T \{d_\ell\} \{d_\ell\}^T [G_2] \{x_k\} \\
& - \frac{i\omega}{2c} (\{x_j\}^T [G_1]^T \{d_\ell\} \{d_\ell\}^T [G_2] \{x_k\} \\
& - \{x_j\}^T [G_2]^T \{d_\ell\} \{d_\ell\}^T [G_1] \{x_k\}) \, ] d\omega \quad (3.27)
\end{aligned}$$

For given spectral density functions of the excitation components, Eq. 3.27 can be used to obtain the mean square response. However, our main aim is to employ the input response spectra which are commonly used to prescribe design earthquakes. For this purpose, we will further simplify Eq. 3.27. Employing the transpose property of the scalar quantities in Eq. 3.27, such as  $\{x_j\}^T [G_1]^T \{d_\ell\} = \{d_\ell\}^T [G_1] \{x_j\}$ , the mean square value defined by this equation can be written in matrix notations as:

$$\text{Ex}[S^2] = \sum_{\ell=1}^3 \{d_\ell\}^T [R_\ell] \{d_\ell\} \quad (3.28)$$

where  $\{d_\ell\}$  is the vector of direction cosines of the  $\ell^{\text{th}}$  principal component. The 3x3 matrix  $[R_\ell]$  is a response matrix, which is defined for the  $\ell^{\text{th}}$  excitation components as follows:

$$\begin{aligned}
[R_\ell] = & \sum_{j=1}^N \sum_{k=1}^N \xi_j \xi_k \{ [\Gamma_{1jk}] \int_{-\infty}^{+\infty} \Phi_\ell(\omega) H_j(\omega) H_k^*(\omega) d\omega \\
& + \xi_j \xi_k \{ [\Gamma_{2jk}] \int_{-\infty}^{+\infty} \Phi_\ell(\omega) \omega^2 H_j(\omega) H_k^*(\omega) d\omega \\
& + \xi_j \xi_k \{ [\Gamma_{3jk}] \int_{-\infty}^{+\infty} \Phi_\ell(\omega) (-i\omega) H_j(\omega) H_k^*(\omega) d\omega \} \quad (3.29)
\end{aligned}$$

where

$$[\Gamma_{1jk}] = [G_1] \{ \gamma_j \} \{ \gamma_k \}^T [G_1]^T \quad (3.30a)$$

$$[\Gamma_{2jk}] = [G_2] \{ \gamma_j \} \{ \gamma_k \}^T [G_2]^T / 4c^2 \quad (3.30b)$$

$$[\Gamma_{3jk}] = ([G_2] \{ \gamma_j \} \{ \gamma_k \}^T [G_1]^T - [G_1] \{ \gamma_j \} \{ \gamma_k \}^T [G_2]^T) / 2c \quad (3.30c)$$

The three terms in Eq. 3.29 are caused by the translational, the rotational and the correlation between translational and rotational excitation components, respectively.

We will now define  $[R_\ell]$  in terms of the response spectra rather than the spectral density functions. For this, the frequency integrals in Eq. 3.29 are split into partial fractions to give the following:

$$[R_\ell] = \sum_{j=1}^N \frac{1}{2} \xi_j^2 \{ [\Gamma'_{1jj}] I_{0\ell}(\omega_j) + [\Gamma'_{2jj}] I_{1\ell}(\omega_j) \}$$

$$+ \sum_{j=1}^N \sum_{k=j+1}^N \xi_j \xi_k \{$$

$$[\Gamma'_{1jk}] ( A_1 I_{0\ell}(\omega_j) + A_2 I_{1\ell}(\omega_j) + A_3 I_{0\ell}(\omega_k) + A_4 I_{1\ell}(\omega_k) )$$

$$+ [\Gamma'_{2jk}] ( B_1 I_{0\ell}(\omega_j) + B_2 I_{1\ell}(\omega_j) + B_3 I_{0\ell}(\omega_k) + B_4 I_{1\ell}(\omega_k) )$$

$$+ [\Gamma'_{3jk}] ( C_1 I_{0\ell}(\omega_j) + C_2 I_{1\ell}(\omega_j) + C_3 I_{0\ell}(\omega_k) + C_4 I_{1\ell}(\omega_k) ) \}$$

$$(3.31)$$

where  $A_1, \dots, A_4, B_1, \dots, B_4$  and  $C_1, \dots, C_4$  are the coefficients of partial fractions and are defined in Appendix C. The

elements of matrices  $[\Gamma'_{1jk}]$ ,  $[\Gamma'_{2jk}]$  and  $[\Gamma'_{3jk}]$  are defined as follows:

$$\Gamma'_{1mnjk} = \sum_{p=1}^6 \sum_{q=1}^6 G_{1mp} G_{1nq} (\gamma_{pj} \gamma_{qk} + \gamma_{qj} \gamma_{pk}) \quad (3.32a)$$

$$\Gamma'_{2mnjk} = \sum_{p=4}^6 \sum_{q=4}^6 G_{2mp} G_{2nq} (\gamma_{pj} \gamma_{qk} + \gamma_{qj} \gamma_{pk}) / 4c^2 \quad (3.32b)$$

$$\Gamma'_{3mnjk} = \sum_{p=1}^6 \sum_{q=1}^6 (G_{2mp} G_{1nq} - G_{1mp} G_{2nq}) (\gamma_{pj} \gamma_{qk} - \gamma_{qj} \gamma_{pk}) / 2c \quad (3.32c)$$

in which  $m=1,2,3$  and  $n=1,2,3$ . The elements  $\Gamma'_{1mnjk}$  and  $\Gamma'_{3mnjk}$  can be further simplified by substituting the elements of matrices  $[G_1]$ ,

$$\Gamma'_{1mnjk} = \gamma_{mj} \gamma_{nk} + \gamma_{nj} \gamma_{mk} \quad (3.33)$$

$$\Gamma'_{3mnjk} = \frac{1}{2c} \left( \sum_{p=4}^6 G_{2mp} (\gamma_{pj} \gamma_{nk} - \gamma_{nj} \gamma_{pk}) - \sum_{q=4}^6 G_{2nq} (\gamma_{mj} \gamma_{qk} - \gamma_{qj} \gamma_{mk}) \right) \quad (3.34)$$

The frequency integrals  $I_{0\ell}(\omega_j)$  and  $I_{1\ell}(\omega_j)$  are defined in Chapter 2. These can be expressed in terms of the psuedo acceleration and relative velocity response spectrum values as in Eqs. 2.8 and 2.14.

For the case when rotational effects of traveling waves are ignored, Eq. 3.31 simplifies to:

$$\begin{aligned}
 [R_\ell] = & \sum_{j=1}^N \xi_j^2 [\Gamma'_{1jj}] I_{0\ell}(\omega_j) \\
 & + \sum_{j=1}^N \sum_{k=j+1}^N \xi_j \xi_k [\Gamma'_{1jk}] [A_1 I_{0\ell}(\omega_j) + A_2 I_{1\ell}(\omega_j) \\
 & \quad + A_3 I_{0\ell}(\omega_k) + A_4 I_{1\ell}(\omega_k)] \quad (3.34)
 \end{aligned}$$

The effects of rotational components on the design response have been numerically evaluated and discussed in section 3.6.

### 3.4.2 NONCLASSICALLY DAMPED STRUCTURES

Using the 2N-dimensional state vector approach, equations similar to those in the preceding section can be derived for the mean square response of nonclassically damped structural systems excited by the correlated components. For the six excitation components, the differential equation in terms of the principal coordinates, similar to Eq. 2.27, can now be written as:

$$\dot{Z}_j - p_j Z_j = \{F_j\}^T \{E'(t)\} \quad (3.35)$$

where  $\{F_j\}$  is a 6x1 vector, the  $\ell^{\text{th}}$  element of which is defined in Eq. 2.28. The response quantity,  $S(t)$ , of design interest can also be written as:

$$S(t) = \sum_{j=1}^{2N} \int_0^t \{q_j\}^T \{E'(\tau)\} e^{p_j(t-\tau)} d\tau \quad (3.36)$$

in which  $\{q_j\}$  is a vector of six elements, with the  $l^{\text{th}}$  element defined as:

$$q_{lj} = -g_j \{\phi_j\}^T [M] \{r_l\} / A_j^* \quad , \quad l=1, \dots, 6 \quad (3.37)$$

Considering the complex and conjugate terms in pairs, the response autocorrelation function can be written as:

$$\begin{aligned} \text{Ex}[S(t_1)S(t_2)] &= \sum_{j=1}^N \sum_{k=1}^N \int_0^{t_1} \int_0^{t_2} \\ & \left( \{q_j\}^T e^{p_j(t_1-\tau_1)} + \{q_j^*\}^T e^{p_j^*(t_1-\tau_1)} \right) \\ & \text{Ex}[\{E'(t_1)\}\{E'(t_2)\}^T] \\ & \left( \{q_k\}^T e^{p_k(t_2-\tau_2)} + \{q_k^*\}^T e^{p_k^*(t_2-\tau_2)} \right) d\tau_1 d\tau_2 \end{aligned} \quad (3.38)$$

Substituting for  $\text{Ex}[\{E'(t_1)\}\{E'(t_2)\}^T]$  from Eq. 3.23, combining the complex and conjugate terms as done in Chapter 2, and after some manipulations, the stationary autocorrelation function can now be written as:

$$\begin{aligned} \text{Ex}[S(t_1)S(t_2)] &= \\ & \sum_{l=1}^3 \sum_{j=1}^N \sum_{k=1}^N \int_{-\infty}^{+\infty} e^{i\omega(t_1-t_2)} \phi_l(\omega) H_j(\omega) H_k^*(\omega) \\ & \{G_j\}^T \left[ [G_1]^T \{d_l\} \{d_l\}^T [G_1] + \frac{\omega^2}{4c^2} [G_2]^T \{d_l\} \{d_l\}^T [G_2] \right. \\ & \left. + \frac{i\omega}{2c} \left( [G_1]^T \{d_l\} \{d_l\}^T [G_2] - [G_2]^T \{d_l\} \{d_l\}^T [G_1] \right) \right] \{G_k^*\} d\omega \end{aligned} \quad (3.39)$$

where  $\{G_j\}$  is a  $6 \times 1$  vector, defined as:

$$\{G_j\} = 2i\omega \{a_j\} + 2 \{A_j\} \quad (3.40)$$

in which the elements of vector  $\{a_j\}$  and  $\{A_j\}$  are defined by Eq. 2.38. Here, however,  $\ell$  varies from 1 to 6. The mean square value is obtained by setting  $t_1=t_2=t$ .

Each term in Eq. 3.39 has two scalar quantities, such as  $\{G_j\}^T [G_1]^T \{d_\ell\}$ . These scalars can also be written in transpose form as was done in Eq. 3.27 to obtain Eq. 3.28. This leads to the mean square response as defined in Eq. 3.28. That is,

$$\text{Ex}\{S^2\} = \sum_{\ell=1}^3 \{d_\ell\}^T [R_\ell] \{d_\ell\} \quad (3.41)$$

where the response matrix  $[R_\ell]$  is now defined as:

$$\begin{aligned} [R_\ell] = & \sum_{j=1}^N \sum_{k=1}^N \int_{-\infty}^{+\infty} \Phi_\ell(\omega) H_j(\omega) H_k^*(\omega) \\ & \{ [G_1] \{G_j\} \{G_k^*\}^T [G_1]^T + \omega^2 [G_2] \{G_j\} \{G_k^*\}^T [G_2]^T / 4c^2 \\ & - \frac{i\omega}{2c} ( [G_2] \{G_j\} \{G_k^*\}^T [G_1]^T - [G_1] \{G_j\} \{G_k^*\}^T [G_2]^T ) \} d\omega \end{aligned} \quad (3.42)$$

Here, also,  $[R_\ell]$  is a  $3 \times 3$  Hermitian matrix. The  $(m,n)^{\text{th}}$  element of this response matrix can be defined as:

$$\begin{aligned}
R_{lmn} &= \sum_{j=1}^N \sum_{k=1}^N \{ \\
&\sum_{p=1}^6 \sum_{q=1}^6 G_{1mp} G_{1nq} \int_{-\infty}^{+\infty} G_{pj} G_{qj}^* \phi_{\ell}(\omega) H_j(\omega) H_k^*(\omega) d\omega \\
&+ \sum_{p=1}^6 \sum_{q=1}^6 G_{2mp} G_{2nq} \\
&\quad \int_{-\infty}^{+\infty} \frac{\omega^2}{4c^2} G_{pj} G_{qj}^* \phi_{\ell}(\omega) H_j(\omega) H_k^*(\omega) d\omega \\
&+ \sum_{p=1}^6 \sum_{q=1}^6 (G_{2mp} G_{1nq} - G_{1mp} G_{nq}) \\
&\quad \left. - \frac{i\omega}{2c} G_{pj} G_{qk}^* \phi_{\ell}(\omega) H_j(\omega) H_k^*(\omega) d\omega \right\}
\end{aligned} \tag{3.43}$$

Each frequency integral in Eq. 3.43, can now be defined in terms of the frequency integrals  $I_{0\ell}$  and  $I_{1\ell}$  by splitting the integrand into partial fractions as follows:

$$\begin{aligned}
R_{lmn} &= 4 \sum_{j=1}^N \{ A_{mj} A_{nj} I_{0\ell}(\omega_j) + a_{mj} a_{nj} I_{1\ell}(\omega_j) \\
&+ \frac{1}{4c^2} \sum_{p=4}^6 \sum_{q=4}^6 G_{2mp} G_{2nq} [A_{pj} A_{qj} I_{1\ell}(\omega_j) + a_{pj} a_{qj} I_{2\ell}(\omega_j)] \} \\
&+ \sum_{j=1}^N \sum_{k=1}^N \{ [A'_{1mn} I_{0\ell}(\omega_j) + A'_{2mn} I_{1\ell}(\omega_j) \\
&\quad + A'_{3mn} I_{0\ell}(\omega_k) + A'_{4mn} I_{1\ell}(\omega_k)] \\
&+ \frac{1}{4c^2} \sum_{p=4}^6 \sum_{q=4}^6 G_{2mp} G_{2nq} [B'_{1pq} I_{0\ell}(\omega_j) + B'_{2pq} I_{1\ell}(\omega_j) \\
&\quad + B'_{3pq} I_{0\ell}(\omega_k) + B'_{4pq} I_{1\ell}(\omega_k) + B'_{5pq} A_{g\ell}] \}
\end{aligned}$$

$$\begin{aligned}
& + \frac{1}{2c} \sum_{p=1}^6 \sum_{q=1}^6 (G_{2mp}G_{1nq} - G_{1mp}G_{2nq}) \\
& \quad [C'_{1pq}I_{0\ell}(\omega_j) + C'_{2pq}I_{1\ell}(\omega_j) \\
& \quad + C'_{3pq}I_{0\ell}(\omega_k) + C'_{4pq}I_{1\ell}(\omega_k)] \} \\
& \hspace{20em} (3.44)
\end{aligned}$$

where the frequency integrals,  $I_{0\ell}(\omega_j)$  and  $I_{1\ell}(\omega_j)$ , are the same as before and the partial fraction factors  $A'_{1pq}$ ,  $A'_{4pq}$ ,  $B'_{1pq}$ ,  $B'_{5pq}$  and  $C'_{1pq}$  and  $C'_{4pq}$  are defined in Appendix C. Eq. 3.44 is applicable to nonclassically damped systems and can be used with prescribed ground spectra to obtain the design response. Again, in Eq. 3.44, the first and second terms in the single and double summation parts on  $j$  and  $k$  are the responses caused by the translational and rotational components of excitation, respectively. Whereas, the third term in double summation over  $j$  and  $k$  is due to the correlation between the translational and rotational components.

For the case of purely translational excitation, that is, when the rotational effects of traveling waves are ignored, Eq. 3.44 simplifies to:

$$\begin{aligned}
R_{\ell mn} = & 4 \sum_{j=1}^N [A_{mj} A_{nj} I_{0\ell}(\omega_j) + a_{mj} a_{nj} I_{1\ell}(\omega_j)] \\
& + \sum_{j=1}^N \sum_{k=1}^N [A'_{1mn} I_{0\ell}(\omega_j) + A'_{2mn} I_{1\ell}(\omega_j) \\
& \quad + A'_{3mn} I_{0\ell}(\omega_k) + A'_{4mn} I_{1\ell}(\omega_k)] \quad (3.45)
\end{aligned}$$

The effects of the rotational excitation components on the response of nonproportionally damped systems are numerically evaluated in Section 3.6.

### 3.5 MAXIMUM DESIGN RESPONSE

Eqs. 3.28 and 3.41 when multiplied by their peak factors will give the design response for any given orientation of a structure relative to the principal components. However, the orientation of a structure relative to the principal components will never be known in advance. Our main interest is to obtain the maximum value of the design response, irrespective of the orientation of the structure. That is, we are interested in the evaluation of the "worst case" response. In this section a methodology to obtain the maximum mean square response is described. The methodology, however, can also be used to obtain the design response, if the peak factor effects are included. This approach is a generalization of the approach proposed by Singh and Ashtia-ny [37] earlier.

Rewrite Eq. 3.28 or 3.41 as follows:

$$\text{Ex}[S^2] = \sum_{\ell=1}^3 \{d_{\ell}\}^T [R_{\ell}] \{d_{\ell}\} = \{d\}^T [R] \{d\} \quad (3.46)$$

where  $\{d\}$  is a  $9 \times 1$  vector and  $[R]$  is a  $9 \times 9$  matrix as:

$$\{d\} = \begin{Bmatrix} \{d_1\} \\ \{d_2\} \\ \{d_3\} \end{Bmatrix} \quad \text{and} \quad [R] = \begin{bmatrix} [R_1] & & 0. \\ & [R_2] & \\ 0. & & [R_3] \end{bmatrix} \quad (3.47)$$

The direction cosines  $\{d_1\}$ ,  $\{d_2\}$  and  $\{d_3\}$  are orthogonal vectors with the following constraints:

$$\{d_{\ell}\}^T \{d_m\} = \begin{cases} 1. & \ell=m \\ 0. & \ell \neq m \end{cases} \quad (3.48)$$

and consequently

$$\{d\}^T \{d\} = \sum_{\ell=1}^3 \{d_{\ell}\}^T \{d_{\ell}\} = 3. \quad (3.49)$$

We are interested in a particular set of  $\{d_1\}$ ,  $\{d_2\}$  and  $\{d_3\}$  such that  $\text{Ex}[S^2]$  is maximum.

For this, the Lagrange multiplier approach can be used.

We define our auxiliary function as:

$$L(\lambda) = \{d\}^T [R] \{d\} - \lambda (\{d\}^T \{d\} - 3) \quad (3.50)$$

where  $\lambda$  is the Lagrange multiplier. For the extreme value of  $L(\lambda)$ , its partial derivative with respect to  $\{d\}$  must be zero. This gives:

$$[R]\{d\} - \lambda\{d\} = 0 \quad (3.51)$$

Eq. 3.51 is equivalent to three independent equations:

$$[R_1]\{d_1\} - \lambda\{d_1\} = 0 \quad (3.52a)$$

$$[R_2]\{d_2\} - \lambda\{d_2\} = 0 \quad (3.52b)$$

$$[R_3]\{d_3\} - \lambda\{d_3\} = 0 \quad (3.52c)$$

These equations are to be solved in conjunction with the constraints given in Eq. 3.48.

Each equation in Eqs. 3.52 is an eigenvalue problem by itself. Corresponding to each set, there will be three eigenvalues and a set of three-orthogonal eigenvectors. Thus, there exist nine possible direction cosines along which if the principal components are applied, they will give an extreme value of  $L(\lambda)$ . These provide local maxima and minima, and a systematic search will have to be made to obtain the absolute maximum value.

The eigenvalues of Eqs. 3.52 directly provide the response values due to the excitation for which matrix  $[R]$  is defined. Thus, if we have solved the eigenvalue problem, for, say the 1<sup>st</sup> excitation components, i.e.,

$$[R_1]\{d_1\} - \lambda_1\{d_1\} = \{0.\} \quad (3.53)$$

the three eigenvalues  $\lambda_{11}$ ,  $\lambda_{12}$  and  $\lambda_{13}$ , respectively, define the response due to the excitation 1 when it is applied

along the  $\{d_1^{(1)}\}$ ,  $\{d_2^{(1)}\}$  and  $\{d_3^{(1)}\}$  directions. Here  $\{d_1^{(i)}\}$  is the eigenvector of Eq. 3.53 for eigenvalue  $\lambda_{1i}$ . To show this, consider Eq. 3.53 for the eigenvalue  $\lambda_{1i}$  as

$$[R_1]\{d_1^{(i)}\} - \lambda_{1i}\{d_1^{(i)}\} = \{0.\} \quad (3.54)$$

Premultiplying this by  $\{d_1^{(i)}\}^T$  and invoking the constraint, Eq. 3.48, we obtain:

$$\lambda_{1i} = \{d_1^{(i)}\}^T [R_1] \{d_1^{(i)}\} \quad (3.55)$$

which, as seen from Eq. 3.28 or Eq. 3.41, is the response due to the 1<sup>st</sup> component of excitation alone. Eq. 3.55 can also be written in general form as:

$$\lambda_{\ell i} = \{d_\ell^{(i)}\}^T [R_\ell] \{d_\ell^{(i)}\} \quad (3.57)$$

where  $\lambda_{\ell i}$  and  $\{d_\ell^{(i)}\}$  are the  $i^{\text{th}}$  eigenpairs for the  $\ell^{\text{th}}$  response matrix,  $[R_\ell]$ . It is also noted that

$$\{d_\ell^{(i)}\}^T [R_\ell] \{d_\ell^{(j)}\} = 0 \quad (3.57)$$

There are 6 possibilities of maximum response in each eigenvector set. Thus, totally there are 18 possible combinations one will have to examine to obtain the global maximum response. The eigenvalues and eigenvectors can be directly used to obtain the responses in various combinations of the axes and excitations. For example, let  $\{d_1^{(i)}\}$  be

the  $i^{\text{th}}$  eigenvectors of  $[R_1]$ , and let the principal components 1, 2 and 3 be applied along the eigenvectors 1, 2 and 3. Then the total mean square response can be obtained from:

$$\text{Ex}(S^2) = \lambda_{11} + \{d_2^{(1)}\}^T [R_2] \{d_2^{(1)}\} + \{d_3^{(1)}\}^T [R_2] \{d_3^{(1)}\} \quad (3.58)$$

in which  $\lambda_{11}$  is the response due to excitation-1 applied along direction  $\{d_1^{(1)}\}$ , the second term represents the response due to excitation-2 applied along direction  $\{d_2^{(1)}\}$ , and the third term represents the response due to excitation-3 applied along direction  $\{d_3^{(1)}\}$ . A more general expression for all possible combinations can be written as:

$$S_{mn} = \lambda_{mn} + \sum_{\substack{k \neq m \text{ (} k=1,2,3 \text{)} \\ \ell \neq n \text{ (} \ell=1,2,3 \text{)}}} \{d_\ell^{(m)}\}^T [R_k] \{d_\ell^{(m)}\} \quad (3.59)$$

$$S'_{mn} = \lambda_{mn} + \sum_{\substack{k \neq m \text{ (} k=1,2,3 \text{)} \\ \ell \neq n \text{ (} \ell=3,2,1 \text{)}}} \{d_\ell^{(m)}\}^T [R_k] \{d_\ell^{(m)}\} \quad (3.60)$$

These eighteen possibilities are enumerated in Appendix D.

Herein, the principal directions represented by the eigenvectors of matrices  $[R_1]$ ,  $[R_2]$  and  $[R_3]$  are called principal response directions.

It is seen that the principal response directions are different for each response quantity because  $\xi_j$  and  $G_{mj}$  are

different. Since the response matrix  $[R_\ell]$  depends upon the  $\ell^{\text{th}}$  excitation spectral density function, the principal response directions will also depend upon the frequency characteristics of the excitation. If the frequency characteristics of the input spectral density function are not significantly different, their response matrices and corresponding principal directions will not be much different either. Especially, when the spectral density functions are proportional, i.e.,

$$\Phi_2(\omega) = \rho_2 \Phi_1(\omega) \quad (3.61a)$$

$$\Phi_3(\omega) = \rho_3 \Phi_1(\omega) \quad (3.61b)$$

then all three sets of principal response directions will be identical. In such a case, the search for the maximum response is simplified considerably, as Eq. 3.58 can then be written as:

$$\text{Ex}(S^2) = \lambda_{11} + \rho_2 \lambda_{12} + \rho_3 \lambda_{13} \quad (3.62)$$

It is seen that this procedure does not require any trial on structural orientations to obtain the worst case response. For an arbitrarily assumed directions of the structural axes, one only needs to establish  $[R_1]$ ,  $[R_2]$  and  $[R_3]$ . Once these have been established, the procedure de-

scribed above can be used to identify the maximum response, without any re-analyses of the structure.

Numerical results showing the application of this methodology are given in the next section.

### 3.6 NUMERICAL RESULTS

In this section, several sets of numerical results are presented for structures subjected to five and six correlated earthquake components. The purpose of this presentation is to: (1) compare the maximum response obtained by Eqs. 3.59 and 3.60 with the conventional response spectrum approach; (2) show that in most cases the directions of the principal excitation axes corresponding to the worst case response are different from the geometrical axis of the structure, and (3) study the effects of the rotational components on the maximum response. The input motions in this study are defined in terms of the spectral density functions,  $\phi_1(\omega)$ ,  $\phi_2(\omega)$  and  $\phi_3(\omega)$ , respectively, of the major, intermediate and minor principal excitation components. These spectral density functions are assumed to be of Kanai-Tajimi form as defined by Eq. 2.73 but with different parameters. These parameters were chosen rather arbitrarily and are given in Table 3.1. These components represent three broad band inputs with different intensities and somewhat different frequency content characteristics.

Three seemingly different types of structure have been considered in this study: 1) two multistory torsional structures with three and six rigid floors supported on columns, and 2) a space frame of an arbitrary shape. The characteristics of these structures and their calculated response are described in the following sections.

### 3.6.1 TORSIONAL STRUCTURE

The three story torsional structure considered here is similar to the one considered in Chapter 2 and shown in Fig. 2.1. For this structure the column stiffnesses in three stories are  $k_1=6k$ ,  $k_2=2k$  and  $k_3=k$ , where  $k$  is the combined stiffness of the columns in the top story. The mass properties of the three floors are  $m_1=3m$ ,  $m_2=2m$  and  $m_3=m$ , where  $m$  = the mass of the top floor. Each floor has 3 degrees-of-freedom: two horizontal translation and a rotation about the vertical axis. The frequency characteristic of this structure can be easily changed by changing the frequency parameter  $\omega^2 = k/m$ . The results have been obtained for three values of this parameter equal to 10., 33.4 and 50. cps. The eccentricity parameter  $e/r$  has also been varied. The values of  $e/r = .01$ ,  $.05$  and  $.30$  have been considered. The modal frequencies and damping ratios obtained by the normal and complex mode approaches are given in Tables 3.2, 3.3 and 3.4.

The response quantities obtained for this structure are: the base shears in two horizontal directions, the base torsional moment and the bending moments about the two axes of a column. Since these quantities are not affected by the vertical excitation significantly, this component of excitation has not been considered. However, the effect of vertical excitation in introducing the rotational components has been considered. Thus, this system is subjected to only five excitation components: two translational components acting in the horizontal plane and three rotational components acting about the two horizontal axes and one vertical axis. Table 3.5 shows the participation factors for these five components for the system with  $e/r=.01$  and  $w = 10$ . cps.

The root mean square values of various response quantities are shown in Tables 3.6 through 3.11. These have been normalized by  $mg$ , the weight of the top slab. The moments have  $mg$ -ft. units. For each response quantity, the numerical values have been obtained by:

1. The worst-case response approach: In this, Eqs. 3.28 and 3.41 have been used for proportionally and nonproportionally damped systems. These values are shown in Column (2) of Tables 3.6 through 3.11.

2. The conventional response spectrum approach with five components: In this, the translational and the rotational

components of excitation are applied along the geometric axes of the structure. The ratio of this value to the maximum value obtained in (1) above is shown in Column (3) of Tables 3.6 through 3.11. The ratio shows the magnitude of under estimation which will result if no search for the worst-case response is made.

3. The worst-case response approach for only translational components: Here the rotational effects of the input are ignored. These values are shown in Column (4) of Tables 3.6 through 3.11. The ratios of the values in Column (4) to the values in Column (2) are shown in Column (6) of the tables, and these show the effect of the rotational components.

4. The conventional response approach with only two principal components: In this case, the principal components are applied along the geometric axes. No rotational components have been considered. The ratio of this value to the maximum value obtained in step (3) is shown in Column (5). This ratio shows the magnitude of possible under estimation of the response if no search for the worst-case response is made.

Tables 3.7 through 3.9 are for the shear wave velocity,  $c=1000$ . fps and Tables 3.10 and 3.11 are for the shear wave velocity,  $c=2000$ . fps.

It is seen that, for  $c=1000$ . fps, the contribution of the rotational components to the response is quite large.

There will be a considerable underestimation of the response, as shown by the ratios in Column (6), if the rotational effects of the excitation are ignored. Furthermore, it is also necessary to make a search for the worst-case response, as established in Section 3.5, otherwise some underestimation of the response is likely to occur. This is shown by the ratios in Columns (3) and (5) of these tables.

A structural model with the floor slab possessing six degrees-of-freedom, instead of three considered above, was also used to examine the effects on the response of the rotational inertias of the slab about the two horizontal axes. The numerical results of the two structural models, however, did not differ much. This was because, in the model with six degrees-of-freedom per floor slab, the axial stiffness of the columns was relatively large to prevent the slab rotations about the horizontal axes.

The results are also shown for a 6-story, 18 degrees-of-freedom structure in Tables 3.12 and 3.13. The length of each story in this model was 14 ft., and thus total height of the structure was 84 ft. Comparing the results in Columns (6) of Tables 3.12 and 3.13 with the corresponding results in previous tables, it is seen that the effect of rotational components is now larger. That is, a taller structure will be affected more by the rotational components. It, there-

fore, seems that the rotational components of an excitation should not be neglected, especially for tall buildings.

The numerical results are also affected by the parameter  $e/r$ ; however, no special trends in the results are observed.

A comparison of the results in the tables for  $c=1000$  and  $2000$  fps clearly shows that an increase in the shear wave velocity reduce the effect of rotational components. This is due to the fact that the terms associated with the rotational components in Eqs. 3.28 and 3.41 are always divided by  $c^2$ .

### 3.6.2 SPACE FRAME STRUCTURE

The space frame structure considered here is shown in Fig. 3.1. In the analytical model, each joint has six degrees-of-freedom. The mass and stiffness properties of the frame are given in Table 3.14. Only a proportionally damped system with a constant modal damping ratio of  $\beta=.02$  is considered. The modal frequencies and the participation factors of the system are given in Table 3.15.

The numerical results of the root mean square response for the axial force, bending moment and maximum flexural stresses in various members are shown in Tables 3.16 through 3.19. The values are in kips-in. units. The results are ob-

tained with and without rotational components. The results with all six components are shown in Columns (2) to (6), and the results for only translational components are shown in Columns (7) to (12).

The response values in Columns (2) and (7) are the worst-case response values. Whereas, those in Columns (3) and (8) are obtained with the principal components applied along the geometric axes. The values in Columns (3) and (8) are reported in the ratio form.

A comparison of the values in Columns (2) and (7) of these tables shows that the rotational components contribute significantly to the responses. in this case again. Of course, this contribution depends upon the shear wave velocity as well as the size of the structure. Also, some response quantities are affected more than others by the rotational components.

Again, it is seen that if no search for the maximum response is made, the calculated value may be underestimated; see Columns (3) and (9). This under-estimation will depend upon the symmetry of the structure and the characteristics of the input motions. Thus, the cases shown here are not typical; there could possibly be some cases where these effects are even more pronounced.

Columns (4) to (6) and (10) to (12) in Tables 3.16 through 3.19 show the orientations of the principal excitations with respect to the structural axes to cause the maximum response, i.e., the worst-case response. This orientation is given in terms of three angles, shown in Fig. 3.1. These angles can be obtained from the direction cosine matrix obtained for the worst-case response. It is seen that the directions for the worst-case response do not necessarily coincide with the structural axes.

## Chapter IV

### RESPONSE FOR SIX CORRELATED EARTHQUAKE COMPONENTS BY MODE ACCELERATION APPROACH

#### 4.1 INTRODUCTION

The previous two chapters were devoted to the analytical development of the response spectrum approaches, which were based on the method of mode displacement of structural dynamics. These approaches required that the seismic inputs be prescribed in terms of the psuedo-acceleration and relative velocity spectra.

Often in these approaches, only a first few modes are used in the analysis, as usually the higher modes do not contribute much to the response. However, there are situations involving certain response quantities or certain structures where the contribution of the high frequency modes can not be neglected without affecting the accuracy of the results. This truncation of the modes leads to the, so-called, "missing mass" effect.

To improve the accuracy of the results with only a first few modes, recently Singh and Mehta [34,38] have proposed an alternative response spectrum approach for the calculation of design response for a single excitation component. This approach is based on the "mode acceleration" method [3,18,45] of structural dynamics. It requires the

seismic inputs to be defined in terms of relative acceleration and relative velocity spectra.

Herein, a similar response spectrum approach, based on the method of mode acceleration, is developed for the calculation of worst-case design response of structures subjected to the six correlated earthquake components. The inputs to this approach are defined in terms of the relative acceleration and relative velocity spectra of the three principal excitation components.

In the next section, the mode acceleration formulation is given for the calculation of mean square and design response for correlated multi-component excitations. The response equations are cast in the same form as in the previous chapter so that the same methodology can be applied to obtain the worst-case design response. The numerical results are presented to demonstrate the advantage of the mode acceleration formulation over the mode displacement formulation given in the Chapter 3.

#### 4.2 ANALYTICAL FORMULATION

Here, we will only consider proportionally damped systems. For a linear multi-degree-of-freedom system with equations of motion as Eq. 3.1, a response quantity,  $S(t)$ , of interest can be written as:

$$S(t) = \sum_{j=1}^N \xi_j V_j(t) \quad (4.1)$$

where,  $V_j(t)$  is defined by the solution of Eq. 2.2 and represents the displacement in mode  $j$ . In Chapter 3, the solution of Eq. 2.2 in terms of Duhamel's integral was substituted in Eq. 4.1 to obtain Eq. 3.25. This equation then formed the basis of the formulation developed in Chapter 3. Since the mode displacement  $V_j(t)$  was directly used in Eq. 4.1, the formulation of Chapter 3 is called the mode displacement formulation.

A different expression is obtained if  $V_j(t)$  in Eq. 4.1 is expressed in terms of modal acceleration  $\ddot{V}_j(t)$  and modal velocity  $\dot{V}_j$ , by employing Eq. 2.2. That is,

$$S(t) = -\sum_{j=1}^N \xi_j [ \{\tilde{x}_j\}^T \{E'(t)\} + 2\beta_j \omega_j \dot{V}_j + \ddot{V}_j ] / \omega_j^2 \quad (4.2)$$

Eq. 4.2 forms the basis of the mode acceleration formulation, to be presented in the following section.

#### 4.2.1 MEAN SQUARE AND DESIGN RESPONSE

We are interested in the evaluation of design response. To obtain this, the mean square response is required. This can be obtained from the autocorrelation function of  $S(t)$ , which can be written as follows:

$$\begin{aligned}
\text{Ex}[S(t_1)S(t_2)] &= \sum_{j=1}^N \sum_{k=1}^N \xi_j \xi_k \\
& [ \{x_j\}^T \text{Ex}[\{E'(t_1)\}\{E'(t_2)\}^T] \{x_k\} \\
& + \{x_j\}^T ( 2\beta_k \omega_k \text{Ex}[\{E'(t_1)\}\dot{V}_k(t_2)] + \text{Ex}[\{E'(t_1)\}\ddot{V}_k(t_2)] ) \\
& + \{x_k\}^T ( 2\beta_j \omega_j \text{Ex}[\{E'(t_2)\}\dot{V}_j(t_1)] + \text{Ex}[\{E'(t_2)\}\ddot{V}_j(t_1)] ) \\
& + 4\beta_j \beta_k \omega_j \omega_k \text{Ex}[\dot{V}_j(t_1)\dot{V}_k(t_2)] + \text{Ex}[\ddot{V}_j(t_1)\ddot{V}_k(t_2)] \\
& + 2\beta_j \omega_j \text{Ex}[\dot{V}_j(t_1)\ddot{V}_k(t_2)] + 2\beta_k \omega_k \text{Ex}[\dot{V}_k(t_2)\ddot{V}_j(t_1)] ] \quad (4.3)
\end{aligned}$$

Various auto- and cross- correlation terms in the above equation have been obtained in terms of the input autocorrelation matrix, Eq. 3.23, and are given in Appendix B. Substituting these in the above equation, the following is obtained for the mean square response:

$$\text{Ex}[S^2] = \sum_{\ell=1}^3 \{d_\ell\}^T [R_\ell] \{d_\ell\} \quad (4.4)$$

The response matrix  $[R_\ell]$  for the  $\ell^{\text{th}}$  excitation can be written as:

$$\begin{aligned}
[R_\ell] &= \sum_{j=1}^N \sum_{k=1}^N (\xi_j \xi_k / \omega_j^2 \omega_k^2) \\
& \{ [\Gamma_{1jk}] \int_{-\infty}^{+\infty} \Phi_\ell(\omega) d\omega + [\Gamma_{2jk}] \int_{-\infty}^{+\infty} \Phi_\ell(\omega) \omega^2 d\omega \} \\
& + \sum_{j=1}^N \sum_{k=1}^N (\xi_j \xi_k / \omega_j^2 \omega_k^2) \left( \int_{-\infty}^{+\infty} \Phi_\ell(\omega) H_j(\omega) H_k^*(\omega) \right)
\end{aligned}$$

$$\begin{aligned}
& [ 4\beta_j \beta_k \omega_j \omega_k \{ [\Gamma_{1jk}] \omega^2 + [\Gamma_{2jk}] \omega^4 + [\Gamma_{3jk}] (-i\omega^3) \} \\
& \quad + [\Gamma_{1jk}] \omega^4 + [\Gamma_{2jk}] \omega^6 + [\Gamma_{3jk}] (-i\omega^5) \\
& \quad + 2(\beta_j \omega_j - \beta_k \omega_k) \{ [\Gamma_{1jk}] (-i\omega^3) + [\Gamma_{2jk}] (-i\omega^5) - [\Gamma_{3jk}] \omega^4 \} \\
& \quad - 2\beta_j \omega_j \{ [\Gamma_{1jk}] (i\omega) + [\Gamma_{2jk}] (i\omega^3) + [\Gamma_{3jk}] \omega^2 \} \\
& \quad - 2\beta_k \omega_k \{ [\Gamma_{1jk}] (-i\omega) + [\Gamma_{2jk}] (-i\omega^3) - [\Gamma_{3jk}] \omega^2 \} \} d\omega \\
& \quad + \int_{-\infty}^{+\infty} \phi_\ell(\omega) (H_j(\omega) + H_k^*(\omega)) \\
& \quad \quad \quad \{ [\Gamma_{1jk}] \omega^2 + [\Gamma_{2jk}] \omega^4 + [\Gamma_{3jk}] -i\omega^3 \} d\omega \quad ) \\
\end{aligned} \tag{4.5}$$

Again,  $[R_\ell]$  is a  $3 \times 3$  Hermitian matrix. To define this matrix in terms of response spectra, the frequency integral in Eq. 4.5 are appropriately split into partial fractions, to give as follows:

$$\begin{aligned}
[R_\ell] = & \\
& \sum_{j=1}^N \sum_{k=1}^N (\xi_j \xi_k / \omega_j \omega_k) ([\Gamma_{1jk}] A_{g\ell}^2 + [\Gamma_{2jk}] \dot{A}_{g\ell}^2) \\
& + \sum_{j=1}^N (\xi_j^2 / 2\omega_j^4) \{ [\Gamma_{1jj}] [2\omega_j^2 (1-2\beta_j^2) I_{1\ell}(\omega_j) - I_{2\ell}(\omega_j)] \\
& \quad + [\Gamma_{2jj}] [2\omega_j^2 (1-2\beta_j^2) I_{2\ell}(\omega_j) - I_{3\ell}(\omega_j)] \} \\
& + \sum_{j=1}^N \sum_{k=j+1}^N (\xi_j \xi_k / \omega_j \omega_k) \\
& \quad \quad \quad \{ 4\beta_j \beta_k \omega_j \omega_k [\Gamma_{1jk}] [A_1 I_{1\ell}(\omega_j) + A_2 I_{2\ell}(\omega_j) + A_3 I_{1\ell}(\omega_k) + A_4 I_{2\ell}(\omega_k)] \}
\end{aligned}$$

$$\begin{aligned}
& + [\Gamma'_{2jk}] [B_1 I_{1\ell}(\omega_j) + B_2 I_{2\ell}(\omega_j) + B_3 I_{1\ell}(\omega_k) + B_4 I_{2\ell}(\omega_k)] \\
& + [\Gamma'_{3jk}] [C_1 I_{1\ell}(\omega_j) + C_2 I_{2\ell}(\omega_j) + C_3 I_{1\ell}(\omega_k) + C_4 I_{2\ell}(\omega_k)] \\
& + [\Gamma'_{1jk}] [A_1 I_{2\ell}(\omega_j) + A_2 I_{3\ell}(\omega_j) + A_3 I_{2\ell}(\omega_k) + A_4 I_{3\ell}(\omega_k)] \\
& + [\Gamma'_{2jk}] [B_1 I_{2\ell}(\omega_j) + B_2 I_{3\ell}(\omega_j) + B_3 I_{2\ell}(\omega_k) + B_4 I_{3\ell}(\omega_k)] \\
& + [\Gamma'_{3jk}] [C_1 I_{2\ell}(\omega_j) + C_2 I_{3\ell}(\omega_j) + C_3 I_{2\ell}(\omega_k) + C_4 I_{3\ell}(\omega_k)] \\
& 4(\beta_j \omega_j - \beta_k \omega_k) ([\Gamma'_{1jk}] [C_1 I_{1\ell}(\omega_j) + C_2 I_{2\ell}(\omega_j) + C_3 I_{1\ell}(\omega_k) + C_4 I_{2\ell}(\omega_k)] \\
& + [\Gamma'_{2jk}] [C_1 I_{2\ell}(\omega_j) + C_2 I_{3\ell}(\omega_j) + C_3 I_{2\ell}(\omega_k) + C_4 I_{3\ell}(\omega_k)] \\
& - \frac{1}{4} [\Gamma'_{3jk}] [A_1 I_{2\ell}(\omega_j) + A_2 I_{3\ell}(\omega_j) + A_3 I_{2\ell}(\omega_k) + A_4 I_{3\ell}(\omega_k)] \\
& - 4([\Gamma'_{1jk}] [(\beta_j \omega_j)^2 I_{1\ell}(\omega_j) + (\beta_k \omega_k)^2 I_{1\ell}(\omega_k)] \\
& + [\Gamma'_{2jk}] [(\beta_j \omega_j)^2 I_{2\ell}(\omega_j) + (\beta_k \omega_k)^2 I_{2\ell}(\omega_k)] \\
& + [\Gamma'_{3jk}] [(-\beta_j \omega_j [\omega_j^2 I_{1\ell}(\omega_j) - I_{2\ell}(\omega_j)] \\
& + \beta_k \omega_k [\omega_k^2 I_{1\ell}(\omega_k) - I_{2\ell}(\omega_k)])] \\
& + [\Gamma'_{1jk}] [\omega_j^2 I_{1\ell}(\omega_j) - I_{2\ell}(\omega_j) + \omega_k^2 I_{1\ell}(\omega_k) - I_{2\ell}(\omega_k)] \\
& + [\Gamma'_{2jk}] [\omega_j^2 I_{2\ell}(\omega_j) - I_{3\ell}(\omega_j) + \omega_k^2 I_{2\ell}(\omega_k) - I_{3\ell}(\omega_k)] \\
& + [\Gamma'_{3jk}] [-\beta_j \omega_j I_{2\ell}(\omega_j) + \beta_k \omega_k I_{2\ell}(\omega_k)] \}
\end{aligned}$$

(4.6)

in which  $A_{g\ell}^2$  and  $\dot{A}_{g\ell}^2$  are the mean square values of the ground acceleration and rate of change of the ground acceleration, respectively, which are defined in terms of the acceleration spectral density function as follows:

$$A_{g\ell}^2 = \int_{-\infty}^{+\infty} \Phi_{\ell}(\omega) d\omega \quad (4.7a)$$

$$\dot{A}_{g\ell}^2 = \int_{-\infty}^{+\infty} \Phi_{\ell}(\omega) \omega^2 d\omega \quad (4.7b)$$

The integrals  $I_{1\ell}(\omega_j)$  and  $I_{2\ell}(\omega_j)$  are mean square values of the relative velocity and relative acceleration response of an oscillator of frequency  $\omega_j$  and damping  $\beta_j$  and are defined as:

$$I_{1\ell}(\omega_j) = \int_{-\infty}^{+\infty} \Phi_{\ell}(\omega) \omega^2 |H_j(\omega)|^2 d\omega \quad (4.8)$$

$$I_{2\ell}(\omega_j) = \int_{-\infty}^{+\infty} \Phi_{\ell}(\omega) \omega^4 |H_j(\omega)|^2 d\omega \quad (4.9)$$

These integrals can be obtained in terms of the relative velocity and relative acceleration response spectra through their respective peak factors. Another integral,  $I_{3\ell}(\omega_j)$ , which is required in Eq 4.6, can also be defined in terms of the above mean square values as follows:

$$\begin{aligned} I_{3\ell}(\omega_j) &= \int_{-\infty}^{+\infty} \Phi_{\ell}(\omega) \omega^6 |H_j(\omega)|^2 d\omega \\ &= A_{g\ell}^2 + 2\omega_j^2 (1 - 2\beta_j^2) I_{2\ell}(\omega_j) - \omega_j^4 I_{1\ell}(\omega_j) \end{aligned} \quad (4.10)$$

The matrix  $[F_\rho]$  in Eq. 4.6 can be further simplified by collecting terms with similar coefficients. An element of this matrix can be written in a simplified form as follows:

$$\begin{aligned}
 R_{\ell mn} = & \\
 & \sum_{j=1}^N \sum_{k=1}^N (\xi_j \xi_k / \omega_j \omega_k) [\Gamma_{1mnjk} A_{g\ell}^2 + \Gamma'_{2mnjk} \dot{A}_{g\ell}^2] \\
 & + \sum_{j=1}^N (\xi_j^2 / 2\omega_j^4) \{ \Gamma'_{1mnjk} [2\omega_j^2 (1-2\beta_j^2) I_{1\ell}(\omega_j) - I_{2\ell}(\omega_j)] \\
 & \quad + \Gamma'_{2mnjk} [\omega_j^4 I_{1\ell}(\omega_j) - \dot{A}_{g\ell}^2] \} \\
 & + \sum_{j=1}^N \sum_{k=j+1}^N (\xi_j \xi_k / \omega_j \omega_k) \\
 & + \{ \Gamma'_{1mnjk} [F_1 I_{1\ell}(\omega_j) + F_2 I_{2\ell}(\omega_j) + F_3 I_{1\ell}(\omega_k) + F_4 I_{2\ell}(\omega_k) + F_5 \dot{A}_{g\ell}^2] \\
 & + \Gamma'_{2mnjk} [F'_1 I_{1\ell}(\omega_j) + F'_2 I_{2\ell}(\omega_j) + F'_3 I_{1\ell}(\omega_k) + F'_4 I_{2\ell}(\omega_k) + F'_5 \dot{A}_{g\ell}^2] \\
 & + \Gamma'_{3mnjk} [F''_1 I_{1\ell}(\omega_j) + F''_2 I_{2\ell}(\omega_j) + F''_3 I_{1\ell}(\omega_k) + F''_4 I_{2\ell}(\omega_k) + F''_5 \dot{A}_{g\ell}^2] \} \\
 & \hspace{15em} (4.11)
 \end{aligned}$$

where  $F_1, \dots, F_5$ ;  $F'_1, \dots, F'_5$ ; and  $F''_1, \dots$  and  $F''_5$  are defined in terms of  $A_1, \dots, A_4$ ,  $B_1, \dots$  and  $B_4$  and are given in Appendix C.  $\Gamma'_{1mnjk}$  etc. are the same as defined in Chapter 3, Eqs. 3.32 and 3.33.

#### 4.2.2 PSUEDO-STATIC RESPONSE

No special advantage is gained if Eq. 4.11 is used in lieu of Eq. 3.31 for the evaluation of  $R_{\ell mn}$ . To obtain accurate response, Eq. 4.11 will also require a complete set of modes, especially for the evaluation of the first two terms. These terms, however, can be obtained by a simple static analysis without an evaluation of the modal quantities.

The following analysis shows that the response associated with the first two terms in Eq. 4.6 is precisely the mean square value of the response of the following psuedo-static problem:

$$[K]\{u_s\} = [M] [r] \{E'\} \quad (4.12)$$

where  $\{u_s\}$  = a vector of the time dependent displacements obtained as a solution of Eq. 4.12, without any consideration of the vibration effects. The response quantity,  $S(t)$ , is related to  $\{u_s\}$  by a simple linear transformation as:

$$S(t) = \{k_i\}^T \{u_s\} \quad (4.13)$$

We will now show that the mean square value of this quantity is directly related to the first term of Eq. 4.6. For this, we expand  $\{u_s\}$  in the vector space of  $\{\phi_j\}$ , the modal vectors of Eq. 3.1, as follows:

$$\{u_s\} = \sum_{j=1}^N V_{sj} \{\phi_j\} \quad (4.14)$$

where  $V_{sj}$  are the coefficients of the expansion. To obtain these coefficients, we substitute Eq. 4.14 into Eq. 4.12, premultiply the result by  $\{\phi_j\}^T$ , and invoke the orthogonality condition of the modes, i.e.,  $\{\phi_j\}^T [K] \{\phi_k\} = \delta_{kj} \omega_j^2$ , to give as follows:

$$V_{sj} = \frac{\{\phi_j\}^T [M] [r] \{E'\}}{\{\phi_j\}^T [K] \{\phi_j\}} \quad (4.15)$$

The denominator in Eq. 4.15 is equal to  $\omega_j^2$ . Substituting for  $\{\phi_j\}^T [M] [r] = \{\chi_j\}^T$  in Eq. 4.15, we obtain

$$V_{sj} = \{\chi_j\}^T \{E'\} / \omega_j^2 \quad (4.16)$$

Substituting for  $V_{sj}$  in Eq. 4.14 gives:

$$\{u_s\} = \sum_{j=1}^N (\{\chi_j\}^T \{E'\}) \{\phi_j\} / \omega_j^2 \quad (4.17)$$

Using Eq. 4.13, the psuedo-static value of the response quantity,  $S(t)$ , can now be defined as:

$$S(t) = \sum_{j=1}^N (\{\chi_j\}^T \{E'\}) \{k_i\}^T \{\phi_j\} / \omega_j^2 \quad (4.18)$$

Since the response mode shape  $\xi_j$  is equal to  $\{k_i\}^T \{\phi_j\}$ , the above equation reduces to:

$$S(t) = \sum_{j=1}^N \xi_j (\{\chi_j\}^T \{E'\}) / \omega_j^2 \quad (4.19)$$

The mean square value of the static response from Eq. 4.19 can then be written as:

$$\text{Ex}[S^2(t)] = \sum_{j=1}^N \sum_{k=1}^N \xi_j \xi_k \{\gamma_j\}^T \text{Ex}[\{E'\}\{E'\}^T] \{\gamma_k\} / \omega_j^2 \omega_k^2 \quad (4.20)$$

The covariance matrix of excitation in Eq. 4.20 can now be defined from Eq. 3.23 by letting  $t_1=t_2=t$  as follows:

$$\begin{aligned} \text{Ex}[\{E'(t)\}\{E'(t)\}^T] &= \sum_{\ell=1}^3 \int_{-\infty}^{+\infty} ( [G_1]^T \{d_\ell\} \{d_\ell\}^T [G_1] \\ &+ \omega^2 [G_2]^T \{d_\ell\} \{d_\ell\}^T [G_2] / 4c^2 ) \phi_\ell(\omega) d\omega \end{aligned} \quad (4.21)$$

The imaginary term associated with the odd powers of  $\omega$  will cancel out when integrated over the frequency domain. Further, substituting for  $A_{g\ell}$  and  $\dot{A}_{g\ell}$  from Eqs. 4.7 in Eq. 4.21, we obtain:

$$\begin{aligned} \text{Ex}[\{E'(t)\}\{E'(t)\}^T] &= \sum_{\ell=1}^3 ( A_{g\ell}^2 [G_1]^T \{d_\ell\} \{d_\ell\}^T [G_1] \\ &+ \dot{A}_{g\ell}^2 [G_2]^T \{d_\ell\} \{d_\ell\}^T [G_2] / 4c^2 ) \end{aligned} \quad (4.22)$$

Substituting Eq. 4.22 in Eq. 4.20,

$$\begin{aligned} \text{Ex}[S^2(t)] &= \sum_{j=1}^N \sum_{k=1}^N \frac{\xi_j \xi_k}{\omega_j^2 \omega_k^2} \\ &\sum_{\ell=1}^3 ( \{\gamma_j\}^T [G_1]^T \{d_\ell\} \{d_\ell\}^T [G_1] \{\gamma_k\} A_{g\ell}^2 + \\ &(1/4c^2) ( \{\gamma_j\}^T [G_2]^T \{d_\ell\} \{d_\ell\}^T [G_2] \{\gamma_k\} \dot{A}_{g\ell}^2 ) \end{aligned} \quad (4.23)$$

In Eq. 4.23, the terms like  $\{\gamma_j\}^T [G_1]^T \{d_\ell\}$  are scalars and, thus, they can also be rewritten as  $\{d_\ell\}^T [G_1] \{\gamma\}$ . Making such changes, Eq. 4.23 can be rewritten as:

$$\text{Ex}[S^2] = \sum_{\ell=1}^3 \{d_\ell\}^T [R_\ell^{(s)}] \{d_\ell\} \quad (4.24)$$

where the response matrix  $[R_\ell^{(s)}]$ , associated with the psuedo-static response, is defined as:

$$\begin{aligned} [R_\ell^{(s)}] = & \\ & \sum_{j=1}^N \sum_{k=1}^N \frac{\xi_j \xi_k}{\omega_j^2 \omega_k^2} ( [G_1] \{\gamma_j\} \{\gamma_k\}^T [G_1]^T A_{g\ell}^2 \\ & + \frac{1}{4c^2} [G_2] \{\gamma_j\} \{\gamma_k\}^T [G_2]^T A_{g\ell}^2 ) \end{aligned} \quad (4.25)$$

which can be rewritten as:

$$\begin{aligned} [R_\ell^{(s)}] = & \sum_{j=1}^N \sum_{k=1}^N \frac{\xi_j \xi_k}{\omega_j^2 \omega_k^2} \{ [\Gamma_{1jk}] A_{g\ell}^2 \\ & + [\Gamma_{2jk}] A_{g\ell}^2 \} \end{aligned} \quad (4.26)$$

Eq. 4.26 is identical to the first two terms of Eq. 4.6. Thus, the first two terms of Eq. 4.6 can be obtained by a psuedo-static analysis of Eq. 4.12.

We will now develop a procedure to obtain this psuedo-static response matrix in terms of  $A_{g\ell}$  and  $\dot{A}_{g\ell}$  without evaluation of the modal quantities.

We rewrite Eq. 4.12 as

$$[K]\{u_s\} = \sum_{p=1}^6 [M]\{r_p\} E_p'(t) \quad (4.27)$$

From this

$$\{u_s\} = \sum_{p=1}^6 \{u_{sp}\} E_p'(t) \quad (4.28)$$

where  $\{u_{sp}\}$  is obtained as a solution of the following linear simultaneous equations:

$$[K]\{u_{sp}\} = [M]\{r_p\} \quad (4.29)$$

The response quantity  $S'(t)$  can also be obtained from Eq. 4.28 as

$$S(t) = \sum_{p=1}^6 S_p' E_p'(t) \quad (4.30)$$

where

$$S_p' = \{k_i\}^T \{u_{sp}\} \quad (4.31)$$

Eq. 4.30 can also be rewritten as:

$$S(t) = \{S'\}^T \{E'\} \quad (4.32)$$

where now  $\{S'\}$  is a 6x1 vector. The mean square value of  $S(t)$  is then obtained as

$$Ex[S^2(t)] = \{S'\}^T Ex[\{E'\}\{E'\}^T] \{S'\} \quad (4.33)$$

Substituting for the covariance matrix from Eq. 4.22 and after some algebraic manipulation, we obtain

$$\begin{aligned} \text{Ex}[S^2(t)] &= \sum_{\ell=1}^3 \{d_{\ell}\}^T \left( [G_1] \{S'\} \{S'\}^T [G_1]^T A_{g\ell}^2 \right. \\ &\quad \left. + \frac{1}{4c^2} [G_2] \{S'\} \{S'\}^T [G_2]^T \dot{A}_{g\ell}^2 \right) \{d_{\ell}\} \end{aligned} \quad (4.34)$$

which can be rewritten as:

$$\text{Ex}[S^2] = \sum_{\ell=1}^3 \{d_{\ell}\}^T [R_{\ell}^{(s)}] \{d_{\ell}\} \quad (4.35)$$

where  $[R_{\ell}^{(s)}]$  is the response matrix associated with the psuedo-static response and is defined as:

$$\begin{aligned} [R_{\ell}^{(s)}] &= [G_1] \{S'\} \{S'\}^T [G_1]^T A_{g\ell}^2 \\ &\quad + \frac{1}{4c^2} [G_2] \{S'\} \{S'\}^T [G_2]^T \dot{A}_{g\ell}^2 \end{aligned} \quad (4.36)$$

By substituting for  $[G_1]$  and  $[G_2]$  from Eq. 3.1, and carrying out the matrix multiplications, a term of this matrix can be defined as follows:

$$\begin{aligned} R_{\ell mn}^{(s)} &= S'_{m \quad n} A_{g\ell}^2 \\ &\quad + \frac{1}{4c^2} \sum_{p=4}^6 \sum_{q=4}^6 G_{2mp} G_{2nq} S'_{p \quad q} \dot{A}_{g\ell}^2 \end{aligned} \quad (4.37)$$

It is seen that in the above equation, the first term is associated with the psuedo-static response for the translatory motion and the second term is due to the rotational effects.

Thus, to evaluate the first term of Eq. 4.6, we first need to obtain the six elements of  $\{S'\}$ . These are obtained

by a simple algebraic solution of linear Eqs. 4.29 and the use of Eq. 4.31. Eq. 4.37 then gives the terms required to define the first term of Eq. 4.6.

The total response, defined by Eq. 4.4, can now be written as a sum of the psuedo-static and dynamic responses. That is,

$$Ex(S^2) = \sum_{\ell=1}^3 \{d_{\ell}\}^T ([R_{\ell}^{(S)}] + [R_{\ell}^{(D)}]) \{d_{\ell}\} \quad (4.38)$$

in which an element of the dynamic response,  $[R_{\ell}^{(D)}]$ , is the same as Eq. 4.11 without the first two terms and a typical element of the static response matrix,  $[R_{\ell}^{(S)}]$ , is given by Eq. 4.37.

The mean square response for the case of purely translation components is obtained by neglecting the terms associated with the rotational effects. In such a case, an element of the response matrix  $[R_{\ell}]$  can be written a

$$\begin{aligned} R_{\ell mn} &= S'_m S'_n A^2_{g\ell} \\ &+ \sum_{j=1}^N (\xi_j^2 / 2\omega_j^4) \{ \Gamma_{lmnjk} [ 2\omega_j^2 (1 - 2\beta_j^2) I_{1\ell}(\omega_j) - I_{2\ell}(\omega_j) ] \\ &+ \sum_{j=1}^N \sum_{k=j+1}^N (\xi_j \xi_k / \omega_j^2 \omega_k^2) \\ &\Gamma_{lmnjk} [ F_1 I_{1\ell}(\omega_j) + F_2 I_{2\ell}(\omega_j) \\ &+ F_3 I_{1\ell}(\omega_k) + F_4 I_{2\ell}(\omega_k) + F_5 A^2_{g\ell} ] \end{aligned} \quad (4.39)$$

Here again, the first term represents the psuedo-static response and the remaining terms represent the dynamic part of the response.

The main advantage in the use of Eq. 4.11 or 4.39 is that only a first few modes are necessary in calculation of the response, because the terms associated with  $I_{1\ell}$  and  $I_{2\ell}$  become small

for the modes with frequencies higher than the input frequency.

To obtain the design response, Eq. 4.11 and 4.39 need to be multiplied by the square of the response peak factor. The peak factor can be evaluated as described in Chapter 2. The numerical results presented here, however, are only for the mean square response.

#### 4.3 THE WORST-CASE MEAN SQUARE RESPONSE

The evaluation of the worst-case response, irrespective of the orientation of the structure, is done in exactly the same manner as in Chapter 3. The only difference being that in Chapter 3 the response matrix  $[R_\ell]$  is defined by the mode displacement approach and here by the mode acceleration approach.

#### 4.4 NUMERICAL RESULTS

The main purpose of the development in this chapter was to alleviate the problem associated with the evaluation of the high frequency modes for the calculation of design response. It was claimed that if the mode acceleration approach is used, the higher modes can be excluded from the summation process without significantly affecting the accuracy of the results. Here, some numerical results are presented which support this claim and also demonstrate the advantages of adopting the mode acceleration approach over the mode displacement approach.

To show this, the torsional multistory structure used in Chapters 2 and 3 has been analyzed again. By changing the frequency parameter  $\omega = \sqrt{k/m}$ , flexible to stiff structural systems can be obtained.

The input to this structure consists of the five earthquake components: two translational components applied in the horizontal plane and three rotational components applied about the two horizontal axes and a vertical axis. The numerical results have been obtained for the root mean square response values of the story shears, torsional moment and column bending moments. To show the effectiveness of the mode acceleration formulation, the response results have been obtained with all nine modes (complete set) as well as

with only the the first three modes. The results are shown in Tables 4.1-4.5 and are in the mg-ft units. The values obtained with all nine modes are called "exact" values. Both formulations, the mode displacement presented in Chapter 3 and the mode acceleration presented in this chapter, provide exactly the same values when all the nine modes are used in the analysis. Two types of response values are obtained for each case:

1. The maximum response, in which the methodology described in section 3.5 was used. These values are shown in Column (1) for nine modes, in Column (3) for 3 modes with the mode displacement approach and in Column (5) for 3 modes with the mode acceleration approach. The values in Column (3) and (5) are shown in the ratio form. That is, they are divided by the values in Column (1).

2. The response, with inputs applied along the geometric axes of the structure, without making any search for the maximum response. These values are designated as "RS" in Tables 4.1 through 4.5 and their ratios to the values in Column (1) are shown in Columns (2), (4) and (6).

The Tables 4.1 through 4.3 are for a stiff system with frequency parameter,  $\omega = 50$  cps. The lowest frequency of this system is 20.8 Table 4.1 is for  $e/r = .01$  and has closely spaced modes, whereas Tables 4.2 and 4.3 are for  $e/r = .05$  and

$e/r=.30$ . The frequencies of the system with  $e/r=.30$  are not closely spaced.

The response ratios shown in Column (3) indicate that the mode displacement approach severely underestimates the response when only the first few modes are used. The mode acceleration approach, however, provides an excellent estimate of the response, even with the first few modes. Similar conclusion can be drawn for the response values shown in Columns (2); (4) and (6). The comparison of values in Column (2) with Column (1), Column (4) with Column (3) and Column (6) with Column (5) shows that if no search is made for the maximum value, the calculated response is likely to be underestimated. This underestimation is about 10 to 18% for the response values shown here. With other structural systems with gross asymmetry in the plan, the underestimation can be significantly large.

Tables 4.4 and 4.5 are for the structural systems which are not so stiff. In these cases it is seen that the mode displacement approach also gives better response values with only the first few modes. This is because the high frequency modes, which are neglected here, are not very dominant now. The values obtained by the mode acceleration approach are even better.

It is, thus, seen that the mode acceleration approach will, in general, provide more accurate response values than the mode displacement approach for the same number of modes used in the analysis. The use of the mode acceleration approach in lieu of the mode displacement approach is, thus, recommended.

It is, however, noted that the mode acceleration approach requires the input to be defined in terms of the relative acceleration and relative velocity spectra. Such prescriptions of the input are, rather, uncommon currently. The psuedo acceleration spectra are more commonly prescribed as the design inputs. However, in principle there should be no special difficulty in the development of the design inputs in the form of the relative spectra.

## Chapter V

### SUMMARY AND CONCLUSIONS

This study is centered around the subject of evaluation of the design response of structures subjected to multicomponent earthquake motions. For design purposes, the earthquake motions are often characterized by the smoothed ground response spectra which supposedly represent the spectral characteristics of the ground motions expected at a site. The analytical development work in this study has, therefore, been directed toward the development of approaches which can employ the ground spectra as inputs in their methodology for the calculation of design response.

The method of the square-of-the-sum-of-the-squares is commonly used for the calculation of the design response from given response spectra. In Chapter 2, this method has been reevaluated and refined to include the modal peak factors in the calculation of design response for the classically as well as nonclassically damped structural systems subjected to three uncorrelated excitation components applied along the structural axes. The concept of the modal correlation often used in the context of closely spaced modes has been further explored, especially for the multicomponent excitations and the nonclassically damped systems.

It is observed that though the correlation between two closely-spaced modes may be strong and significant for one component of excitation, it loses its significance when multicomponents are considered. In fact, the significance of this correlation, and thus the importance of the double summation terms in the mode combination procedures, can not be assessed in a straightforward manner when nonproportionally damped systems under multicomponent excitations are considered. Since the evaluation of the double summation terms in the mode combination rules does not pose any special problem, their inclusion in all the cases is advocated, irrespective of the closeness of the modal frequencies.

As several assumptions are made in the development of response spectrum procedures, a comprehensive numerical simulation study involving an ensemble of acceleration time histories has been conducted for the validation of the proposed approaches. For the time history analysis of the proportionally damped systems, an already available modal superposition approach has been used. For nonproportionally damped structures, a new modal superposition time history integration approach has been developed and used. The results obtained by the response spectrum approaches for time history ensemble spectra as input have been compared with the time history ensemble results, both for the proportionally and nonproportionally damped structures. The compari-

son shows that the response spectrum approaches both for the proportionally and nonproportionally damped structures can be used for the accurate predictions of the design responses from the ground spectra. The inclusion of the modal peak factors in the spectrum approaches can improve the numerical accuracy of the results. For the calculation of the peak factors, the easy-to-use band-limited white noise spectral density function, with cut-off frequency encompassing the frequencies of the input, can be employed. In an overall sense, the results presented in Chapter 2 validate the applicability of the response spectrum approaches for the proportionally and nonproportionally damped linear structures for the calculation of the design response.

In Chapter 3, the effect of the inevitable correlation between the earthquake components, experienced by structures along arbitrary sets of axes, is considered. Based on the assumption of the existence of the principal excitation directions, as observed by Penzien, et. al. [26,27], the correlation between the translation as well as the rotational components of excitation has been evaluated. The rotational components are expressed in terms of the spatial derivative of the translation components and the shear wave velocity, as was done by Newmark [23]. The correlation matrix of the six components applied along any arbitrary set of structural axes is expressed in terms of the autocorrelation of the

principal components and the direction cosines of the principal excitation axes. A procedure is developed to obtain the maximum value of a structural response quantity, irrespective of the orientation of the structure. The numerical results obtained by this procedure are presented for the proportionally and nonproportionally damped structures. It is shown that a search for the maximum response, as described in this chapter, should be made; otherwise the calculated response may be significantly underestimated.

The numerical results, showing the effect of the rotational components, have also been presented in Chapter 3. It is shown that the contribution of the rotational components can be very large. This contribution increases with the size of the structure. For example, a taller structure will be affected more than a shorter structure. Likewise, a larger structure in plan will also be affected more than a smaller structure because of differential movement caused by the passage of the seismic shear wave. The effect of the rotational components, however, decreases with higher shear wave velocity. The results indicate that the effect of the rotational components can not be ignored simply on the basis of a preconceived notion that these components are unimportant. The results presented here clearly demonstrate the importance of the rotational components. However, further

research in this area, especially with a more advanced model of seismic wave propagation to define these components is also necessary.

In Chapter 4, the approach of Chapter 3 is applied to develop a response spectrum approach based on the mode acceleration method of structural dynamics. The use of such an approach is especially desirable if the high frequency structural modes contribute to the response significantly. This happens in stiff structural systems. In the commonly used mode displacement approach, such high modes must be calculated explicitly and included in the modal analysis. In the mode acceleration formulation, these modes, however, need not be calculated explicitly; their effect can be included through a simple static analysis of the structure. The input in this approach must be prescribed in terms of the relative acceleration and relative velocity spectra of the ground motion. Again, the formulation in this chapter considers all six earthquake components. The possible correlation between the six components is also considered. The solution is cast in such a form that the maximum response evaluation methodology, developed in Chapter 3 can be used. The numerical results, demonstrating the benefits of this alternative formulation, and also the importance of the rotational components in the calculation of the design response, are presented.

## REFERENCES

1. Amin, M. and Ang, A. H. S., "Nonstationary Stochastic Model of Earthquake Motion", Journal of Engineering Mechanics Division, ASCE, Vol. 94, No. EM2, April 1968.
2. Amin, M. and Gungor, I., "Random Vibration in Seismic Analysis- An Evaluation", Proceedings, ASCE National Meeting on Structural Engineering, Baltimore, MD, April 19-23, 1971.
3. Bisplinghoff, R.L., Isakson, G. and Pian, T.H., "Method in Transient Stress Analysis", Journal of the Aeronautical Science, Vol. 17, No. 5, May 1950.
4. Bogdanoff, J.L., Goldberg, J.E. and Schiff A.J., "The Effect of Ground Transmission Time on the Response of Long Structures", Bulletin of Seismological Society of America, Vol. 55, No. 3, pp. 627-640, June 1965.
5. Caughey, T.K., "Classical Normal Modes in Damped Linear Dynamic System", Journal of Applied Mechanics, Vol. 27, June 1960, pp.269-271.
6. Clough, R.W. and Mojtahedi, S., "Earthquake Response Analysis Considering Non-Proportional Damping", Journal of Earthquake Engineering and Structural Dynamics, Vol. 4, pp. 489-496 (1976).
7. Clough, R.W. and Penzin, J., Dynamics of Structures, McGraw Hill, 1975.
8. Chu, S.L., Amin, M. and Singh, S., "Spectral Treatment of Actions of Three Earthquake Components on Structures", Nuclear Engineering and Design, Vol.21, pp. 126-136, 1976.
9. DerKiureghian, A., "A Response Spectra Method For Random Vibration Analysis of MDF Systems", Journal of Earthquake Engineering and Structural Dynamics, Vol. 9, pp. 419-435 (1981).
10. Foss, K.A., "Coordinates Which Uncouple the Equations of Motion of Damped Linear Dynamic System", Journal of Applied Mechanics, Vol. 25, Sept. 1958, pp. 361-364.

11. Gaspirani, D. and Vanmarcke, E.H., "Simulated Earthquake Motions Compatible With Prescribed Response Spectra", Publication No. 76-4, Department of Civil Engineering, M.I.T., Jan. 1975.
12. Ghafory-Ashtiany, M., "Seismic Response of Structural System With Random Parameters", M.S. Thesis, Department of Engineering Science and Mechanics, Virginia Polytechnic Institute and State University. May 1981.
13. Housner, G.W., "Design Spectrum", Chapter 5, Earthquake Engineering, Ed. R.L. Weigel, Printice Hall, Inc. Englewood Cliffs, NJ. 1970.
14. Itoh T., "Damped vibration Mode Superposition Method for Dynamic Response Analysis", Journal of Earthquake Engineering and Structural Dynamics, Vol. 2, pp. 47-57 (1973)
15. Kanai, K., "An Empirical Formula for the Spectrum of Strong Earthquake Motions", Bulletin of Earthquake Research Institute, University of Tokyo, Vol. 39, pp. 85-95 (1961).
16. Kubo, C.L. and Penzin, J., "Analysis of Three-Dimensional Strong Ground Motions Along Principal Axes, San Fernando Earthquake", Journal of Earthquake Engineering and Structural Dynamics, Vol. 7, pp. 265-278 (1979).
17. Kubo, C.L. and Penzin, J., "Simulation of Three-Dimensional Strong Ground Motions Along Principal Axes, San Fernando Earthquake", Journal of Earthquake Engineering and Structural Dynamics, Vol. 7, pp. 279-294 (1979).
18. Leonard, J.W., "An Improved Modal Synthesis Method for Transient Response of Piping System", 3rd SMIRT Conference, Paper K7/2, September 1-15, 1979.
19. Longuet-Higgins, M.S. "On the Statistical Distribution of the Height of Sea Waves", Journal of Marine Res. Vol. 2, 245-266 (1952)
20. Mason A.B., "Some Observations on the Random Response of Linear and Nonlinear Dynamical System", Report No. EERL 79-01, Earthquake Engr. Research Laboratory, California Inst. of Technology, Pasadena, Calif., Jan. 1979.
21. Meirovitch, L., Analytical Method in Vibration, Macmillan Co., New York, 1967.

22. Nathan, N.D. and MacKenzie, J.R., "Rotational Components of Earthquake Motion", Canadian Journal of Civil Engineering, Vol. 2, pp. 430-436 (1975).
23. Newmark, N.M., "Torsion in Symmetrical Building", Proceeding of the Fourth World Conference on Earthquake Engineering, Santiago, Chile, 2, A.3, 19-32.
24. Newmark, N.M., Blume, J.A. and Kapur, K.K., "Seismic Design Spectra for Nuclear Power Plants", Journal of Power Division, ASCE, Vol. 99, 1973.
25. Nigam N.C. and Jennings, P.C., "Calculation of Response Spectra from Strong Motion Earthquake Records", Bulletin of Seismological Society of America, Vol. 59, No. 2, April 1969, pp. 909-922.
26. Penzin, J. and Watabe, M., "Characteristics of 3-Dimensional Earthquake Ground Motions", Journal of Earthquake Engineering and Structural Dynamics, Vol. 3, pp. 365-373 (1975).
27. Penzin, J. and Watabe, M., "Simulation of 3-Dimensional Earthquake Ground Motions", Bulletin of international Institute of Seismology and Earthquake Engineering, Vol. 12, pp. 103-115 (1976).
28. Rosenblueth, E., "Tall Building Under Five-Components Earthquake" Proceedings, ASCE, Journal of Structural Division, Vol. 102, No. 2, Feb. 1976, pp. 453-459.
29. Rosenblueth E., "The Six Components of Earthquakes", Proceeding of the Twelfth Regional Conference on Planning and Design of Tall Buildings, Sydney, Australia, 1973, pp. 63-81.
30. Rosenblueth E. and Elorduy, "Response of Linear System to Certain Transient Displacement", Proceeding of The Fourth World Conference on Earthquake Engineering, Vol. 1, Santiago, Chile, 1969.
31. Singh, A.K., Chu, S.L. and Singh, S., "Influence of Closely Spaced Modes in Response Spectrum Method of Analysis", Proceedings, ASCE Specialty Conference on Structural Design of Nuclear Plant Facilities, Chicago, IL. Dec. 1973.
32. Singh, M.P., "Seismic Design Input For Secondary Systems" ASCE, Journal of the Structural Division, Vol.

- 106, No. ST2, Proceeding Paper 15207, Feb. 1980, pp. 505-517.
33. Singh, M.P., "Seismic Response by SRSS for Nonproportional Damping", Journal of the Engineering Mechanics Division, ASCE, Vol. 106, No. EM6, Proc. Paper 15948, Dec. 1980, pp. 1405-1419.
  34. Singh, M.P., "Seismic Response Combination of High Frequency Modes", Proceeding of 7th European Conference on Earthquake Engineering, Athen, Greece, Sept. 20-25, 1982.
  35. Singh, M.P., and Chu, S.L., "Stochastic Consideration in Seismic Analysis of Structures", Journal of Earthquake Engineering and Structural Dynamics, Vol. 4, pp. 295-307 (1976)
  36. Singh, M.P., and Ghafory-Ashtiany, M., "Seismic Stability Evaluation of Earth Structures", Report No. VPI-E-80.30, Virginia Polytechnic Institute and State University. August 1980.
  37. Singh, M.P., and Ghafory-Ashtiany, M., "Maximum Response of Nonproportionally and Proportionally Damped Systems Under Multicomponent Earthquakes", Report No. VPI-E-83-10, Virginia Polytechnic Institute and State University. March 1983.
  38. Singh, M.P. and Mehta, K.B., "Seismic Design Response by an Alternative SRSS Rule", Report No. VPI-E-83-12, Virginia Polytechnic Institute and State University. March 1983.
  39. Tajimi, H., "A Statical Method of Determining the Maximum Response of a Building Structure During an Earthquake", Proc. of second WCEE, Tokyo, Vol. 2, pp. 781-797, Science Council of Japan, 1960.
  40. Tso, W.K. and Hsu, T.I., "Torsional Spectrum for Earthquake Motion", Journal of Earthquake Engineering and Structural Dynamics, Vol. 6, pp. 375-382 (1978)
  41. U.S. Nuclear Regulatory Commission, "Design response Spectrum For Nuclear Power Plants", Nuclear Regulatory Guide No. 1.60, Washington D.C., 1975.
  42. Vanmarcke, E.H., "Seismic Structural Response", Chapter 8, in Seismic Risk and Engineering Decisions, Ed. C.

- Lomnitz and E. Rosenblueth, Elsevier scientific Publishing Co., New York, 1976.
43. Vanmarcke, E.H., "Properties of Spectral Moments With Applications to Random Vibration" Journal of Engineering Mechanic Division, ASCE, Vol. 98, No. EM2, Proc. Paper 8859, April 1972, pp.425-446.
  44. Vanmarcke, E.H, "On the Distribution of the First Passage Time for Normal Stationary Random Process", Journal of Applied Mechanics, Vol. 42, March 1975, pp.215-220.
  45. William, D., "Displacement of Linear Elastic System Under a Given Transient Load", The Aeronautical Quarterly, Vol. 1, August 1949, pp.123-136.

TABLE 2.1  
DYNAMIC CHARACTERISTICS OF STRUCTURE IN FIG. 2.1,  $e/r=.01$

Mode No.	COMPLEX MODE APPROACH		NORMAL MODE APPROACH			
	Frequency	Damping	Frequency	Damping	Participation fact.	
	cps.	Ratio	cps.	Ratio	$x_1$ -direc	$x_2$ -direc
1	4.4475	.0222	4.4163	.0226	0.8309	-0.8309
2	4.4480	.0109	4.4482	.0225	1.1709	1.1709
3	4.4489	.0336	4.4797	.0224	-0.8251	0.8251
4	12.4620	.0623	12.3760	.0619	0.2378	-0.2378
5	12.4630	.0256	12.7640	.0623	0.3351	0.3351
6	12.4650	.0991	12.5520	.0628	-0.2361	0.2361
7	18.0080	.0901	17.8830	.0895	-0.0913	0.0913
8	18.0100	.0365	18.0100	.0901	-0.1287	-0.1287
9	18.0130	.1437	18.1380	.0907	0.0907	-0.0907

TABLE 2.2  
DYNAMIC CHARACTERISTICS OF STRUCTURE IN FIG. 2.1,  $e/r=.05$

Mode No.	COMPLEX MODE APPROACH		NORMAL MODE APPROACH			
	Frequency	Damping	Frequency	Damping	Participation fact.	
	cps.	Ratio	cps.	Ratio	$x_1$ -direc	$x_2$ -direc
1	4.3041	.0214	4.2937	.0215	0.8425	-0.8425
2	4.4500	.0222	4.4482	.0223	1.1709	1.1709
3	4.5952	.0231	4.6082	.0231	-0.8132	0.8132
4	12.3206	.0587	12.0307	.0602	0.2411	-0.2411
5	12.4998	.0481	12.4635	.0623	0.3351	0.3351
6	12.5713	.0804	12.9119	.0646	-0.2328	0.2328
7	17.9356	.0892	17.3847	.0870	-0.0926	0.0926
8	17.9999	.0492	18.0102	.0901	-0.1287	-0.1287
9	18.0953	.1321	18.6581	.0933	0.0894	-0.0894

TABLE 2.3

MODAL CORRELATION COEFFICIENTS FOR PROPORTIONALLY DAMPED STRUCTURE SHOWN IN FIG. 2.1,  $e/r=0.01$

Excitation Along  $x_1$

j \ i	Mode Number								
	1	2	3	4	5	6	7	8	9
1	1.0								
2	0.973	1.0							
3	0.901	0.974	1.0						
4	0.168	0.173	0.179	1.0					
5	0.169	0.174	0.180	0.999	1.0				
6	0.170	0.176	0.181	0.995	0.999	1.0			
7	0.215	0.222	0.229	0.758	0.763	0.766	1.0		
8	0.216	0.223	0.229	0.758	0.763	0.766	1.000	1.0	
9	0.217	0.223	0.230	0.758	0.762	0.765	0.999	1.000	1.0

Excitation Along  $x_1$  And  $x_2$

j \ i	Mode Number								
	1	2	3	4	5	6	7	8	9
1	1.0								
2	-0.064	1.0							
3	0.901	-0.064	1.0						
4	0.170	0.002	0.182	1.0					
5	0.006	0.177	-0.003	0.013	1.0				
6	0.172	0.002	0.184	0.995	0.014	1.0			
7	0.217	0.004	0.231	0.755	0.037	0.764	1.0		
8	0.008	0.225	-0.001	0.033	0.760	0.038	0.010	1.0	
9	0.219	0.004	0.232	0.755	0.037	0.763	0.299	0.009	1.0

TABLE 2.4

MODAL CORRELATION COEFFICIENTS FOR PROPORTIONALLY DAMPED STRUCTURE SHOWN IN FIG. 2.1,  $e/r=0.05$

Excitation Along  $x_1$

j \ i	Mode Number								
	1	2	3	4	5	6	7	8	9
1	1.0								
2	0.567	1.0							
3	0.244	0.618	1.0						
4	0.140	0.170	0.188	1.0					
5	0.145	0.174	0.194	0.965	1.0				
6	0.150	0.181	0.200	0.908	0.978	1.0			
7	0.185	0.219	0.242	0.739	0.767	0.779	1.0		
8	0.188	0.223	0.245	0.738	0.763	0.773	0.991	1.0	
9	0.191	0.226	0.249	0.739	0.762	0.771	0.969	0.992	1.0

Excitation Along  $x_1$  And  $x_2$

j \ i	Mode Number								
	1	2	3	4	5	6	7	8	9
1	1.0								
2	0.016	1.0							
3	0.298	-0.018	1.0						
4	0.143	0.002	0.190	1.0					
5	0.024	0.177	-0.006	-0.000	1.0				
6	0.153	0.002	0.202	0.907	0.017	1.0			
7	0.187	0.003	0.243	0.737	0.037	0.776	1.0		
8	0.029	0.225	-0.005	0.016	0.760	0.030	0.011	1.0	
9	0.193	0.004	0.250	0.736	0.037	0.768	0.969	0.009	1.0

TABLE 2.5

MODAL CORRELATION COEFF. FOR BASE SHEARS AND TORSIONAL MOM.  
FOR NONPROPORTIONALLY DAMPED STRUC. SHOWN IN FIG 2.1,  
 $e/r=.01$

Base Story Shear in  $x_1$ 

j \ i	Mode Number								
	1	2	3	4	5	6	7	8	9
1	1.000								
2	-0.940	1.000							
3	-0.975	0.858	1.000						
4	0.124	-0.087	-0.136	1.000					
5	-0.090	0.063	0.098	-0.921	1.000				
6	-0.157	0.109	0.172	-0.967	0.820	1.000			
7	0.157	-0.110	-0.173	0.678	-0.529	-0.708	1.000		
8	-0.125	0.087	0.138	-0.539	0.420	0.560	-0.937	1.000	
9	-0.185	0.130	0.206	-0.765	0.597	0.811	-0.972	0.854	1.000

Base Story Shear in  $x_2$ 

j \ i	Mode Number								
	1	2	3	4	5	6	7	8	9
1	1.000								
2	-0.940	1.000							
3	-0.979	0.861	1.000						
4	0.122	-0.086	-0.150	1.000					
5	-0.091	0.063	0.112	-0.924	1.000				
6	-0.140	0.098	0.173	-0.982	0.848	1.000			
7	0.154	-0.108	-0.189	0.678	-0.526	-0.743	1.000		
8	-0.126	0.089	0.155	-0.552	0.427	0.607	-0.943	1.000	
9	-0.168	0.118	0.206	-0.735	0.573	0.804	-0.988	0.890	1.000

## Torsional Moment

j \ i	Mode Number								
	1	2	3	4	5	6	7	8	9
1	1.000								
2	-0.940	1.000							
3	-0.979	0.861	1.000						
4	-0.041	0.030	0.049	1.000					
5	0.034	-0.025	-0.042	-0.907	1.000				
6	0.046	-0.034	-0.055	-0.974	0.806	1.000			
7	-0.054	0.039	0.065	0.214	-0.147	-0.272	1.000		
8	0.048	-0.035	-0.059	-0.093	0.065	-0.125	-0.904	1.000	
9	0.061	-0.045	-0.074	-0.308	0.215	0.379	-0.974	0.804	1.000

TABLE 2.6

MODAL CORRELATION COEFF. FOR BENDING MOMENTS IN COL. 1 FOR  
NONPROPORTIONALLY DAMPED STRUCTURE SHOWN IN FIG. 2.1,  
 $e/r=.01$

Bending Moment in  $x_1$ 

j \ i	Mode Number									
	1	2	3	4	5	6	7	8	9	
1	1.000									
2	-0.920	1.000								
3	-0.714	0.492	1.000							
4	-0.009	0.027	-0.106	1.000						
5	0.009	-0.021	0.070	-0.909	1.000					
6	0.061	-0.074	0.120	-0.445	0.385	1.000				
7	-0.008	0.030	-0.125	0.279	-0.189	-0.532	1.000			
8	0.014	-0.029	0.094	-0.150	0.101	0.438	-0.907	1.000		
9	0.052	-0.071	0.147	-0.098	0.078	0.802	-0.478	0.486	1.000	

Bending Moment in  $x_2$ 

j \ i	Mode Number									
	1	2	3	4	5	6	7	8	9	
1	1.000									
2	-0.668	1.000								
3	-0.962	0.488	1.000							
4	-0.030	0.038	0.025	1.000						
5	-0.126	0.076	0.145	-0.388	1.000					
6	0.038	-0.049	-0.031	0.975	0.376	1.000				
7	-0.048	0.050	0.045	0.205	0.106	-0.268	1.000			
8	-0.161	0.105	0.182	-0.308	0.423	0.364	-0.290	1.000		
9	0.035	-0.047	-0.028	-0.325	-0.037	0.405	-0.966	0.377	1.000	

TABLE 2.7

MODAL CORRELATION COEFF. FOR BASE SHEARS AND TORSIONAL MOM.  
FOR NONPROPORTIONALLY DAMPED STRUC. SHOWN IN FIG 2.1,  
 $e/r=.05$

Base Story Shear in  $x_1$ 

j \ i	Mode Number									
	1	2	3	4	5	6	7	8	9	
1	1.000									
2	0.170	1.000								
3	-0.430	0.128	1.000							
4	0.024	-0.071	-0.141	1.000						
5	0.005	0.123	0.187	-0.558	1.000					
6	-0.023	0.088	0.166	-0.983	0.533	1.000				
7	0.008	-0.119	-0.196	0.641	-0.303	-0.702	1.000			
8	-0.004	0.118	0.189	-0.599	0.298	0.657	-0.976	1.000		
9	0.001	0.153	0.237	-0.727	0.430	0.799	-0.961	0.932	1.000	

Base Story Shear in  $x_2$ 

j \ i	Mode Number									
	1	2	3	4	5	6	7	8	9	
1	1.000									
2	-0.642	1.000								
3	0.338	-0.677	1.000							
4	0.116	-0.121	0.127	1.000						
5	-0.125	0.132	-0.138	-0.928	1.000					
6	-0.024	0.025	-0.025	-0.583	0.243	1.000				
7	0.132	-0.138	0.144	0.615	-0.424	-0.659	1.000			
8	-0.123	0.129	-0.134	-0.560	0.386	0.601	-0.978	1.000		
9	-0.134	0.140	-0.146	-0.638	0.442	0.682	-0.991	0.945	1.000	

## Torsional Moment

j \ i	Mode Number									
	1	2	3	4	5	6	7	8	9	
1	1.000									
2	-0.637	1.000								
3	0.068	-0.718	1.000							
4	0.066	0.075	-0.126	1.000						
5	0.015	0.096	-0.088	-0.428	1.000					
6	-0.085	-0.160	0.210	-0.647	-0.410	1.000				
7	0.088	0.112	-0.176	0.220	0.398	-0.540	1.000			
8	-0.053	-0.053	0.096	-0.169	-0.164	0.324	-0.915	1.000		
9	-0.106	-0.133	0.210	-0.276	-0.400	0.634	-0.979	0.822	1.000	



TABLE 2.8

MODAL CORRELATION COEFF. FOR BENDING MOMENTS IN COL. 1 FOR  
NONPROPORTIONALLY DAMPED STRUC. SHOWN IN FIG. 2.1,  $e/r=.05$

Bending Moment in  $x_1$ 

j \ i	Mode Number									
	1	2	3	4	5	6	7	8	9	
1	1.000									
2	-0.658	1.000								
3	-0.452	-0.013	1.000							
4	0.191	-0.070	-0.201	1.000						
5	-0.016	0.034	0.026	-0.222	1.000					
6	-0.191	0.057	0.197	-0.859	-0.302	1.000				
7	0.223	-0.095	-0.237	0.605	0.281	-0.768	1.000			
8	-0.172	0.079	0.185	-0.484	-0.181	0.592	-0.900	1.000		
9	-0.233	0.093	0.246	-0.620	-0.327	0.805	-0.960	0.750	1.000	

Bending Moment in  $x_2$ 

j \ i	Mode Number									
	1	2	3	4	5	6	7	8	9	
1	1.000									
2	-0.725	1.000								
3	0.554	-0.744	1.000							
4	0.087	-0.068	0.058	1.000						
5	-0.146	0.156	-0.146	-0.781	1.000					
6	0.110	-0.158	0.156	-0.197	-0.457	1.000				
7	0.049	-0.026	0.019	0.297	-0.120	-0.251	1.000			
8	-0.130	0.140	-0.131	-0.522	0.452	0.036	-0.787	1.000		
9	0.005	-0.050	0.055	-0.157	-0.083	0.378	-0.941	0.548	1.000	

TABLE 2.9

MODAL CORREL. COEFF. FOR BASE SHEARS AND TORS. MOM. FOR  
NONPROP. DAMPED STRUC. SHOWN IN FIG. 2.1 FOR TWO INPUTS,  
 $e/r=.01$

EXCITATION ALONG  $x_1$  AND  $x_2$   
Base Story Shear in  $x_1$

j \ i	Mode Number								
	1	2	3	4	5	6	7	8	9
1	1.000								
2	-0.716	1.000							
3	-0.744	0.140	1.000						
4	0.124	-0.066	-0.105	1.000					
5	-0.066	0.064	0.010	-0.657	1.000				
6	-0.112	0.010	0.172	-0.693	0.015	1.000			
7	0.157	-0.084	-0.134	0.682	-0.380	-0.508	1.000		
8	-0.092	0.091	0.014	-0.399	0.439	0.008	-0.667	1.000	
9	-0.131	0.011	0.205	-0.545	0.008	0.811	-0.694	0.008	1.000

Base Story Shear in  $x_2$

j \ i	Mode Number								
	1	2	3	4	5	6	7	8	9
1	1.000								
2	-0.716	1.000							
3	-0.747	0.140	1.000						
4	0.122	-0.065	-0.116	1.000					
5	-0.066	0.065	0.011	-0.658	1.000				
6	-0.100	0.009	0.172	-0.704	0.016	1.000			
7	0.154	-0.082	-0.146	0.682	-0.376	-0.533	1.000		
8	-0.092	0.091	0.015	-0.404	0.439	0.009	-0.668	1.000	
9	-0.119	0.010	0.205	-0.524	0.008	0.804	-0.705	0.008	1.000

Torsional Moment

j \ i	Mode Number								
	1	2	3	4	5	6	7	8	9
1	1.000								
2	-0.717	1.000							
3	-0.746	0.140	1.000						
4	-0.028	0.010	0.035	1.000					
5	0.009	-0.009	-0.001	-0.649	1.000				
6	0.033	-0.003	-0.055	-0.695	0.015	1.000			
7	-0.025	0.001	0.045	0.237	-0.117	-0.195	1.000		
8	-0.000	-0.000	0.000	-0.101	0.086	0.002	-0.644	1.000	
9	0.044	-0.004	-0.074	-0.218	0.002	0.379	-0.692	0.007	1.000



TABLE 2.10

MODAL CORREL. COEFF. FOR BASE SHEARS AND TORS. MOM. FOR  
NONPROP. DAMPED STRUC. SHOWN IN FIG. 2.1 FOR TWO INPUTS,  
 $e/r=.05$

EXCITATION ALONG  $x_1$  AND  $x_2$   
Base Story Shear in  $x_1$

j \ i	Mode Number									
	1	2	3	4	5	6	7	8	9	
1	1.000									
2	-0.244	1.000								
3	-0.043	-0.271	1.000							
4	0.075	-0.098	0.005	1.000						
5	-0.076	0.116	-0.028	-0.792	1.000					
6	-0.025	0.069	0.103	-0.739	0.282	1.000				
7	0.075	-0.130	-0.020	0.628	-0.347	-0.616	1.000			
8	-0.089	0.103	-0.075	-0.486	0.337	0.287	-0.803	1.000		
9	-0.012	0.120	0.154	-0.520	0.225	0.782	-0.742	0.250	1.000	

Base Story Shear in  $x_2$

j \ i	Mode Number									
	1	2	3	4	5	6	7	8	9	
1	1.000									
2	0.088	1.000								
3	0.412	0.043	1.000							
4	-0.037	-0.131	0.065	1.000						
5	0.080	0.124	-0.046	-0.882	1.000					
6	-0.026	0.004	-0.026	-0.284	0.026	1.000				
7	-0.045	-0.147	0.076	0.515	-0.450	-0.517	1.000			
8	0.122	0.111	-0.019	-0.311	0.417	0.187	-0.792	1.000		
9	-0.077	0.109	-0.107	-0.473	0.226	0.660	-0.764	0.239	1.000	

Torsional Moment

j \ i	Mode Number									
	1	2	3	4	5	6	7	8	9	
1	1.000									
2	-0.214	1.000								
3	-0.248	-0.266	1.000							
4	0.050	-0.006	-0.049	1.000						
5	-0.044	0.088	-0.021	-0.821	1.000					
6	-0.004	-0.150	0.120	-0.186	-0.393	1.000				
7	0.021	0.062	-0.069	0.160	0.077	-0.406	1.000			
8	0.008	-0.000	-0.009	-0.107	0.056	0.071	-0.746	1.000		
9	-0.049	-0.110	0.137	-0.110	-0.239	0.621	-0.753	0.173	1.000	

TABLE 2.11

MODAL PEAK FACTORS FOR THREE DIFFERENT INPUTS,  $e/r=.05$ ,  $s=$   
7 SEC.,  $p = 0.5$

Mode Number (1)	Response Spectra	Kanai-Tajimi SDF		White Noise SDF	
	$C_{1dj}$ (2)	$C_{2dj}$ (3)	$C_{1vj}$ (4)	$C_{2dj}$ (5)	$C_{1vj}$ (6)
1	2.830	2.719	2.986	2.870	3.003
2	2.843	2.739	2.998	2.883	3.014
3	2.857	2.759	3.010	2.896	3.025
4	3.190	3.188	3.295	3.221	3.274
5	3.180	3.194	3.305	3.232	3.280
6	3.201	3.200	3.315	3.243	3.287
7	3.241	3.231	3.395	3.333	3.335
8	3.283	3.233	3.404	3.343	3.340
9	3.210	3.235	3.413	3.354	3.345

TABLE 2.12

KANAI-TAJIMI SPECTRAL DENSITY FUNCTION, EQ. 2.73

i	$s_i$ ft <sup>2</sup> -Sec/rad	$\omega_i$ Rad/Sec	$\beta_i$
1	0.0015	13.5	0.3925
2	0.000495	23.5	0.3600
3	0.000375	39.0	0.3350

TABLE 2.14

MEAN BENDING MOMENT RESPONSES OF COL. 1 OF STRUCTURE IN FIG. 2.1 FOR 15 SEC. INPUTS IN  $x_1$ -DIREC.,  $e/r=.01$

	Type of Response Quantity (1)	Time History Response (2)	RS Time History (3)	RS With Peak Factor Time History		
				Resp. Spectra (4)	Kanai-Tajimi (5)	White Noise (6)
C O M P O S I T I O N A L	Bending Moment in $x_1$ -Direc.	42.0384	0.95	0.95	0.79	0.88
	Bending Moment in $x_2$ -Direc.	3.0408	0.78	0.73	---	---
N O M O D A L	Bending Moment in $x_1$ -Direc.	49.5760	0.99	1.01	1.10	1.03
	Bending Moment in $x_2$ -Direc.	3.9945	1.42	1.23	1.28	1.22
E R R O R	$x_1$ -Direc.	17.9	23.4			
	$x_2$ -Direc.	31.4	138.0			

TABLE 2.13

MEAN BASE SHEAR AND TORSIONAL MOMENT RESPONSE OF STRUCTURE IN FIG 2.1 FOR 15 SEC. INPUTS IN  $x_1$ -DIREC.,  $e/r=.01$

	Type of Response Quantity (1)	Time History Response (2)	RS Time History (3)	RS With Peak Factor Time History		
				Resp. Spectra (4)	Kanai-Tajimi (5)	White Noise (6)
C O M P O S I T I O N A L	Base Shear in $x_1$ -Direc	24.1824	1.00	1.01	1.09	1.03
	Base Shear in $x_2$ -Direc	0.6982	1.13	0.80	1.50	1.00
	Torsional Moment	2.5668	1.10	1.00	1.01	1.00
N O M O D A L	Base Shear in $x_1$ -Direc	28.4551	0.99	1.00	1.10	1.03
	Base Shear in $x_2$ -Direc	0.5265	1.62	1.37	1.46	1.14
	Torsional Moment	3.1378	1.41	1.23	1.27	1.12
P E R C E N T	$x_1$ -Direc.	17.7	16.6			
	$x_2$ -Direc.	-14.7	22.4			
	Torsion	34.8	72.9			

TABLE 2.15

MEAN BASE SHEAR AND TORSIONAL MOMENT RESPONSE OF STRUCTURE  
IN FIG. 2.1 FOR 30 SEC. INPUTS IN  $x_1$ -DIREC.,  $e/r=0.01$

	Type of Response Quantity (1)	Time History Response (2)	RS	RS With Peak Factor		
			Time History (3)	Time History (4)	Resp. Spectra (4)	Kanai-Tajimi (5)
C O M P O S I T I O N A L	Base Shear in $x_1$ -Direc	28.7411	1.03	1.04	1.10	1.05
	Base Shear in $x_2$ -Direc	0.8856	1.22	0.42	1.47	1.10
	Torsional Moment	3.0679	1.11	1.01	1.05	1.01
N O M O D A L	Base Shear in $x_1$ -Direc	34.5225	1.03	1.04	1.11	1.06
	Base Shear in $x_2$ -Direc	0.7160	1.38	1.29	1.31	1.08
	Torsional Moment	4.1635	0.81	1.17	1.17	1.12
P E R C E N T	$x_1$ -Direc.	20.1	20.0			
	$x_2$ -Direc.	-16.4	-5.4			
	Torsion	20.4	50.9			

TABLE 2.16

MEAN BENDING MOMENT RESPONSES OF COL. 1 OF STRUCTURE IN FIG.  
2.1 FOR 30 SEC. INPUTS IN  $x_1$ -DIREC.,  $e/r=0.01$

	Type of Response Quantity (1)	Time History Response (2)	RS	RS With Peak Factor		
			Time History (3)	Time History (4)	Resp. Spectra (4)	Kanai-Tajimi (5)
C O M P O S I T I O N A L	Bending Moment in $x_1$ -Direc.	50.1255	0.96	0.97	0.84	0.92
	Bending Moment in $x_2$ -Direc.	3.8340	1.08	1.07	---	---
N O M O D A L	Bending Moment in $x_1$ -Direc.	60.3229	1.03	1.03	1.11	1.06
	Bending Moment in $x_2$ -Direc.	5.2751	1.25	1.18	1.18	1.13
E R R O R	$x_1$ -Direc.	20.3	28.1			
	$x_2$ -Direc.	31.8	52.1			

TABLE 2.17

MEAN BASE SHEAR AND TORSIONAL MOMENT RESPONSE OF STRUCTURE  
IN FIG. 2.1 FOR 15 SEC. INPUTS IN  $x_1$ -DIREC.,  $e/r=.05$

	Type of Response Quantity (1)	Time History Response (2)	RS Time History (3)	RS With Peak Factor Time History		
				Resp. Spectra (4)	Kanai-Tajimi (5)	White Noise (6)
C O M P L E X	Base Shear in $x_1$ -Direc	22.8879	0.88	0.91	1.14	1.00
	Base Shear in $x_2$ -Direc	7.5267	1.35	1.19	1.19	1.13
	Torsional Moment	8.3714	1.18	0.92	1.04	1.04
N O R M A L	Base Shear in $x_1$ -Direc	25.8960	0.92	0.95	1.09	0.99
	Base Shear in $x_2$ -Direc	7.0282	1.33	1.14	1.19	1.08
	Torsional Moment	10.3500	1.18	1.07	1.05	1.07
P E R C E N T	$x_1$ -Direc.	13.1	18.4			
	$x_2$ -Direc.	-6.6	-8.0			
	Torsion	23.6	23.4			

TABLE 2.18

MEAN BENDING MOMENT RESPONSES OF COL. 1 OF STRUCTURE IN FIG.  
2.1 FOR 15 SEC. INPUTS IN  $x_1$ -DIREC.,  $e/r=.05$

	Type of Response Quantity (1)	Time History Response (2)	RS Time History (3)	RS With Peak Factor Time History		
				Resp. Spectra (4)	Kanai-Tajimi (5)	White Noise (6)
C O M P L E X	Bending Moment in $x_1$ -Direc.	39.4383	0.92	0.95	1.15	1.02
	Bending Moment in $x_2$ -Direc.	15.5099	1.31	1.08	1.14	1.11
N O R M A L	Bending Moment in $x_1$ -Direc.	45.3322	0.95	0.97	1.09	1.01
	Bending Moment in $x_2$ -Direc.	16.7141	1.26	1.11	1.12	1.10
E R R O R	$x_1$ -Direc.	15.0	18.9			
	$x_2$ -Direc.	7.8	3.7			

TABLE 2.19

MEAN BASE SHEAR AND TORSIONAL MOMENT RESPONSE OF STRUCTURE  
IN FIG. 2.1 FOR 30 SEC. INPUTS IN  $x_1$ -DIREC.,  $e/r=.05$

	Type of Response Quantity (1)	Time History Response (2)	RS Time History (3)	RS With Peak Factor Time History		
				Resp. Spectra (4)	Kanai-Tajimi (5)	White Noise (6)
COMPOUND ELEMENT	Base Shear in $x_1$ -Direc	27.1730	1.00	1.03	1.17	1.08
	Base Shear in $x_2$ -Direc	9.8576	1.20	1.14	1.12	1.06
	Torsional Moment	10.7569	1.07	0.98	0.99	0.98
NORMAL MODE	Base Shear in $x_1$ -Direc	30.9376	1.00	1.02	1.12	1.05
	Base Shear in $x_2$ -Direc	9.1545	1.19	1.12	1.12	1.03
	Torsional Moment	13.0475	1.09	1.05	1.02	1.02
PERCENT	$x_1$ -Direc.	13.9	13.8			
	$x_2$ -Direc.	-7.1	-8.0			
	Torsion	21.3	23.7			

TABLE 2.20

MEAN BENDING MOMENT RESPONSES OF COL. 1 OF STRUCTURE IN FIG.  
2.1 FOR 30 SEC. INPUTS IN  $x_1$ -DIREC.,  $e/r=.05$

	Type of Response Quantity (1)	Time History Response (2)	RS Time History (3)	RS With Peak Factor Time History		
				Resp. Spectra (4)	Kanai-Tajimi (5)	White Noise (6)
COMPOUND ELEMENT	Bending Moment in $x_1$ -Direc.	47.7437	1.01	1.03	1.16	1.07
	Bending Moment in $x_2$ -Direc.	21.1113	1.15	1.05	1.06	1.02
NORMAL MODE	Bending Moment in $x_1$ -Direc.	55.1707	1.00	1.00	1.10	1.05
	Bending Moment in $x_2$ -Direc.	22.4227	1.12	1.06	1.05	1.02
ERROR	$x_1$ -Direc.	15.6	15.1			
	$x_2$ -Direc.	6.2	3.5			

TABLE 2.21

MEAN BASE SHEAR AND TORSIONAL MOMENT RESPONSE OF STRUCTURE  
IN FIG. 2.1 FOR 15 SEC. INPUTS IN  $x_1$  &  $x_2$ -DIREC.,  $e/r=.05$

	Type of Response Quantity (1)	Time History Response (2)	RS Time History (3)	RS With Peak Factor Time History		
				Resp. Spectra (4)	Kanai-Tajimi (5)	White Noise (6)
C O M P O S I T I O N A L	Base Shear in $x_1$ -Direc	24.1900	0.96	0.98	1.13	1.03
	Base Shear in $x_2$ -Direc	32.6554	1.00	1.01	1.07	1.02
	Torsional Moment	16.7561	1.22	1.10	1.07	1.11
N O M I N A L	Base Shear in $x_1$ -Direc	26.5838	0.96	0.98	1.09	1.01
	Base Shear in $x_2$ -Direc	27.6810	0.92	0.95	1.08	0.99
	Torsional Moment	14.6672	1.17	1.06	1.04	1.06
P E R C E N T	$x_1$ -Direc.	10.3	10.5			
	$x_2$ -Direc.	-15.0	-21.6			
	Torsion	-11.4	-16.1			

TABLE 2.22

MEAN BENDING MOMENT RESPONSES OF COL. 1 OF STRUCTURE IN FIG.  
2.1 FOR 15 SEC. INPUTS IN  $x_1$  &  $x_2$ -DIREC.,  $e/r=.05$

	Type of Response Quantity (1)	Time History Response (2)	RS Time History (3)	RS With Peak Factor Time History		
				Resp. Spectra (4)	Kanai-Tajimi (5)	White Noise (6)
C O M P O S I T I O N A L	Bending Moment in $x_1$ -Direc.	46.4398	0.99	1.00	1.08	1.02
	Bending Moment in $x_2$ -Direc.	58.2417	1.05	1.05	1.08	1.06
N O M I N A L	Bending Moment in $x_1$ -Direc.	48.6731	0.98	0.99	1.06	1.01
	Bending Moment in $x_2$ -Direc.	49.6462	0.97	0.99	1.09	1.02
E R R O R	$x_1$ -Direc.	4.8	3.8			
	$x_2$ -Direc.	-14.8	-20.9			

TABLE 2.23

MEAN BASE SHEAR AND TORSIONAL MOMENT RESPONSE OF STRUCTURE  
IN FIG. 2.1 FOR 15 SEC. INPUTS IN  $x_1$ -DIREC.,  $e/r=.3$

	Type of Response Quantity (1)	Time History Response (2)	RS Time History (3)	RS With Peak Factor Time History		
				Resp. Spectra (4)	Kanai-Tajimi (5)	White Noise (6)
C O M P O S I T I O N A L	Base Shear in $x_1$ -Direc	20.0987	0.92	0.95	1.24	1.06
	Base Shear in $x_2$ -Direc	17.9893	0.94	0.92	0.84	0.88
	Torsional Moment	14.5467	0.91	0.93	0.81	0.87
N O M O D A L	Base Shear in $x_1$ -Direc	20.4091	0.92	0.95	1.24	1.06
	Base Shear in $x_2$ -Direc	17.8975	0.94	0.92	0.84	0.88
	Torsional Moment	14.8616	0.90	0.92	0.80	0.86
P E R C E N T	$x_1$ -Direc.	1.5	1.4			
	$x_2$ -Direc.	-0.5	-0.5			
	Torsion	2.2	1.3			

TABLE 2.24

MEAN BENDING MOMENT RESPONSES OF COL. 1 OF STRUCTURE IN FIG.  
2.1 FOR 15 SEC. INPUTS IN  $x_1$ -DIREC.,  $e/r=.3$

	Type of Response Quantity (1)	Time History Response (2)	RS Time History (3)	RS With Peak Factor Time History		
				Resp. Spectra (4)	Kanai-Tajimi (5)	White Noise (6)
C O M P O S I T I O N A L	Bending Moment in $x_1$ -Direc.	33.4334	0.93	0.96	1.09	1.01
	Bending Moment in $x_2$ -Direc.	30.3383	0.95	0.93	0.90	0.90
N O M O D A L	Bending Moment in $x_1$ -Direc.	34.0675	0.93	0.96	1.08	1.00
	Bending Moment in $x_2$ -Direc.	30.2386	0.95	0.93	0.91	0.91
E R R O R	$x_1$ -Direc.	1.9	1.9			
	$x_2$ -Direc.	-0.3	-0.1			

TABLE 2.25

MEAN BASE SHEAR AND TORSIONAL MOMENT RESPONSE OF STRUCTURE  
IN FIG. 2.1 FOR 30 SEC. INPUTS IN  $x_1$ -DIREC.,  $e/r=.3$

	Type of Response Quantity (1)	Time History Response (2)	RS Time History (3)	RS With Peak Factor Time History		
				Resp. Spectra (4)	Kanai-Tajimi (5)	White Noise (6)
COMPLETED EX	Base Shear in $x_1$ -Direc	23.4013	1.00	1.03	1.25	1.11
	Base Shear in $x_2$ -Direc	20.9401	1.00	0.99	0.92	0.95
	Torsional Moment	17.4004	0.91	0.94	0.84	0.88
NORMAL MODELS	Base Shear in $x_1$ -Direc	23.7054	1.00	1.03	1.24	1.11
	Base Shear in $x_2$ -Direc	20.8217	1.00	0.99	0.92	0.95
	Torsional Moment	17.6861	0.91	0.93	0.84	0.88
ERROR	$x_1$ -Direc.	1.3	1.3			
	$x_2$ -Direc.	-0.5	-0.6			
	Torsion	1.4	1.6			

TABLE 2.26

MEAN BENDING MOMENT RESPONSES OF COL. 1 OF STRUCTURE IN FIG.  
2.1 FOR 30 SEC. INPUTS IN  $x_1$ -DIREC.,  $e/r=.3$

	Type of Response Quantity (1)	Time History Response (2)	RS Time History (3)	RS With Peak Factor Time History		
				Resp. Spectra (4)	Kanai-Tajimi (5)	White Noise (6)
COMPLETED EX	Bending Moment in $x_1$ -Direc.	39.4743	0.98	1.00	1.11	1.05
	Bending Moment in $x_2$ -Direc.	36.5436	0.97	0.97	0.92	0.93
NORMAL MODELS	Bending Moment in $x_1$ -Direc.	40.2641	0.98	1.00	1.11	1.04
	Bending Moment in $x_2$ -Direc.	36.5004	0.97	0.96	0.92	0.93
% ERROR	$x_1$ -Direc.	2.0	1.8			
	$x_2$ -Direc.	-0.1	-0.2			

TABLE 2.27

MEAN+1 SDV BASE SHEAR AND TORSIONAL MOMENT RESPONSE OF  
STRUCTURE IN FIG. 2.1 FOR 15 SEC. INPUTS IN  $x_1$ -DIREC.,  
 $e/r=.01$

	Type of Response Quantity (1)	Time History Response (2)	RS With Peak Factor			
			RS Time History (3)	Resp. Spectra (4)	Kanai-Tajimi (5)	White Noise (6)
COMPODLE X	Base Shear in $x_1$ -Direc	28.7081	1.00	1.00	1.05	1.02
	Base Shear in $x_2$ -Direc	0.8389	1.11	0.83	1.33	1.02
	Torsional Moment	2.9815	1.08	1.01	1.03	1.00
NORMD A L	Base Shear in $x_1$ -Direc	34.3384	0.99	0.99	1.06	1.02
	Base Shear in $x_2$ -Direc	0.7083	1.39	1.23	1.27	1.09
	Torsional Moment	4.0719	1.25	1.14	1.15	1.13
P E R R C E O N R T	$x_1$ -Direc.	19.6	19.0			
	$x_2$ -Direc.	-15.6	5.3			
	Torsion	36.6	58.0			

TABLE 2.28

MEAN+1 SDV BENDING MOMENT RESPONSES OF COL. 1 OF STRUCTURE  
IN FIG. 2.1 FOR 15 SEC. INPUTS IN  $x_1$ -DIREC.,  $e/r=.01$

	Type of Response Quantity (1)	Time History Response (2)	RS With Peak Factor			
			RS Time History (3)	Resp. Spectra (4)	Kanai-Tajimi (5)	White Noise (6)
COMPODLE X	Bending Moment in $x_1$ -Direc.	49.7289	0.94	0.94	0.84	0.99
	Bending Moment in $x_2$ -Direc.	3.9170	0.87	0.84	---	---
NORMD A L	Bending Moment in $x_1$ -Direc.	59.7547	0.99	1.00	1.06	1.02
	Bending Moment in $x_2$ -Direc.	5.1956	1.26	1.15	1.15	1.12
% R R O R	$x_1$ -Direc.	20.2	26.5			
	$x_2$ -Direc.	32.6	92.2			

TABLE 2.29

MEAN+1 SDV BASE SHEAR AND TORSIONAL MOMENT RESPONSE OF  
STRUCTURE IN FIG. 2.1 FOR 30 SEC. INPUTS IN  $x_1$ -DIREC.,  
 $e/r=.01$

	Type of Response Quantity (1)	Time History Response (2)	RS Time History (3)	RS With Peak Factor Time History		
				Resp. Spectra (4)	Kanal-Tajimi (5)	White Noise (6)
COMPLEX	Base Shear in $x_1$ -Direc	32.0267	1.01	1.03	1.09	1.06
	Base Shear in $x_2$ -Direc	1.0599	1.19	0.87	1.35	1.10
	Torsional Moment	3.5650	1.14	1.07	1.10	1.07
NORMAL MODE	Base Shear in $x_1$ -Direc	39.7997	1.02	1.01	1.07	1.04
	Base Shear in $x_2$ -Direc	0.8713	1.23	1.18	1.17	1.03
	Torsional Moment	4.9136	1.13	1.10	1.08	1.05
PERCENT	$x_1$ -Direc.	21.8	21.8			
	$x_2$ -Direc.	-17.8	-15.0			
	Torsion	37.8	36.4			

TABLE 2.30

MEAN+1 SDV BENDING MOMENT RESPONSES OF COL. 1 OF STRUCTURE  
IN FIG. 2.1 FOR 30 SEC. INPUTS IN  $x_1$ -DIREC.,  $e/r=.01$

	Type of Response Quantity (1)	Time History Response (2)	RS Time History (3)	RS With Peak Factor Time History		
				Resp. Spectra (4)	Kanal-Tajimi (5)	White Noise (6)
COMPLEX	Bending Moment in $x_1$ -Direc.	56.6765	0.97	0.98	0.91	0.96
	Bending Moment in $x_2$ -Direc.	4.7725	1.32	1.29	---	---
NORMAL MODE	Bending Moment in $x_1$ -Direc.	69.8549	1.01	1.00	1.07	0.95
	Bending Moment in $x_2$ -Direc.	6.2817	1.15	1.10	1.08	1.05
ERROR	$x_1$ -Direc.	21.1	26.2			
	$x_2$ -Direc.	31.6	13.2			

TABLE 2.31

MEAN+1 SDV BASE SHEAR AND TORSIONAL MOMENT RESPONSE OF  
STRUCTURE IN FIG. 2.1 FOR 15 SEC. INPUTS IN  $x_1$ -DIREC.,  
 $e/r=.05$

	Type of Response Quantity (1)	Time History Response (2)	RS With Peak Factor Time History			
			RS Time History (3)	Resp. Spectra (4)	Kanai-Tajimi (5)	White Noise (6)
COMPOULEX	Base Shear in $x_1$ -Direc	26.9092	0.94	0.96	1.12	1.02
	Base Shear in $x_2$ -Direc	9.7278	1.21	1.11	1.09	1.07
	Torsional Moment	10.3743	1.10	1.01	1.00	1.01
NORMDAIL	Base Shear in $x_1$ -Direc	30.8444	0.95	0.97	1.07	1.00
	Base Shear in $x_2$ -Direc	9.0535	1.20	1.08	1.09	1.03
	Torsional Moment	12.9587	1.09	1.03	0.99	1.02
PERCENT	$x_1$ -Direc.	14.6	15.7			
	$x_2$ -Direc.	-6.9	-7.9			
	Torsion	24.9	23.5			

TABLE 2.32

MEAN+1 SDV BENDING MOMENT RESPONSES OF COL. 1 OF STRUCTURE  
IN FIG. 2.1 FOR 15 SEC. INPUTS IN  $x_1$ -DIREC.,  $e/r=.05$

	Type of Response Quantity (1)	Time History Response (2)	RS With Peak Factor Time History			
			RS Time History (3)	Resp. Spectra (4)	Kanai-Tajimi (5)	White Noise (6)
COMPOULEX	Bending Moment in $x_1$ -Direc.	46.0620	0.97	0.99	1.13	1.04
	Bending Moment in $x_2$ -Direc.	20.1079	1.17	1.07	1.06	1.04
NORMDAIL	Bending Moment in $x_1$ -Direc.	53.8456	0.97	0.98	1.07	1.01
	Bending Moment in $x_2$ -Direc.	21.4019	1.15	1.06	1.04	1.04
ERROR	$x_1$ -Direc.	16.9	16.9			
	$x_2$ -Direc.	6.4	3.8			

TABLE 2.33

MEAN+1 SDV BASE SHEAR AND TORSIONAL MOM. RESPONSE OF  
STRUCTURE IN FIG. 2.1 FOR 15 SEC. INPUTS IN  $x_1$ -& $x_2$ -DIREC.,  
 $e/r=0.05$

	Type of Response Quantity (1)	Time History Response (2)	RS Time History (3)	RS With Peak Factor Time History		
				Resp. Spectra (4)	Kanai-Tajimi (5)	White Noise (6)
COMPODLEEX	Base Shear in $x_1$ -Direc	28.5099	1.00	1.01	1.11	1.05
	Base Shear in $x_2$ -Direc	39.8522	0.98	0.98	1.01	0.99
	Torsional Moment	21.3731	1.09	1.01	0.96	1.01
NORMDAEL	Base Shear in $x_1$ -Direc	31.9329	0.98	0.98	1.05	1.01
	Base Shear in $x_2$ -Direc	33.4897	0.94	0.95	1.04	0.98
	Torsional Moment	18.9684	1.03	0.97	0.93	0.96
PERCENT	$x_1$ -Direc.	12.0	9.1			
	$x_2$ -Direc.	-16.0	-19.4			
	Torsion	-11.3	-15.7			

TABLE 2.34

MEAN+1 SDV BENDING MOMENT RESPONSES OF COL. 1 OF STRUCTURE  
IN FIG. 2.1 FOR 15 SEC. INPUTS IN  $x_1$ -& $x_2$ -DIREC.,  $e/r=0.05$

	Type of Response Quantity (1)	Time History Response (2)	RS Time History (3)	RS With Peak Factor Time History		
				Resp. Spectra (4)	Kanai-Tajimi (5)	White Noise (6)
COMPODLEEX	Bending Moment in $x_1$ -Direc.	53.9901	1.02	1.03	1.08	1.04
	Bending Moment in $x_2$ -Direc.	70.7030	1.01	1.01	1.02	1.01
NORMDAEL	Bending Moment in $x_1$ -Direc.	57.6737	0.99	0.99	1.04	1.01
	Bending Moment in $x_2$ -Direc.	59.6700	0.97	0.97	1.01	1.00
% ERROR	$x_1$ -Direc.	6.8	3.7			
	$x_2$ -Direc.	-15.6	-19.4			

TABLE 2.35  
DYNAMIC CHARACTERISTICS OF STRUCTURE IN FIG. 2.13

Mode Number	Frequency cps.	Damping Ratio	Participation Factor
1	1.064	.0113	318.984
2	3.168	.0274	-104.733
3	5.200	.0455	60.908
4	7.117	.0611	41.404
5	8.850	.0776	29.975
6	10.438	.0890	22.180
7	11.765	.1008	16.298
8	12.825	.1102	11.512
9	13.605	.1169	7.734
10	14.085	.1245	3.603

TABLE 2.36

MEAN STORY SHEAR RESPONSES OF STRUCTURE IN FIG. 2.13 FOR 15  
SEC. INPUTS

Story Number (1)	Time History Response ( $\times 10^6$ ) (2)	RS Time History (3)	Rs With Peak Factor Time History		
			Resp. Spectra (4)	Kanai- Tajimi (5)	White Noise (6)
1	0.4717	0.96	0.99	1.13	1.02
2	0.4541	0.97	1.00	1.12	1.01
3	0.4262	0.92	1.01	1.11	1.02
4	0.3962	0.99	1.02	1.10	1.02
5	0.3666	0.98	1.01	1.08	1.00
6	0.3328	0.96	1.00	1.06	0.98
7	0.2910	0.94	1.00	1.03	0.96
8	0.2388	0.92	0.99	1.01	0.95
9	0.1735	0.90	0.98	0.99	0.94
10	0.0928	0.89	0.98	0.97	0.94

TABLE 2.37

MEAN STORY SHEAR RESPONSES OF STRUCTURE IN FIG. 2.13 FOR 30  
SEC. INPUTS

Story Number (1)	Time History Response ( $\times 10^6$ ) (2)	RS Time History (3)	Rs With Peak Factor Time History		
			Resp. Spectra (4)	Kanai- Tajimi (5)	White Noise (6)
1	0.6739	0.99	1.03	1.11	1.04
2	0.6546	1.00	1.03	1.09	1.03
3	0.6221	1.00	1.03	1.08	1.02
4	0.5840	0.99	1.02	1.07	1.01
5	0.5418	0.97	1.01	1.04	0.99
6	0.4880	0.96	1.00	1.02	0.97
7	0.4207	0.94	0.99	1.01	0.96
8	0.3414	0.93	0.99	0.99	0.95
9	0.2454	0.91	0.98	0.97	0.94
10	0.1298	0.89	0.98	0.96	0.94

TABLE 2.38

MEANS AND COEFFICIENTS OF VARIATION OF RESPONSE RATIOS GIVEN  
IN TABLES 2.13 THROUGH 2.34

	Type of Response	Without Peak Factor		With Peak Factor					
		Mean	COV.	Resp. Spectra		Kanai-Tajimi		White Noise	
				Mean	COV.	Mean	COV.	Mean	COV.
C O M P O S I T I O N A L E X	x1-Shear	0.98	0.04	1.00	0.05	1.14	0.04	1.05	0.03
	x2-Shear	1.08	0.12	0.96	0.18	1.12	0.17	1.02	0.06
	Torsion	1.04	0.10	0.98	0.05	0.96	0.10	0.97	0.07
	x1-Mom.	0.97	0.03	0.98	0.03	1.02	0.11	0.99	0.06
	x2-Mom.	1.04	0.14	1.00	0.12	1.02	0.07	1.00	0.06
N O M O D A L	x1-Shear	0.98	0.04	0.99	0.03	1.12	0.05	1.04	0.03
	x2-Shear	1.13	0.19	1.08	0.12	1.10	0.14	1.01	0.06
	Torsion	1.04	0.15	0.99	0.20	0.99	0.14	0.99	0.09
	x1-Mom.	0.98	0.03	0.99	0.02	1.07	0.03	1.01	0.03
	x2-Mom.	1.09	0.13	1.05	0.08	1.06	0.09	1.03	0.08
Overall Mean and COV		1.033	0.128	1.001	0.112	1.058	0.117	1.012	0.065

TABLE 3.1

PARAMETERS OF THE SPECTRAL DENSITY FUNCTIONS OF THE  
PRINCIPAL COMPONENTS

Excitation in Direction	i	$S_{\xi i}$ ft <sup>2</sup> -Sec/rad	$\omega_{\xi i}$ Rad/Sec	$\beta_{\xi i}$
1	1	0.0015	13.5	0.3925
	2	0.000495	23.5	0.3600
	3	0.000375	39.0	0.3350
2	1	0.0010	15.5	0.5000
	2	0.00033	27.5	0.4000
	3	0.00025	42.0	0.3000
3	1	0.0005	10.5	0.3000
	2	0.000165	19.5	0.2000
	3	0.000125	33.0	0.1800

TABLE 3.2  
 DYNAMIC CHARACTERISTICS OF STRUCTURE IN FIG. 2.1 FOR  $e/r=.01$   
 AND  $w=10$  cps.

Mode No.	COMPLEX MODE APPROACH		NORMAL MODE APPROACH	
	Frequency cps.	Damping Ratio	Frequency cps.	Damping Ratio
1	6.2367	.0064	6.2362	.0097
2	6.2375	.0129	6.2369	.0097
3	8.3126	.0499	8.2941	.0500
4	12.7959	.0195	12.7943	.0293
5	12.8008	.0391	12.7959	.0293
6	16.0028	.0794	16.0341	.0792
7	17.7107	.0275	17.7211	.0206
8	17.7189	.0138	17.7211	.0207
9	36.8324	.0194	36.8473	.0194

TABLE 3.5  
 PARTICIPATION FACTORS OF STRUCTURE IN FIG. 2.1  $e/r=.01$  AND  
 $w=10$  cps. FOR THE EXCITATION COMPONENTS

Mode No.	Participation factors in $x_k$ direction				
	$x_1$	$x_2$	$x_4$	$x_5$	$x_6$
1	1.437	-1.437	62.30	62.30	0.028
2	1.437	1.437	-62.31	62.30	0.000
3	-0.031	0.031	-1.14	-1.14	1.574
4	-0.071	0.071	-7.29	-7.29	0.028
5	-0.072	-0.072	7.30	7.30	-0.078
6	-0.037	0.037	-0.45	-0.45	0.107
7	0.666	0.666	-8.03	8.03	0.000
8	-0.665	0.665	-8.03	-8.03	-0.040
9	-0.003	0.003	-0.04	-0.04	1.515

TABLE 3.3  
 DYNAMIC CHARACTERISTIC OF STRUCTURES IN FIG. 2.1 FOR  $e/r=.01$   
 AND  $w=33.4$  cps.

Mode No.	COMPLEX MODE APPROACH		NORMAL MODE APPROACH	
	Frequency cps.	Damping Ratio	Frequency cps.	Damping Ratio
1	20.8464	.0064	20.8420	.0097
2	20.8468	.0129	20.8455	.0097
3	27.7855	.0499	27.7239	.0500
4	42.7679	.0195	42.7606	.0293
5	42.7844	.0391	42.7643	.0293
6	53.4845	.0794	53.5906	.0792
7	59.1926	.0275	59.2417	.0206
8	59.2207	.0138	59.2347	.0207
9	123.1072	.0194	123.1527	.0194

TABLE 3.4  
 DYNAMIC CHARACTERISTICS OF STRUCTURE IN FIG. 2.1 FOR  $e/r=.01$   
 AND  $w=50$  cps.

Mode No.	COMPLEX MODE APPROACH		NORMAL MODE APPROACH	
	Frequency cps.	Damping Ratio	Frequency cps.	Damping Ratio
1	31.1429	.0127	31.0945	.0100
2	31.1429	.0069	31.1847	.0097
3	41.6840	.0498	41.5749	.0498
4	63.8978	.0199	63.7959	.0296
5	63.9182	.0391	63.9754	.0293
6	80.1976	.0778	80.2826	.0772
7	88.5897	.0281	88.6053	.0206
8	88.6289	.0143	88.7469	.0222
9	184.4679	.0194	184.5359	.0194

TABLE 3.6

BASE SHEARS, TORSIONAL MOMENT AND COLUMN BENDING MOMENTS FOR  
STRUCTURE IN FIG 2.1,  $c=1000$ . fps,  $e/r=.01$ ,  $w=10$ . cps.

	Type of Response (1)	Translational and Rotational Excitations		Translational Excitation in $x_1$ -& $x_2$ -Direc.		4/2 (6)
		Maximum Resp. (2)	RS Max. (3)	Maximum Resp. (4)	RS Max. (5)	
C O M P O S I T I O N A L	Shear in $x_1$ -Direc.	18.075	0.900	11.876	1.000	.657
	Shear in $x_2$ -Direc.	25.422	0.869	16.527	0.964	.650
	Torsional Moment	0.329	0.986	0.206	0.986	.626
	Moment in $x_1$ -Direc.	45.121	0.900	29.625	1.000	.657
	Moment in $x_2$ -Direc.	63.435	0.869	39.741	0.964	.626
N O M I N A L	Shear in $x_1$ -Direc.	20.795	0.898	13.592	1.000	.654
	Shear in $x_2$ -Direc.	20.795	0.870	13.592	0.961	.654
	Torsional Moment	0.314	0.995	0.198	0.990	.631
	Moment in $x_1$ -Direc.	51.902	0.898	33.905	1.000	.653
	Moment in $x_2$ -Direc.	51.902	0.869	33.905	0.961	.653

TABLE 3.7

BASE SHEARS, TORSIONAL MOMENT AND COLUMN BENDING MOMENTS FOR  
STRUCTURE IN FIG 2.1,  $c=1000$ . fps,  $e/r=.01$ ,  $w=50$ . cps.

	Type of Response (1)	Translational and Rotational Excitations		Translational Excitation in $x_1$ -& $x_2$ -Direc.		4/2 (6)
		Maximum Resp. (2)	RS Max. (3)	Maximum Resp. (4)	RS Max. (5)	
C O M P D L E E X	Shear in $x_1$ -Direc.	4.319	0.921	3.349	1.000	.775
	Shear in $x_2$ -Direc.	4.319	0.829	3.349	0.867	.775
	Torsional Moment	0.074	0.984	0.001	0.996	.014
	Moment in $x_1$ -Direc.	10.793	0.921	8.362	1.000	.775
	Moment in $x_2$ -Direc.	10.793	0.829	8.362	0.867	.775
N O R M A L	Shear in $x_1$ -Direc.	4.319	0.921	3.349	1.000	.775
	Shear in $x_2$ -Direc.	4.319	0.829	3.349	0.867	.775
	Torsional Moment	0.073	0.984	0.001	0.996	0.014
	Moment in $x_1$ -Direc.	10.794	0.921	8.362	1.000	.775
	Moment in $x_2$ -Direc.	10.794	0.829	8.362	0.867	.775

TABLE 3.8

BASE SHEARS, TORSIONAL MOMENT AND COLUMN BENDING MOMENTS FOR  
STRUCTURE IN FIG 2.1,  $c=1000$ . fps,  $e/r=.3$ ,  $w=10$ . cps.

	Type of Response (1)	Translational and Rotational Excitations		Translational Excitation in $x_1$ -& $x_2$ -Direc.		4/2 (6)
		Maximum Resp. (2)	$\frac{RS}{Max.}$ (3)	Maximum Resp. (4)	$\frac{RS}{Max.}$ (5)	
C O M P O S I T E	Shear in $x_1$ -Direc.	17.734	0.903	11.513	1.000	.649
	-----	-----	-----	-----	-----	-----
	Shear in $x_2$ -Direc.	18.073	0.894	11.742	0.983	.650
	-----	-----	-----	-----	-----	-----
	Torsional Moment	3.869	0.981	2.998	0.981	.775
E X P O S U R E	-----	-----	-----	-----	-----	-----
	Moment in $x_1$ -Direc.	43.621	0.893	27.875	1.000	.639
	-----	-----	-----	-----	-----	-----
	Moment in $x_2$ -Direc.	44.392	0.885	28.404	0.983	.640
	-----	-----	-----	-----	-----	-----
N O M I N A L	-----	-----	-----	-----	-----	-----
	Shear in $x_1$ -Direc.	17.819	0.902	11.557	1.000	.649
	-----	-----	-----	-----	-----	-----
	Shear in $x_2$ -Direc.	17.819	0.893	11.557	0.984	.649
	-----	-----	-----	-----	-----	-----
Torsional Moment	3.831	0.982	2.972	0.982	.776	
A E L	-----	-----	-----	-----	-----	-----
	Moment in $x_1$ -Direc.	43.820	0.893	27.981	1.000	.639
	-----	-----	-----	-----	-----	-----
Moment in $x_2$ -Direc.	43.820	0.884	27.981	0.984	.639	

TABLE 3.9

BASE SHEARS, TORSIONAL MOMENT AND COLUMN BENDING MOMENTS FOR  
STRUCTURE IN FIG 2.1,  $c=1000$ . fps,  $e/r=.3$ ,  $w=50$ . cps.

	Type of Response (1)	Translational and Rotational Excitations		Translational Excitation in $x_1$ -& $x_2$ -Direc.		4/2 (6)
		Maximum Resp. (2)	$\frac{RS}{Max.}$ (3)	Maximum Resp. (4)	$\frac{RS}{Max.}$ (5)	
C O M P L E X	Shear in $x_1$ -Direc.	4.329	0.921	3.352	1.000	.774
	Shear in $x_2$ -Direc.	4.329	0.830	3.352	0.867	.774
	Torsional Moment	0.066	0.775	0.032	0.996	.485
	Moment in $x_1$ -Direc.	10.538	0.917	8.107	1.000	.769
	Moment in $x_2$ -Direc.	10.539	0.826	8.107	0.867	.769
N O M I N A L	Shear in $x_1$ -Direc.	4.329	0.921	3.352	1.000	.774
	Shear in $x_2$ -Direc.	4.329	0.830	3.352	0.867	.774
	Torsional Moment	0.068	0.982	0.032	0.996	0.471
	Moment in $x_1$ -Direc.	10.539	0.917	8.107	1.000	.769
	Moment in $x_2$ -Direc.	10.539	0.826	8.107	0.867	.769

TABLE 3.10

BASE SHEARS, TORSIONAL MOMENT AND COLUMN BENDING MOMENTS FOR  
STRUCTURE IN FIG 2.1,  $c=2000$ . fps,  $e/r=.01$ ,  $w=10$ . cps.

	Type of Response (1)	Translational and Rotational Excitations		Translational Excitation in $x_1$ -& $x_2$ -Direc.		4/2 (6)
		Maximum Resp. (2)	RS Max. (3)	Maximum Resp. (4)	RS Max. (5)	
C O M P O S I T I O N A L E X	Shear in $x_1$ -Direc.	13.701	0.959	11.876	1.000	.869
	Shear in $x_2$ -Direc.	19.136	0.925	16.527	0.964	.864
	Torsional Moment	0.244	0.988	0.206	0.986	.844
	Moment in $x_1$ -Direc.	34.185	0.959	29.625	1.000	.867
	Moment in $x_2$ -Direc.	47.738	0.925	39.741	0.964	.832
N O R M A L	Shear in $x_1$ -Direc.	15.708	0.958	13.592	1.000	.856
	Shear in $x_2$ -Direc.	15.708	0.923	13.592	0.961	.856
	Torsional Moment	0.234	0.992	0.198	0.990	.846
	Moment in $x_1$ -Direc.	39.191	0.958	33.905	1.000	.865
	Moment in $x_2$ -Direc.	39.191	0.923	33.905	0.961	.865

TABLE 3.11

BASE SHEARS, TORSIONAL MOMENT AND COLUMN BENDING MOMENTS FOR  
STRUCTURE IN FIG 2.1,  $c=2000$ . fps,  $e/r=.3$ ,  $w=10$ . cps.

	Type of Response (1)	Translational and Rotational Excitations		Translational Excitation in $x_1$ -& $x_2$ -Direc.		4/2 (6)
		Maximum Resp. (2)	RS Max. (3)	Maximum Resp. (4)	RS Max. (5)	
C O M P L E X	Shear in $x_1$ -Direc.	13.037	0.983	11.513	1.000	.883
	Shear in $x_2$ -Direc.	13.291	0.969	11.742	0.983	.883
	Torsional Moment	3.227	0.981	2.998	0.981	.929
	Moment in $x_1$ -Direc.	31.736	0.979	27.875	1.000	.878
	Moment in $x_2$ -Direc.	32.309	0.966	28.404	0.983	.879
N O R M A L	Shear in $x_1$ -Direc.	13.089	0.983	11.557	1.000	.883
	Shear in $x_2$ -Direc.	13.089	0.969	11.557	0.984	.883
	Torsional Moment	3.198	0.982	2.972	0.982	.929
	Moment in $x_1$ -Direc.	31.860	0.979	27.981	1.000	.878
	Moment in $x_2$ -Direc.	31.860	0.966	27.981	0.984	.877

TABLE 3.12

BASE SHEARS, TORSIONAL MOMENTS AND COL. BENDING MOM. FOR A SIX STORY STRUCT. IN FIG. 2.1,  $c=1000$  fps,  $e/r=.3$ ,  $w=33.4$  cps.

	Type of Response (1)	Translational and Rotational Excitations		Translational Excitations		4/2 (6)
		Maximum Resp. (2)	RS Max. (3)	Maximum Resp. (4)	RS Max. (5)	
N O M R O M D A E L	Shear in $x_1$ -Direc.	30.138	0.767	12.835	0.997	.426
	Shear in $x_2$ -Direc.	30.138	0.762	12.835	0.984	.426
	Torsional Moment	10.060	0.999	7.744	0.998	.770
	Moment in $x_1$ -Direc.	51.692	0.754	20.540	0.995	.397
	Moment in $x_2$ -Direc.	51.692	0.752	20.540	0.989	.397

TABLE 3.13

BASE SHEARS, TORSIONAL MOMENTS AND COL. BENDING MOM. FOR A SIX STORY STRUCT. IN FIG. 2.1,  $c=2000$  fps,  $e/r=.3$ ,  $w=33.4$  cps.

	Type of Response (1)	Translational and Rotational Excitations		Translational Excitations		4/2 (6)
		Maximum Resp. (2)	RS Max. (3)	Maximum Resp. (4)	RS Max. (5)	
N O M R O M D A E L	Shear in $x_1$ -Direc.	17.904	0.895	12.835	0.997	.717
	Shear in $x_2$ -Direc.	17.904	0.887	12.835	0.984	.717
	Torsional Moment	9.363	0.998	7.744	0.998	.827
	Moment in $x_1$ -Direc.	30.683	0.859	20.540	0.995	.669
	Moment in $x_2$ -Direc.	30.683	0.855	20.540	0.989	.669

TABLE 3.14

MASS, STIFFNESS, AND CROSS SECTIONAL PROPERTIES OF THE SPACE  
FRAME IN FIG. 3.1

Member Number	Length (inch)	d (in.)	A (in.)	I <sub>x</sub> Ksi	I <sub>y</sub> Ksi	I <sub>z</sub> Ksi
1	301.	12.75	36.9	641.7	641.7	1283.4
2	312.	12.75	36.9	641.7	641.7	1283.4
3	354.	12.75	36.9	641.7	641.7	1283.4
4	294.	12.75	36.9	641.7	641.7	1283.4
5	71.	10.75	11.91	160.7	160.7	321.4
6	101.	10.75	11.91	160.7	160.7	321.4
7	108.	10.75	11.91	160.7	160.7	321.4
8	51.	10.75	11.91	160.7	160.7	321.4

JOINT COORDINATES IN INCH

joint Number	x <sub>1</sub> (inch)	x <sub>2</sub> (in.)	x <sub>3</sub> (in.)
1	48.0	0.0	0.0
2	90.0	78.0	0.0
3	-6.0	95.0	6.0
4	-6.0	-12.0	6.0
5	48.0	18.0	300.0
6	88.0	76.0	312.0
7	0.0	90.0	360.0
8	0.0	0.0	300.0

TABLE 3.15

NATURAL FREQUENCIES AND PARTICIPATION FACTORS FOR THE SIX COMPONENTS OF EXCITATION OF SPACE FRAME IN FIG. 3.1

Mode No.	Frequency cps.	Participation factors in $x_p$ direction					
		$x_1$	$x_2$	$x_3$	$x_4$	$x_5$	$x_6$
1	0.564	-0.5460	2.3337	-0.1074	-774.17	-141.40	-121.33
2	0.633	2.2605	0.5021	0.1388	-116.31	686.11	-160.03
3	1.210	0.2753	0.5557	-0.0448	-174.15	74.00	95.06
4	2.673	0.0984	0.0759	-0.5542	-253.73	180.40	-0.5346
5	8.831	0.0562	-0.0302	-0.3229	-79.29	98.53	-1.8484
6	10.276	0.0098	-0.0208	0.3323	126.48	-121.03	9.0406
7	11.853	-0.0346	-0.0142	0.0190	17.51	-2.78	2.0906
8	13.241	-0.1365	0.0757	1.2742	383.52	-378.99	12.3191
9	13.990	0.0478	0.0056	-0.6682	-201.43	192.39	-0.5572
10	15.541	-0.0937	0.1096	1.1526	304.69	-308.01	-3.5955
11	26.0278	0.0053	0.0138	-0.2616	-92.31	93.54	3.1276
12	37.9432	-0.0015	0.0051	-0.0959	-60.98	30.19	0.5635
13	52.2059	-0.0119	0.0026	0.0010	-9.13	-22.05	0.6944
14	69.2649	0.0049	-0.0071	0.6293	231.97	-218.81	-0.4793
15	81.4734	0.0144	0.0104	1.0235	314.65	-326.39	-0.7878
16	86.4329	0.0092	0.0276	0.7315	206.00	-215.84	-0.5446
17	93.7806	0.0030	0.0047	0.0175	2.79	-2.95	-0.1664
18	101.5223	-0.0065	0.0137	0.0177	-0.57	4.77	-0.2279
19	106.8117	-0.0057	0.0021	-0.0048	-10.36	22.25	0.5578
20	110.2381	-0.0011	0.0112	0.0361	10.18	-8.87	0.4846
21	117.7470	-0.0029	-0.0237	-0.0450	-14.50	25.65	0.6562
22	127.9208	0.0010	0.0116	0.0565	17.86	-19.76	0.5118
23	140.8611	0.0035	0.0124	0.1291	35.81	-22.49	-0.3713
24	161.7969	-0.0011	-0.0012	-0.0263	-6.71	-0.65	0.1323

TABLE 3.16

AXIAL FORCES IN THE SPACE FRAME OF FIG. 3.1,  $c=1000$ . fps

Member No.	SIX COMPONENTS EXCITATION					3 TRANSLATIONAL EXCITATION					
	Max. Response	RS Max.	Angle in Deg.			Max. Response	RS Max.	(7) (2)	Angle in Deg.		
			(4)	(5)	(6)				(9)	(10)	(11)
(1)	(2)	(3)	(4)	(5)	(6)	(7)	(8)	(9)	(10)	(11)	(12)
1	14.884	.895	117	22	12	5.570	.932	.374	110	-3	3
2	15.472	.911	117	24	1	3.719	.991	.236	17	-3	3
3	16.886	.879	117	23	46	4.324	.918	.256	108	3	72
4	24.111	.842	117	25	10	5.738	.914	.238	13	-2	95
5	7.962	.906	117	24	42	0.682	.904	.086	15	12	88
6	5.884	.897	117	25	15	1.686	.979	.170	13	-7	6
7	10.002	.903	117	20	84	2.286	.835	.229	78	2	72
8	13.163	.915	116	24	70	0.639	.824	.049	14	-6	28

TABLE 3.17

BENDING MOMENTS ABOUT x3-AXIS IN THE SPACE FRAME OF FIG. 3.1,  $c=1000$ . fps

Member No.	SIX COMPONENTS EXCITATION					3 TRANSLATIONAL EXCITATION					
	Max. Response	RS Max.	Angle in Deg.			Max. Response	RS Max.	(7) (2)	Angle in Deg.		
			(4)	(5)	(6)				(9)	(10)	(11)
(1)	(2)	(3)	(4)	(5)	(6)	(7)	(8)	(9)	(10)	(11)	(12)
1	195.44	.962	32	-18	16	144.53	.994	.740	11	-3	2
2	228.15	.926	43	-22	12	154.85	.986	.679	12	-3	94
3	147.24	.988	5	-10	23	124.83	.992	.848	12	-3	9
4	197.36	.967	34	-15	14	149.96	.997	.760	8	-4	2
5	137.05	.838	110	10	123	103.32	.839	.753	101	2	1
6	308.83	.816	119	23	11	108.21	.989	.350	8	-2	99
7	106.06	.803	118	23	79	23.56	.754	.222	144	-84	71
8	299.35	.854	119	24	8	125.59	.991	.420	9	-3	108

TABLE 3.18  
 COMBINED NORMAL STRESSES IN THE SPACE FRAME OF FIG. 3.1,  
 c=1000. fps

Member No.	SIX COMPONENTS EXCITATION					3 TRANSLATIONAL EXCITATION					
	Max. Response	RS Max.	Angle in Deg.			Max. Response	RS Max.	(7) (2)	Angle in Deg.		
			(4)	(5)	(6)				(10)	(11)	(12)
(1)	(2)	(3)	(4)	(5)	(6)	(7)	(8)	(9)	(10)	(11)	(12)
1	1.934	.987	16	-6	16	1.818	.989	.940	19	-3	3
2	2.026	.951	124	19	1	1.629	.990	.804	20	-3	3
3	1.778	.990	16	-6	11	1.681	.991	.945	21	-3	3
4	2.180	.988	16	-6	16	2.099	.990	.963	17	-3	3
5	6.222	.850	111	13	43	4.247	.858	.683	101	2	3
6	10.245	.809	119	23	12	3.254	.963	.318	10	-2	94
7	5.056	.844	112	12	98	3.466	.828	.685	103	3	84
8	10.956	.861	119	24	8	4.471	.979	.408	11	-3	97

TABLE 3.19  
 AXIAL FORCES IN THE SPACE FRAME OF FIG. 3.1, c=2000. fps

Member No.	SIX COMPONENTS EXCITATION					3 TRANSLATIONAL EXCITATION					
	Max. Response	RS Max.	Angle in Deg.			Max. Response	RS Max.	(7) (2)	Angle in Deg.		
			(4)	(5)	(6)				(10)	(11)	(12)
(1)	(2)	(3)	(4)	(5)	(6)	(7)	(8)	(9)	(10)	(11)	(12)
1	8.886	.913	116	19	1	5.570	.932	.627	110	-3	3
2	8.233	.936	121	23	1	3.719	.991	.452	17	-3	3
3	9.229	.889	116	21	77	4.324	.918	.469	108	3	72
4	12.707	.873	118	26	12	5.738	.914	.451	13	-2	95
5	4.011	.909	116	25	28	0.682	.904	.170	15	12	88
6	3.202	.939	130	24	12	1.686	.979	.527	13	-7	6
7	5.362	.896	113	17	93	2.286	.835	.426	78	2	72
8	6.603	.915	116	24	81	0.639	.824	.097	14	-6	28

TABLE 4.1

BASE SHEAR, TORSIONAL MOMENT AND COLUMN BENDING MOMENT OF  
STRUCTURE IN FIG. 2.1,  $e/r=.01$ ,  $w=50$  cps.

Type of Response	Exact Response Value 9 Modes		Approximate Response Using 3 Modes By			
	Maximum Resp. (1)	SRSS Max. (2)	Mode Displc.		Mode Accl.	
			R-Max. A-Max. (3)	SRSS A-Max. (4)	R-Max. A-Max. (5)	SRSS A-Max. (6)
Base Shear in $x_1$ -Direction	4.319	.921	.786	.702	.990	.913
Base Shear in $x_2$ -Direction	4.319	.829	.786	.642	.990	.821
Torsional Moment	0.073	.984	.430	.423	1.000	.984
Bending Mom. of Col.1 in $x_1$ -Direc.	10.794	.921	.786	.701	.990	.913
Bending Mom. of Col.2 in $x_2$ -Direc.	10.801	.829	.786	.642	.990	.913

TABLE 4.2

BASE SHEAR, TORSIONAL MOMENT AND COLUMN BENDING MOMENT OF  
STRUCTURE IN FIG. 2.1,  $e/r=.05$ ,  $w=50$  cps.

Type of Response	Exact Response Value 9 Modes		Approximate Response Using 3 Modes By			
	Maximum Resp. (1)	SRSS Max. (2)	Mode Displc.		Mode Accl.	
			R-Max. A-Max. (3)	SRSS A-Max. (4)	R-Max. A-Max. (5)	SRSS A-Max. (6)
Base Shear in $x_1$ -Direction	4.319	.921	.786	.702	.991	.913
Base Shear in $x_2$ -Direction	4.319	.829	.786	.643	.991	.821
Torsional Moment	0.065	.982	.600	.585	1.077	1.062
Bending Mom. of Col.1 in $x_1$ -Direc.	10.753	.920	.787	.702	.990	.820
Bending Mom. of Col.2 in $x_2$ -Direc.	10.844	.830	.756	.642	.990	.821

TABLE 4.3

BASE SHEAR, TORSIONAL MOMENT AND COLUMN BENDING MOMENT OF  
STRUCTURE IN FIG. 2.1,  $e/r=.3$ ,  $w=50$  cps.

Type of Response	Exact Response Value 9 Modes		Approximate Response Using 3 Modes By			
	Maximum Resp. (1)	SRSS Max. (2)	Mode Displc.		Mode Accl.	
			R-Max. A-Max. (3)	SRSS A-Max. (4)	R-Max. A-Max. (5)	SRSS A-Max. (6)
Base Shear in $x_1$ -Direction	4.329	.921	.800	.718	.991	.913
Base Shear in $x_2$ -Direction	4.329	.830	.800	.656	.991	.822
Torsional Moment	0.068	.982	2.221	2.103	1.371	1.357
Bending Mom. of Col.1 in $x_1$ -Direc.	10.539	.917	.802	.715	.991	.909
Bending Mom. of Col.2 in $x_2$ -Direc.	11.117	.834	.798	.662	.991	.825

TABLE 4.4

BASE SHEAR, TORSIONAL MOMENT AND COLUMN BENDING MOMENT OF  
STRUCTURE IN FIG. 2.1,  $e/r=.01$ ,  $w=33.4$  cps.

Type of Response	Exact Response Value 9 Modes		Approximate Response Using 3 Modes By			
	Maximum Resp. (1)	SRSS Max. (2)	Mode Displc.		Mode Accl.	
			R-Max. A-Max. (3)	SRSS A-Max. (4)	R-Max. A-Max. (5)	SRSS A-Max. (6)
Base Shear in $x_1$ -Direction	6.186	.849	.886	.725	.980	.832
Base Shear in $x_2$ -Direction	6.186	.798	.886	.694	.980	.780
Torsional Moment	0.072	.984	.472	.468	1.032	1.015
Bending Mom. of Col.1 in $x_1$ -Direc.	34.593	.849	.396	.324	.438	.372
Bending Mom. of Col.2 in $x_2$ -Direc.	34.628	.798	.396	.310	.438	.349

TABLE 4.5

BASE SHEAR, TORSIONAL MOMENT AND COLUMN BENDING MOMENT OF  
STRUCTURE IN FIG. 2.1,  $e/r=.01$ ,  $w=10$  cps.

Type of Response	Exact Response Value 9 Modes		Approximate Response Using 3 Modes By			
	Maximum Resp. (1)	SRSS Max. (2)	Mode Displc.		Mode Accl.	
			R-Max. A-Max. (3)	SRSS A-Max. (4)	R-Max. A-Max. (5)	SRSS A-Max. (6)
Base Shear in $x_1$ -Direction	20.796	.898	.988	.885	.996	.894
Base Shear in $x_2$ -Direction	20.796	.870	.988	.860	.996	.866
Torsional Moment	0.314	.995	.965	.961	.987	.983
Bending Mom. of Col.1 in $x_1$ -Direc.	51.902	.898	.989	.885	.996	.893
Bending Mom. of Col.2 in $x_2$ -Direc.	52.077	.870	.988	.860	.996	.866

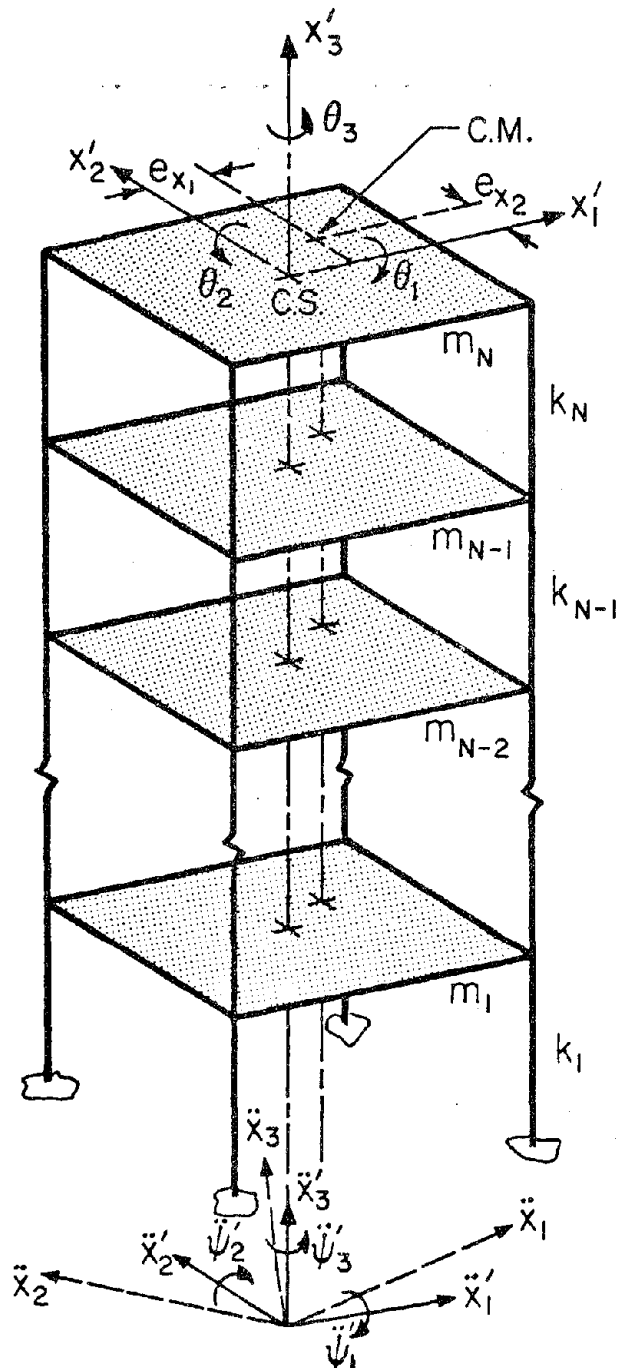
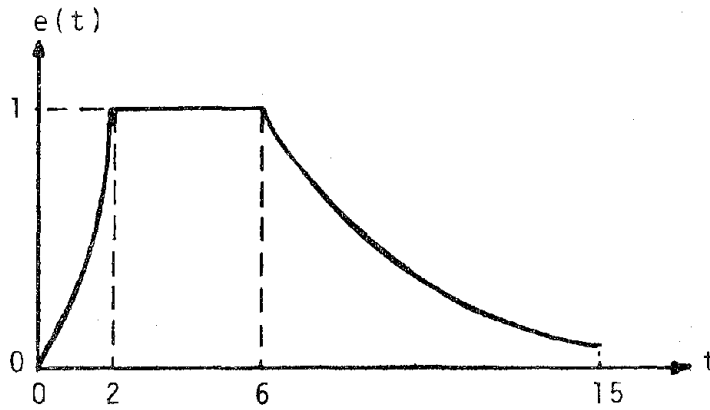
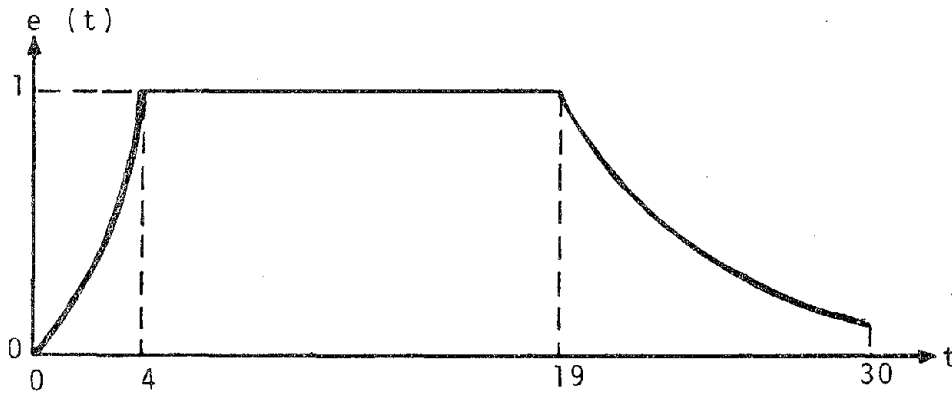


Figure 2.1: A MULTISTORY TORSIONAL BUILDING WITH ECCENTRIC MASS AND STIFFNESS CENTERS



a, 15 SECOND TIME HISTORY



b, 30 SECOND TIME HISTORY

Figure 2.2: INTENSITY ENVELOPE FUNCTION FOR 15 AND 30 SECONDS TIME HISTORIES

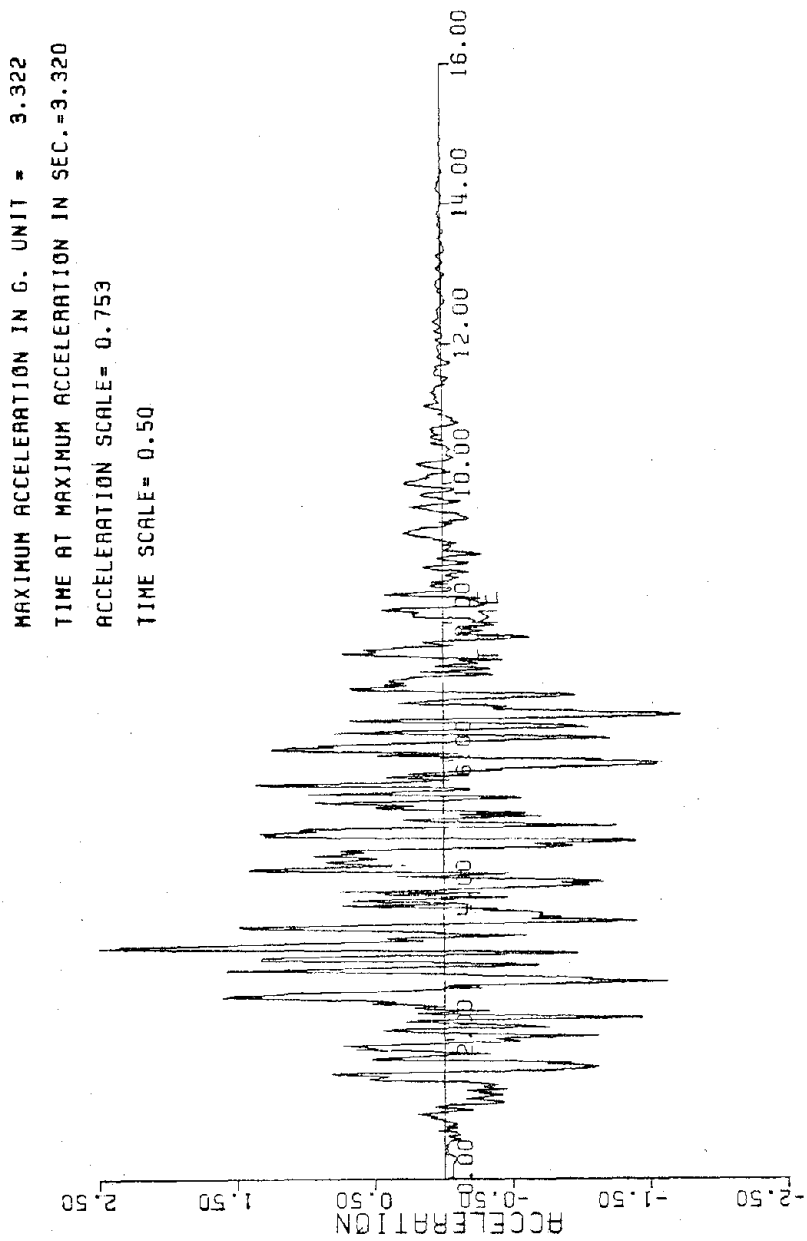


Figure 2.3: A TYPICAL SYNTHETIC ACCELERATION TIME HISTORY OF 15 SECONDS DURATION

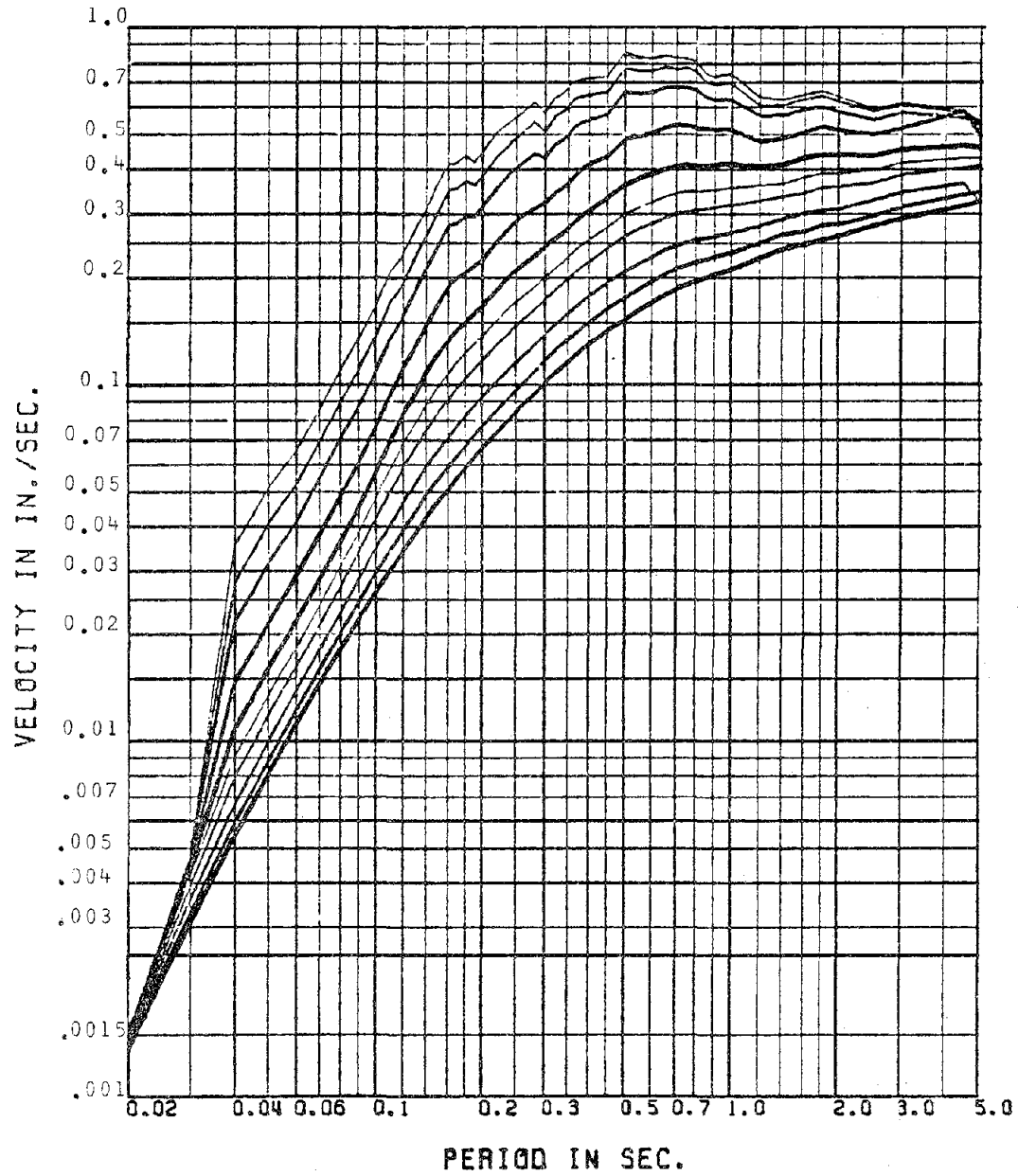


Figure 2.4: MEAN RELATIVE VELOCITY SPECTRA FOR  
 .5, 1, 2, 5, 10, 15, 20, 30, 40 AND 50 PERCENT DAMPING  
 VALUE FOR 15 SEC. TIME HISTORIES

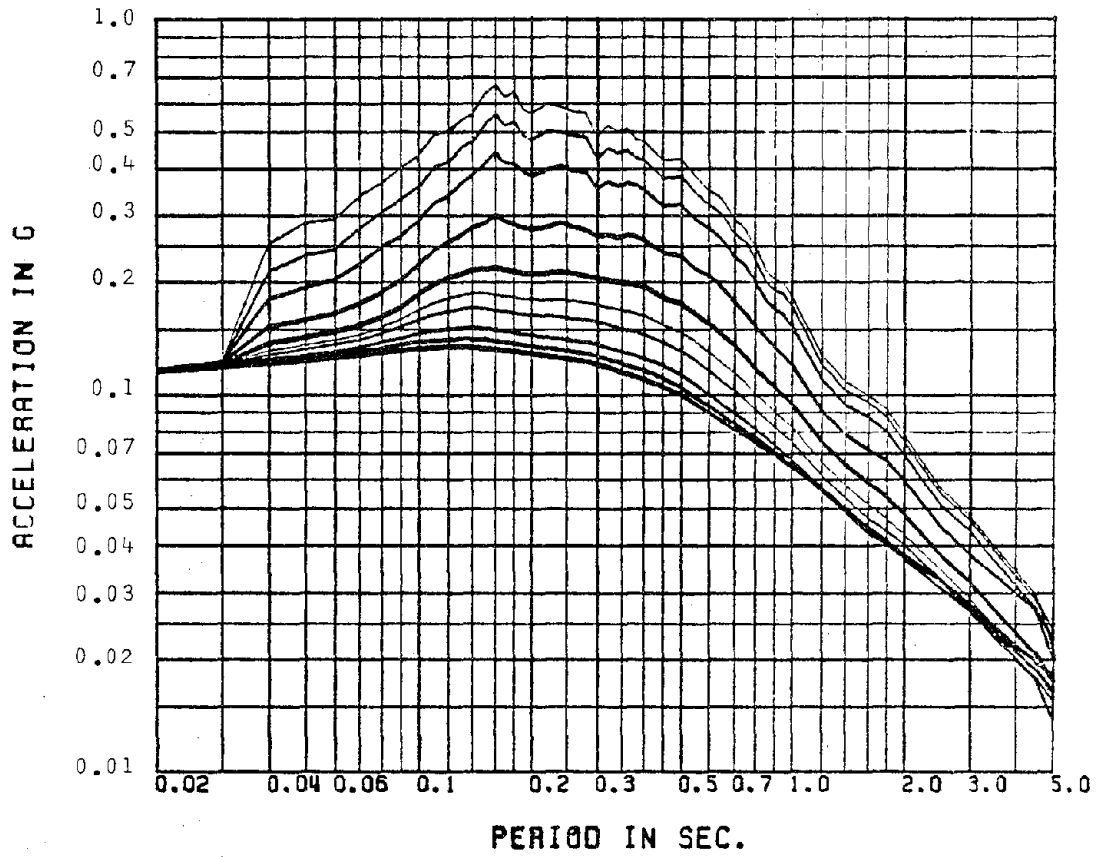


Figure 2.5: MEAN PSUEDO ACCELERATION SPECTRA FOR  
.5, 1, 2, 5, 10, 15, 20, 30, 40 AND 50 PERCENT DAMPING  
VALUE FOR 15 SEC. TIME HISTORIES

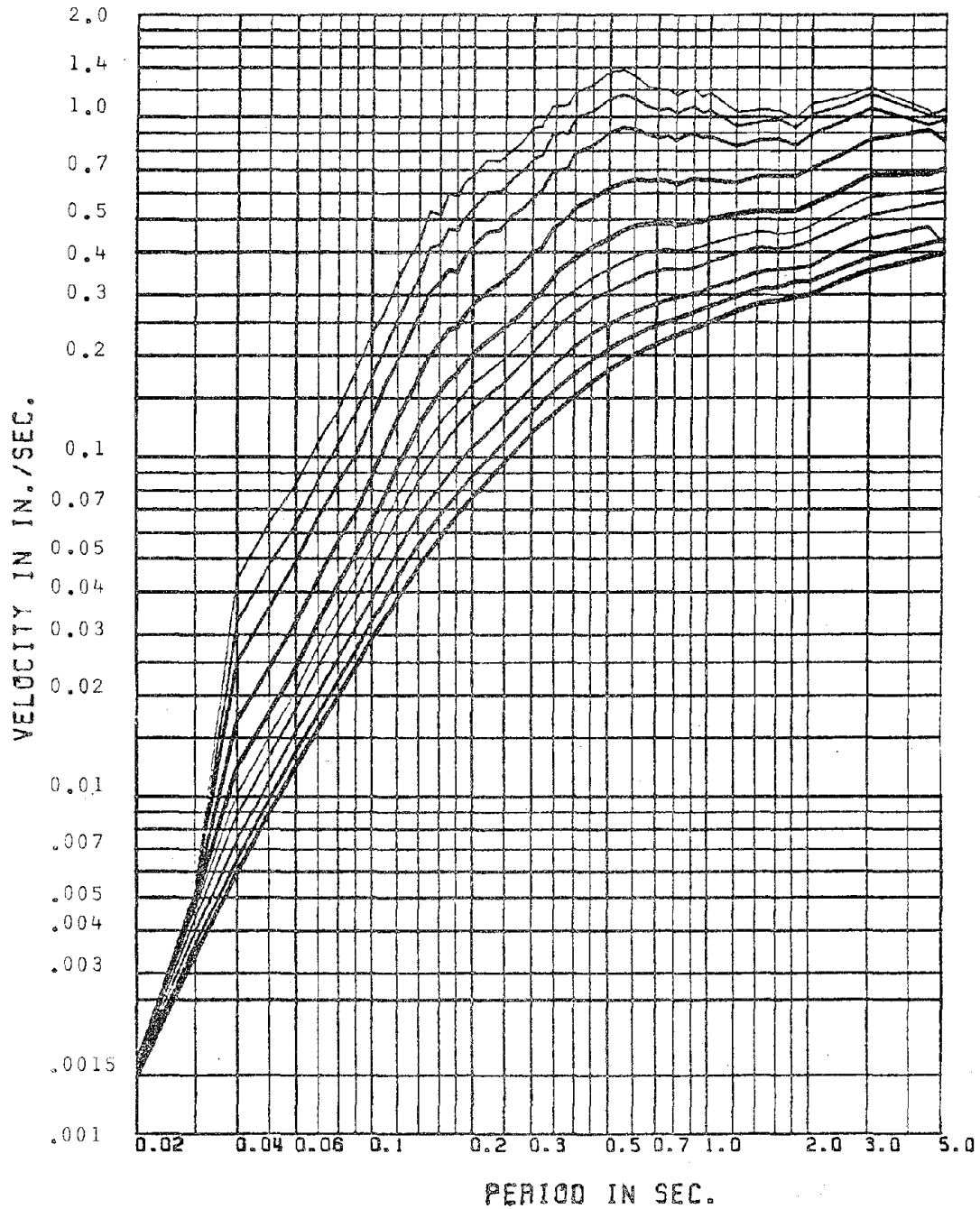


Figure 2.6: MEAN RELATIVE VELOCITY SPECTRA FOR  
 .5, 1, 2, 5, 10, 15, 20, 30, 40 AND 50 PERCENT DAMPING  
 VALUE FOR 30 SEC. TIME HISTORIES

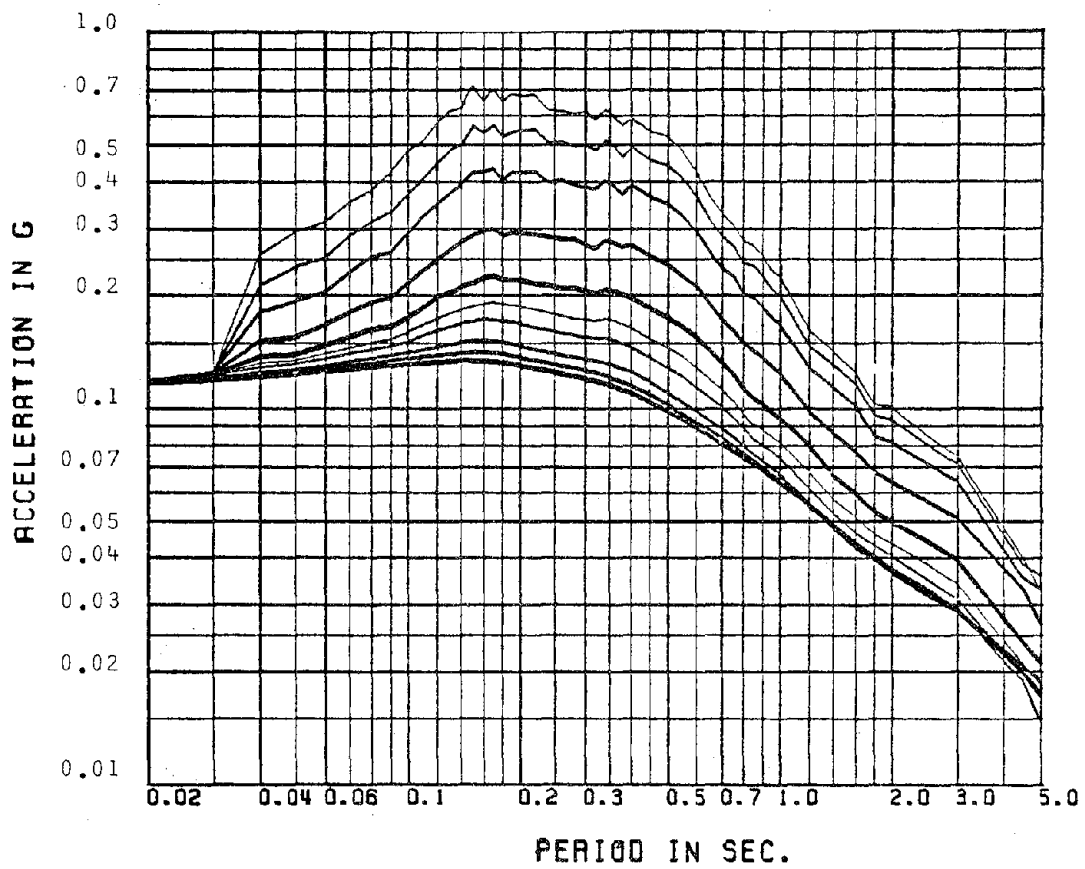


Figure 2.7: MEAN PSUEDO ACCELERATION SPECTRA FOR  
.5, 1, 2, 5, 10, 15, 20, 30, 40 AND 50 PERCENT DAMPING  
VALUE FOR 30 SEC. TIME HISTORIES

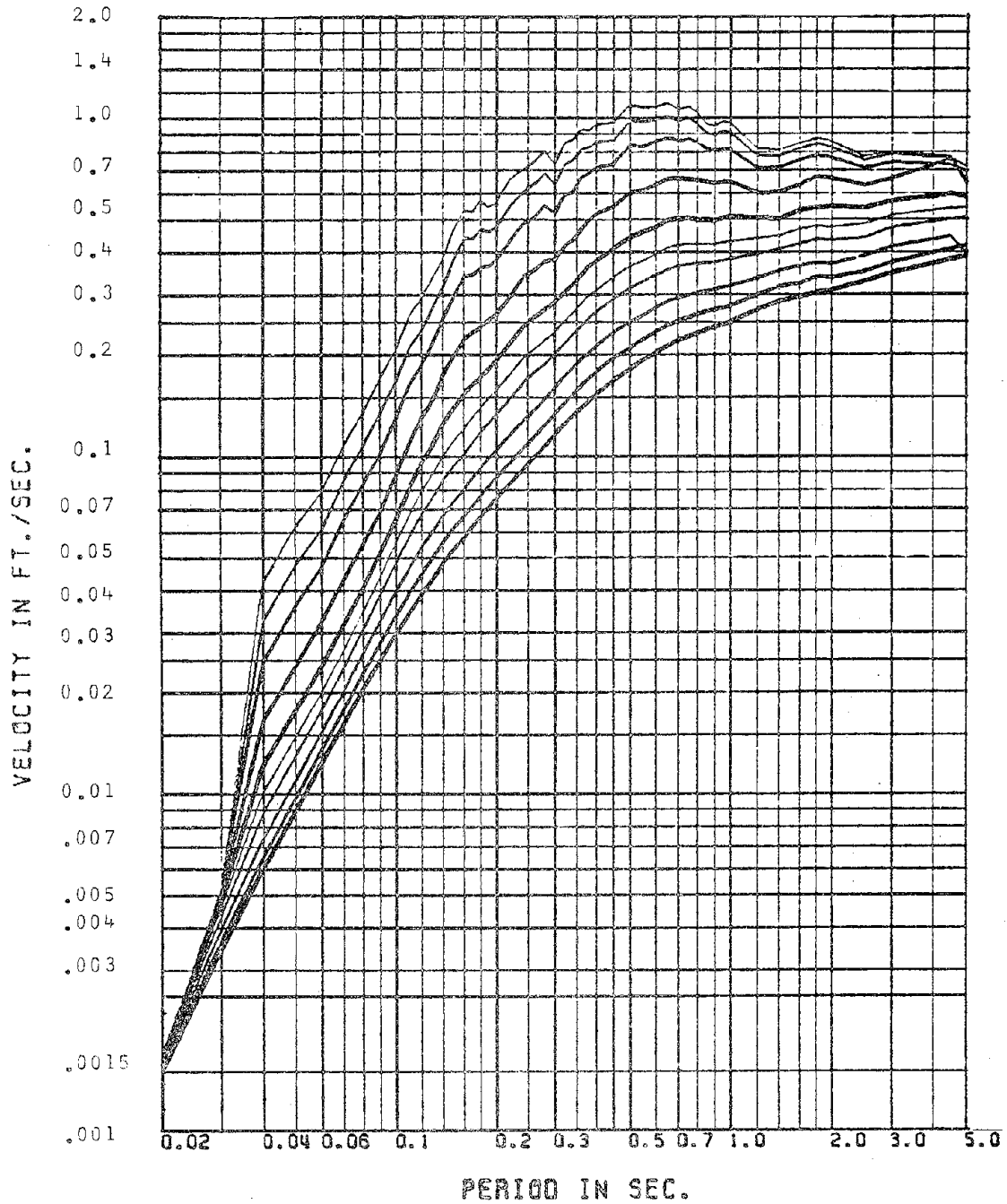


Figure 2.8: MEAN + 1 STD. REL. VELOCITY SPECTRA FOR  
.5, 1, 2, 5, 10, 15, 20, 30, 40 AND 50 PERCENT DAMPING  
VALUE FOR 15 SEC. TIME HISTORIES

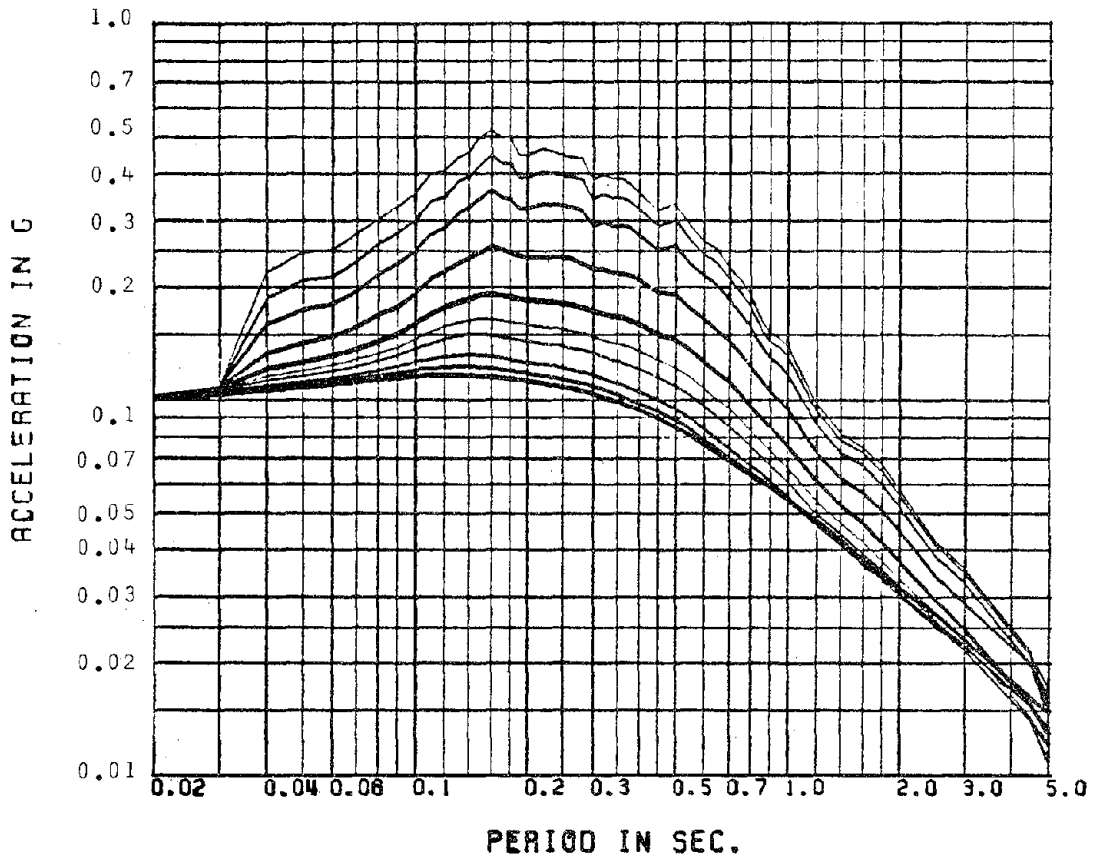


Figure 2.9: MEAN +1 STD. PSUEDO ACCEL. SPECTRA FOR  
.5,1,2,5,10,15,20,30,40 AND 50 PERCENT DAMPING  
VALUE FOR 15 SEC. TIME HISTORIES

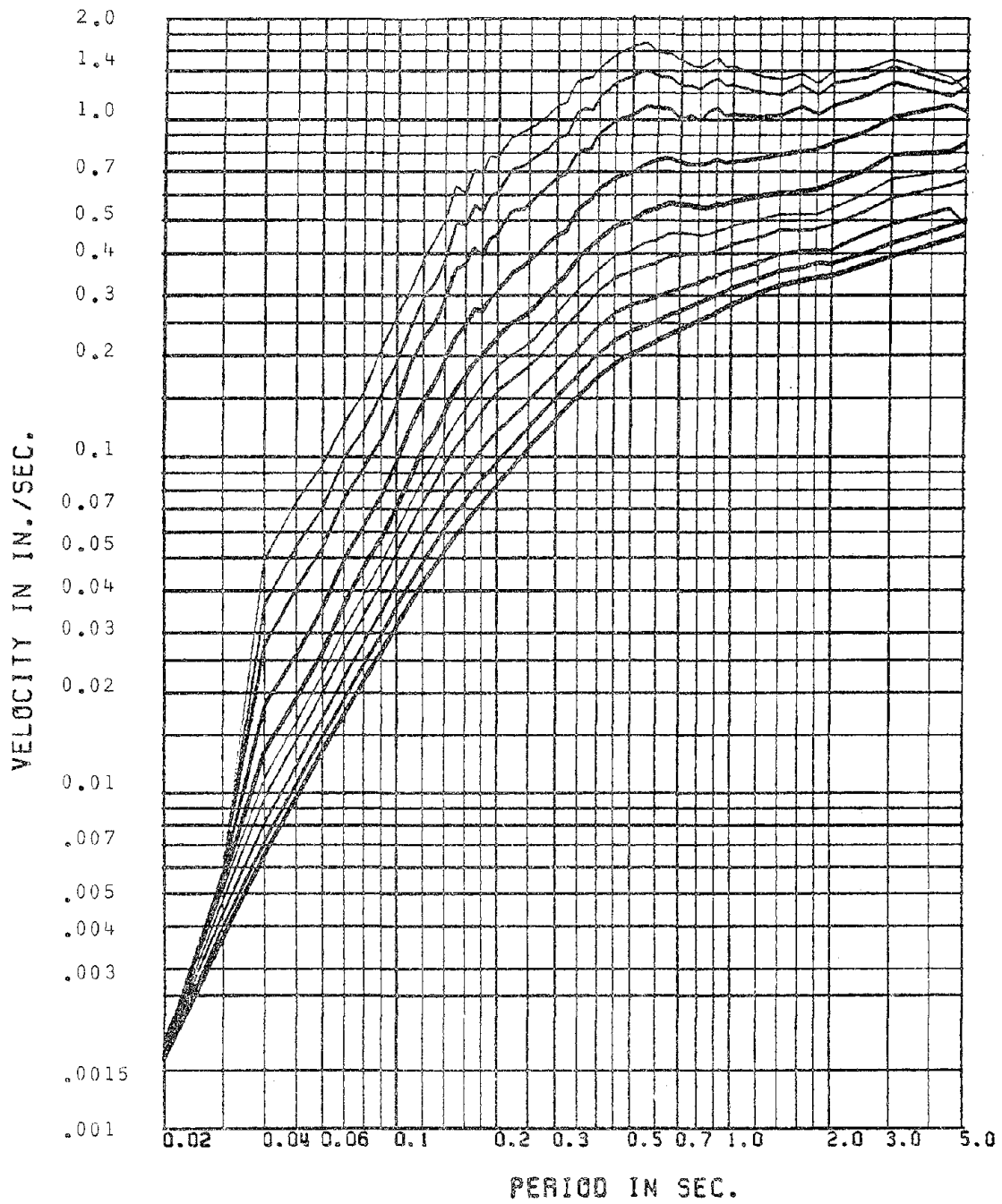


Figure 2.10: MEAN + 1 STD. REL. VELOCITY SPECTRA FOR  
 .5, 1, 2, 5, 10, 15, 20, 30, 40 AND 50 PERCENT DAMPING  
 VALUE FOR 30 SEC. TIME HISTORIES

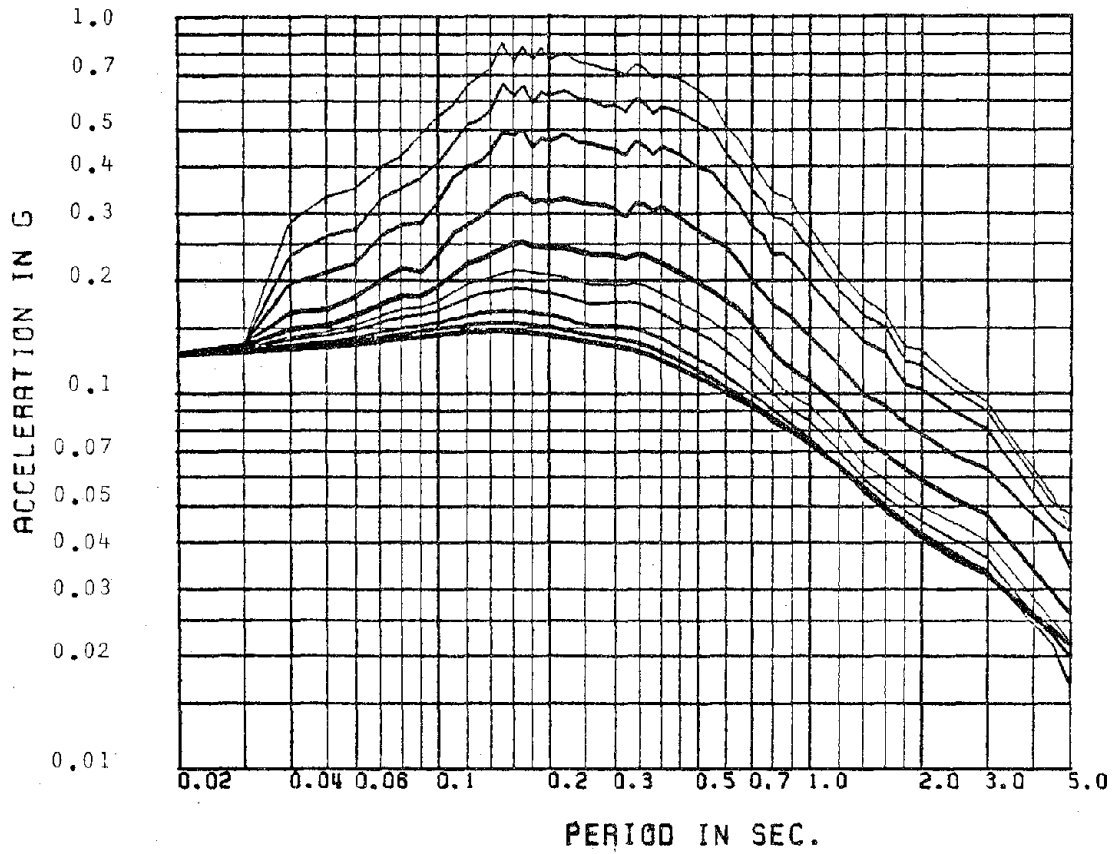


Figure 2.11: MEAN + 1 STD. PSUEDO ACCEL. SPECTRA FOR  
.5, 1, 2, 5, 10, 15, 20, 30, 40 AND 50 PERCENT DAMPING  
VALUE FOR 30 SEC. TIME HISTORIES

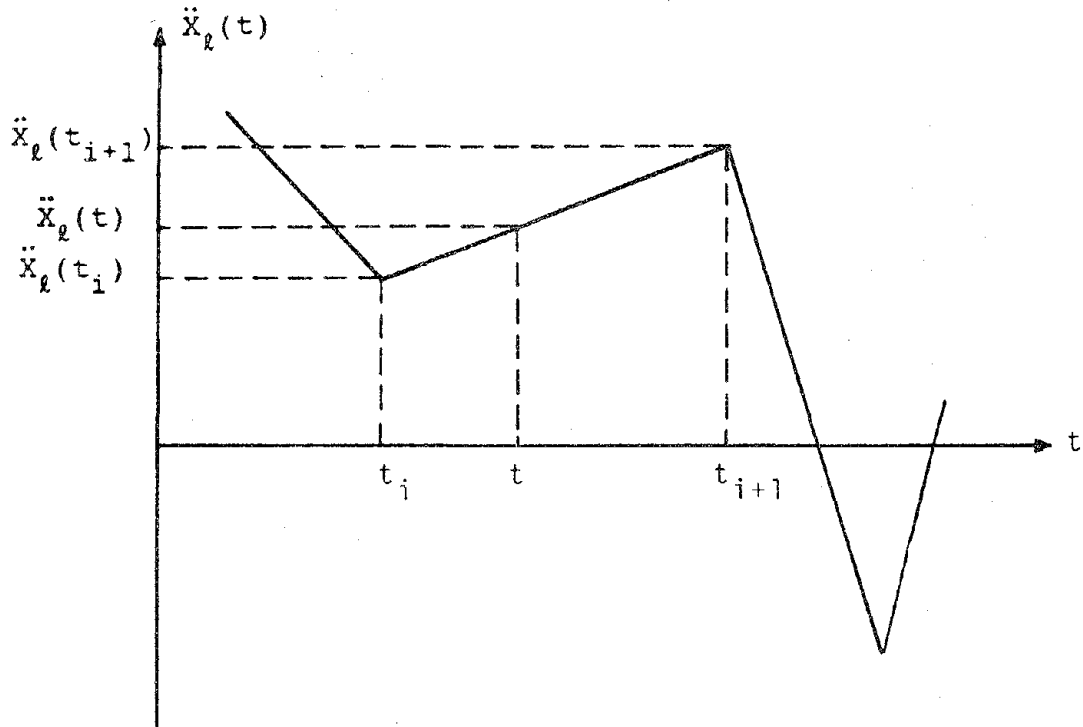


Figure 2.12: DIGITIZED TIME HISTORY

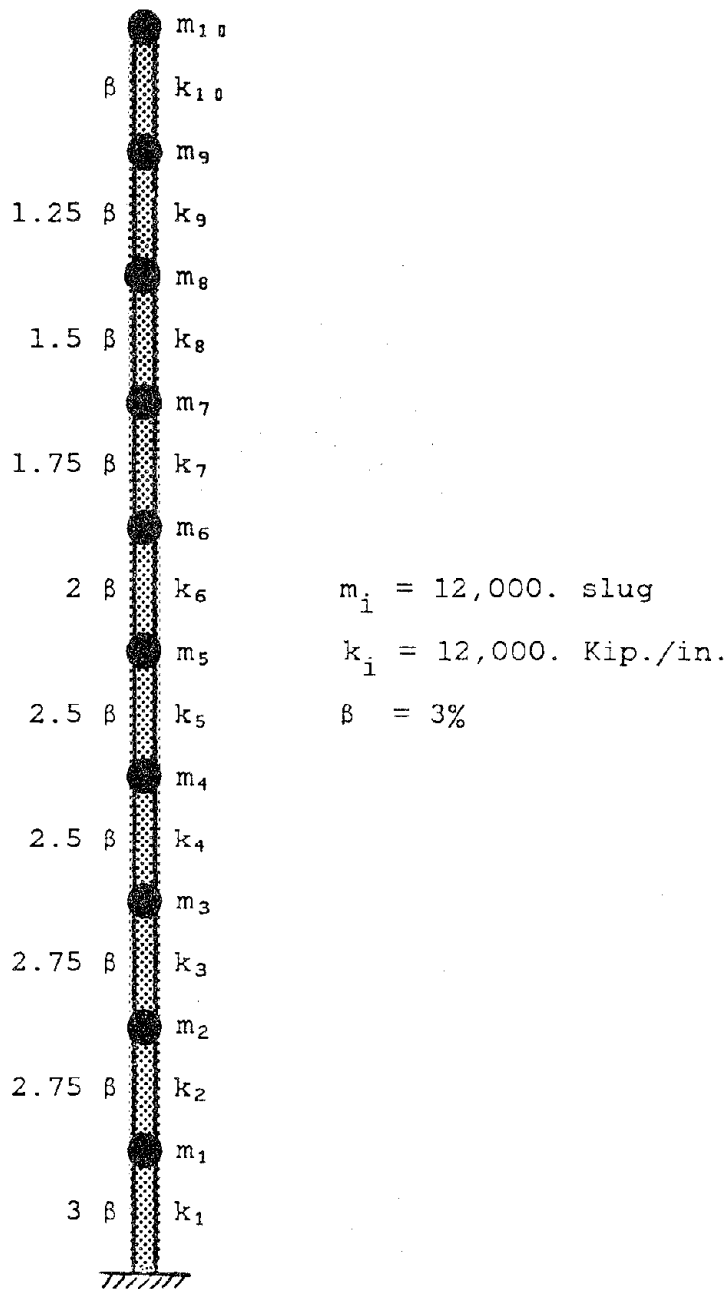


Figure 2.13: SHEAR STRUCTURE MODEL WITH 10 DEGREES-OF-FREEDOM

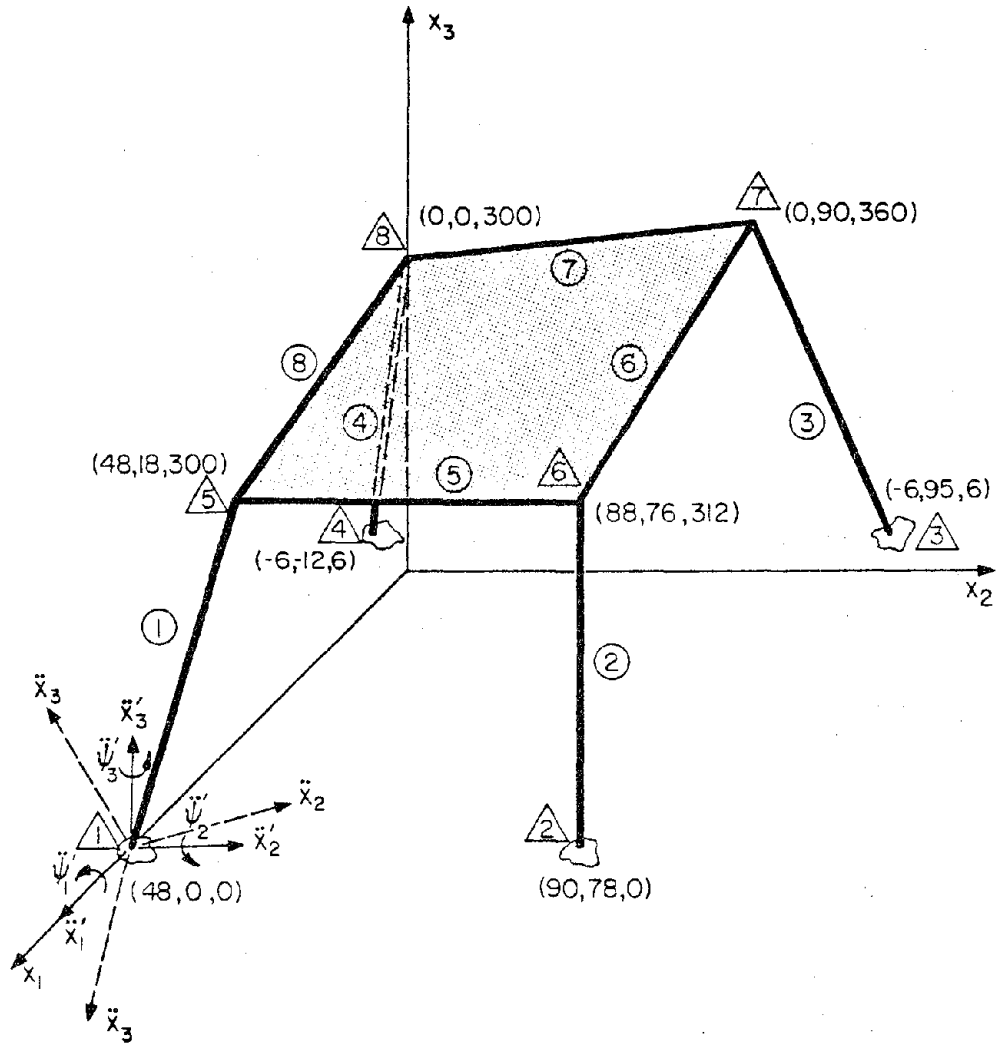


Figure 3.1: A SPACE FRAME STRUCTURE

## Appendix A

### TIME HISTORY ANALYSIS OF NONCLASSICALLY DAMPED SYSTEMS

To cross check the formulation developed in section 2.7, here an alternative formulation is developed. Using the particular solution obtained by Eq. 2.79, the complete solution of  $Z_j$ , can then be written as:

$$Z_j = c_j e^{p_j t} + \sum_{\ell=1}^3 F_{\ell j} \int_0^t \ddot{X}_{\ell}(\tau) e^{p_j(t-\tau)} d\tau \quad (\text{A.1})$$

where  $t$  is again measured from  $t_i$ . For  $\ddot{X}_{\ell}(\tau)$  varying linearly between any two consecutive time steps, the above equation also can be written as:

$$Z_j = c_j e^{p_j t} + \sum_{\ell=1}^3 F_{\ell j} \int_0^t (a_{\ell} + b_{\ell} \tau) e^{p_j(t-\tau)} d\tau \quad (\text{A.2})$$

For a linear behaving structure, response quantity  $S(t)$ , which is linearly related to the displacement vector  $\{u\}$  can be written as:

$$S(t) = \sum_{j=1}^{2N} g_j Z_j \quad (\text{A.3})$$

in which  $g_j =$  the  $j^{\text{th}}$  modal response is defined by Eq. 2.33. Combining complex and conjugate pairs of the above equation:

$$S(t) = \sum_{j=1}^N (g_j Z_j + g_j^* Z_j^*) \quad (\text{A.4})$$

$$S(t) = \sum_{j=1}^N 2 \operatorname{Re}(g_j Z_j) = \sum_{j=1}^N S_j(t) \quad (\text{A.5})$$

where

$$S_j(t) = 2 \operatorname{Re} \left[ g_j c_j e^{p_j t} + \sum_{\ell=1}^3 \int_0^t g_j F_{\ell j} (a_{\ell} + b_{\ell} t) e^{p_j(t-\tau)} d\tau \right] \quad (\text{A.6})$$

Substituting for  $g_j c_j = r_j + i s_j$ ,  $p_j = -\beta_j \omega_j + i \omega_{dj}$  and  $g_j F_{\ell j} = q_{\ell j} = a_{\ell j} + i b_{\ell j}$ . The real part of Eq. A.6 become:

$$\begin{aligned} S_j(t) = & 2 e^{-\beta_j \omega_j t} [r_j \operatorname{Cos}(\omega_{dj} t) - s_j \operatorname{Sin}(\omega_{dj} t)] \\ & + 2 \sum_{\ell=1}^3 \int_0^t (a_{\ell} + b_{\ell} \tau) e^{-\beta_j \omega_j(t-\tau)} \\ & [a_{\ell j} \operatorname{Cos} \omega_{dj}(t-\tau) - b_{\ell j} \operatorname{Sin} \omega_{dj}(t-\tau)] d\tau \end{aligned} \quad (\text{A.7})$$

To obtain unknown real and imaginary parts,  $r_j$  and  $s_j$ , of the constant of integration, the initial condition on the response will be used. To apply the initial conditions we also need the derivative of  $S_j(t)$ .

$$\begin{aligned} \dot{S}_j(t) = & 2 e^{-\beta_j \omega_j t} \{-\beta_j \omega_j [r_j \operatorname{Cos}(\omega_{dj} t) - s_j \operatorname{Sin}(\omega_{dj} t)] \\ & - \omega_{dj} [r_j \operatorname{Sin}(\omega_{dj} t) + s_j \operatorname{Cos}(\omega_{dj} t)]\} \\ & + \sum_{\ell=1}^3 (2 a_{\ell j} (a_{\ell} + b_{\ell} t) + 2 \int_0^t (a_{\ell} + b_{\ell} \tau) e^{-\beta_j \omega_j(t-\tau)} \\ & \{-\beta_j \omega_j [a_{\ell j} \operatorname{Cos} \omega_{dj}(t-\tau) - b_{\ell j} \operatorname{Sin} \omega_{dj}(t-\tau)] \} \end{aligned}$$

$$-\omega_{dj} [a_{\ell j} \sin \omega_{dj}(t-\tau) + b_{\ell j} \cos \omega_{dj}(t-\tau)] \} dr ) \quad (\text{A.8})$$

Applying the initial conditions,  $S_j(t=0)$  and  $\dot{S}_j(t=0)$ , on Eqs. A.7 and A.8 and proceeding similarly as explained in Chapter 2, the unknown value of  $r_j$  and  $s_j$  can be written as:

$$r_j = \frac{1}{2} S_j(t=0) \quad (\text{A.9})$$

$$s_j = \frac{1}{2\omega_{dj}} [-\beta_j \omega_j S_j(t=0) - \dot{S}_j(t=0) + 2 \sum_{\ell=1}^3 a_{\ell j} \ddot{X}_{\ell}(t=0)] \quad (\text{A.10})$$

where  $S_j(t=0)$  and  $\dot{S}_j(t=0)$  are the same as  $S_j$  and  $\dot{S}_j$  at the time step  $t_i$ . Substituting  $r_j$  and  $s_j$  in Eqs. A.7 and A.8, the solution at  $t=h$ , that is at time step  $t_{i+1}$  can be obtained as:

$$S_j(t_{i+1}) = e^{-\beta_j \omega_j h} \{ S_j(t_i) \cos(\omega_{dj} h) - \frac{1}{\omega_{dj}} [-\beta_j \omega_j S_j(t_i) - \dot{S}_j(t_i) + \sum_{\ell=1}^3 2a_{\ell j} \ddot{X}_{\ell}(t_i)] \sin(\omega_{dj} h) \} + \sum_{\ell=1}^3 2(a_{\ell j} P_{\ell c j} - b_{\ell j} P_{\ell s j}) \quad (\text{A.11})$$

and

$$\begin{aligned}
\dot{S}_j(t_{i+1}) = & e^{-\beta_j \omega_j h} \{-\beta_j \omega_j [S_j(t_i) \text{Cos}(\omega_{dj} h) \\
& - \frac{1}{\omega_{dj}} \{-\beta_j \omega_j S_j(t_i) - \dot{S}_j(t_i) \\
& + \sum_{\ell=1}^3 2a_{\ell j} \ddot{X}_\ell(t_i)\} \text{Sin}(\omega_{dj} h)] \\
& - \omega_{dj} S_j(t_i) \text{Sin}(\omega_{dj} h) \\
& - [-\beta_j \omega_j \dot{S}_j(t_i) - \dot{S}_j(t_i) + 2 \sum_{\ell=1}^3 a_{\ell j} \ddot{X}_\ell(t_i)] \text{Cos}(\omega_{dj} h) \} \\
& + \sum_{\ell=1}^3 [2 a_{\ell j} (a_\ell + b_\ell t) \\
& - \beta_j \omega_j (a_{\ell j} P_{\ell c j} - b_{\ell j} P_{\ell s j}) - \omega_{dj} (a_{\ell j} P_{\ell s j} + b_{\ell j} P_{\ell c j})]
\end{aligned} \tag{A.12}$$

Where  $P_{\ell c j}$  and  $P_{\ell s j}$  are defined as:

$$P_{\ell c j} = \int_0^h (a_\ell + b_\ell \tau) e^{-\beta_j \omega_j (h-\tau)} \text{Cos } \omega_{dj} (h-\tau) d\tau \tag{A.13}$$

$$P_{\ell s j} = \int_0^h (a_\ell + b_\ell \tau) e^{-\beta_j \omega_j (h-\tau)} \text{Sin } \omega_{dj} (h-\tau) d\tau \tag{A.14}$$

The closed form solution of the above integrals can be written as:

$$\begin{aligned}
P_{\ell c j} = & (1/h\omega_j^2) \{ \ddot{X}_\ell(t_i) [e^{-\beta_j \omega_j h} (hP_1 - \frac{P_2}{\omega_j^2}) - (1-2\beta_j^2)] \\
& + \ddot{X}_\ell(t_{i+1}) [e^{-\beta_j \omega_j h} (P_2/\omega_j^2) + (\beta_j \omega_j h + (1-2\beta_j^2))] \}
\end{aligned} \tag{A.15}$$

$$\begin{aligned}
P_{\ell sj} = & (1/h\omega_j^2) \{ \ddot{X}_\ell(t_i) [e^{-\beta_j \omega_j h} (hP_3 - \frac{P_4}{\omega_j^2}) + 2\beta_j(1-\beta_j^2)] \\
& + \ddot{X}_\ell(t_{i+1}) [e^{-\beta_j \omega_j h} (\frac{P_4}{\omega_j^2}) + \beta_j(1 - 2\sqrt{(1-\beta_j^2)})] \}
\end{aligned}
\tag{A.16}$$

in which  $P_1$ ,  $P_2$ ,  $P_3$  and  $P_4$  defined as:

$$P_1 = -\beta_j \omega_j \text{Cos}(\omega_{dj} h) + \omega_{dj} \text{Sin}(\omega_{dj} h) \tag{A.17a}$$

$$P_2 = \omega_j^2 (2\beta_j^2 - 1) \text{Cos}(\omega_{dj} h) - 2\beta_j \omega_j \omega_{dj} \text{Sin}(\omega_{dj} h) \tag{A.17b}$$

$$P_3 = -\omega_{dj} \text{Cos}(\omega_{dj} h) - \beta_j \omega_j \text{Sin}(\omega_{dj} h) \tag{A.17c}$$

$$P_4 = 2\beta_j \omega_j \omega_{dj} \text{Cos}(\omega_{dj} h) + \omega_j^2 (2\beta_j^2 - 1) \text{Sin}(\omega_{dj} h) \tag{A.17d}$$

Thus, using Eqs. A.11 and A.12,  $S_j(t_{i+1})$  and  $\dot{S}_j(t_{i+1})$  at the end of each time step can be obtained by knowing the initial value at that time step,  $S_j(t_i)$  and  $\dot{S}_j(t_i)$ . A complete solution of these equations at all discrete time points can be obtained for a digitized acceleration time history if the initial values of  $S_j$  and  $\dot{S}_j$  in the first step are known. By the same procedure, explained in section 2.7, the initial values of  $S_j$  and  $\dot{S}_j$  at  $t=0$  can be obtained as:

$$S_j(t=0) = \sum_{j=1}^{2N} g_j Z_j(t=0) \tag{A.18}$$

$$\dot{S}_j(t=0) = \sum_{j=1}^{2N} g_j \dot{Z}_j(t=0) \quad (\text{A.19})$$

in which  $Z_j(t=0)$  is defined by Eq. 2.90 and  $\dot{Z}_j(t=0)$ , similar to  $Z_j(t=0)$ , can be written as:

$$\dot{Z}_j(t=0) = \{\phi_j\} [A] \{\dot{Y}\}_{t=0} / A_j^* \quad (\text{A.20})$$

Therefore, if the system starting acceleration ( $\{\ddot{u}\}$ ), velocity ( $\{\dot{u}\}$ ) and displacement ( $\{u\}$ ) is known. The initial value of  $Z_j$  and  $\dot{Z}_j$  at  $t=0$  will be known, so as  $S_j$  and  $\dot{S}_j$  at  $t=0$ .

Now Substituting for  $P_{\ell c j}$  and  $P_{\ell s j}$  from Eqs. A.13 and A.14 in Eqs. A.11 and A.12. These two simultaneous equations can be written in the following matrix form:

$$\begin{Bmatrix} S_j \\ S_j \end{Bmatrix}_{t_{i+1}} = \begin{bmatrix} A_{11} & A_{12} \\ A_{21} & A_{22} \end{bmatrix} \begin{Bmatrix} S_j \\ S_j \end{Bmatrix}_{t_i} + \sum_{\ell=1}^3 \begin{bmatrix} B_{11}^{(\ell)} & B_{12}^{(\ell)} \\ B_{21}^{(\ell)} & B_{22}^{(\ell)} \end{bmatrix} \begin{Bmatrix} \ddot{X}_\ell(t_i) \\ \ddot{X}_\ell(t_{i+1}) \end{Bmatrix} \quad (\text{A.21})$$

where the elements of the two matrices are defined as follows:

$$A_{11} = e^{-\beta_j \omega_j h} [\omega_{dj} \cos(\omega_{dj} h) + \beta_j \omega_j \sin(\omega_{dj} h)] / \omega_{dj} \quad (\text{A.22})$$

$$A_{12} = e^{-\beta_j \omega_j h} \sin(\omega_{dj} h) / \omega_{dj} \quad (\text{A.23})$$

$$A_{21} = -e^{-\beta_j \omega_j h} \frac{\omega_j^2}{\omega_{dj}} \sin(\omega_{dj} h) \quad (\text{A.24})$$

$$A_{22} = e^{-\beta_j \omega_j h} [\omega_{dj} \cos(\omega_{dj} h) - \beta_j \omega_j \sin(\omega_{dj} h)] / \omega_{dj} \quad (\text{A.25})$$

$$\begin{aligned} B_{11}^{(\ell)} = & \frac{2}{\omega_j^2} \left\{ e^{-\beta_j \omega_j h} \left[ a_{\ell j} \left( P_1 - \frac{1}{h \omega_j^2} P_2 \right) \right. \right. \\ & \left. \left. - b_{\ell j} \left( P_3 - \frac{1}{h \omega_j^2} P_4 \right) \right] - \frac{a_{\ell j}}{\omega_{dj}} \omega_j^2 \sin(\omega_{dj} h) \right. \\ & \left. - \frac{1}{\omega_j^2 h} \left[ a_{\ell j} \omega^2 (1 - 2\beta_j^2) + 2b_{\ell j} \beta_j \omega_j \omega_{dj} \right] \right\} \end{aligned} \quad (\text{A.26})$$

$$\begin{aligned} B_{12}^{(\ell)} = & \frac{2}{\omega_j^2} e^{-\beta_j \omega_j h} \frac{1}{h \omega_j^2} (a_{\ell j} P_2 - b_{\ell j} P_4) \\ & + a_{\ell j} \left[ \beta_j \omega_j + \frac{1}{h} (1 - 2\beta_j^2) \right] - b_{\ell j} \left[ \omega_{dj} - \frac{2}{\omega_j h} \beta_j \omega_{dj} \right] \end{aligned} \quad (\text{A.27})$$

$$\begin{aligned}
E_{21}^{(\ell)} = & \frac{2}{\omega_j^2} e^{-\beta_j \omega_j h} [-(a_{\ell j} \beta_j \omega_j + b_{\ell j} \omega_{dj}) (P_1 - \frac{1}{h \omega_j^2} P_2) \\
& + (b_{\ell j} \beta_j \omega_j - a_{\ell j} \omega_{dj}) (P_3 - \frac{1}{h \omega_j^2} P_4) \\
& - \frac{a_{\ell j}}{\omega_{dj}} \omega_j^2 \{ \omega_{dj} \cos(\omega_{dj} h) - \beta_j \omega_j \sin(\omega_{dj} h) \} ] \\
& + \frac{1}{h \omega_j^2} [ (a_{\ell j} \beta_j \omega_j + b_{\ell j} \omega_{dj}) \omega_j^2 (1 - 2\beta_j^2) \\
& - 2 (b_{\ell j} \beta_j \omega_j - a_{\ell j} \omega_{dj}) \beta_j \omega_j \omega_{dj} ]
\end{aligned}$$

(A.28)

$$\begin{aligned}
E_{22}^{(\ell)} = & \frac{2}{\omega_j^2} \{ -e^{-\beta_j \omega_j h} \frac{1}{h \omega_j^2} [ (a_{\ell j} \beta_j \omega_j + b_{\ell j} \omega_{dj}) P_2 \\
& + (b_{\ell j} \beta_j \omega_j - a_{\ell j} \omega_{dj}) P_4 ] + a_{\ell j} \omega_j^2 \\
& - (a_{\ell j} \beta_j \omega_j + b_{\ell j} \omega_{dj}) [ \beta_j \omega_j + \frac{1}{h} (1 - 2\beta_j^2) ] \\
& + (b_{\ell j} \beta_j \omega_j - a_{\ell j} \omega_{dj}) [ \omega_{dj} - \frac{2}{\omega_j h} \beta_j \omega_{dj} ] \}
\end{aligned}$$

(A.29)

## Appendix B

## CORRELATION TERMS IN EQUATION 4.3

In this Appendix, various auto- and cross- correlation terms required in Eq. 4.3 are obtained

B.1

$$\text{Term: } \underline{\{\gamma_j\}^T \text{Ex}[\{E'(t_1)\}\dot{V}_k(t_2)]}$$

This term can be written as:

$$T1 = \{\gamma_j\}^T \text{Ex}[\{E'(t_1)\}\dot{V}_k(t_2)] = \frac{\partial}{\partial t_2} \{\gamma_j\}^T \text{Ex}[\{E'(t_1)\}V_k(t_2)] \quad (\text{B.1})$$

Substituting for  $V_k(t_2)$ , as solution of Eq. 2.2 as:

$$V_k(t_2) = - \{\gamma_k\}^T \int_0^{t_2} \{E'(\tau)\} h_k(t_2-\tau) d\tau \quad (\text{B.2})$$

we obtain:

$$\begin{aligned} T1 &= \frac{-\partial}{\partial t_2} \{\gamma_j\}^T \int_0^{t_2} \text{Ex}[\{E'(t_1)\}\{\gamma_k\}^T \{E'(\tau)\}] h_k(t_2-\tau) d\tau \\ &= \frac{-\partial}{\partial t_2} \{\gamma_j\}^T \int_0^{t_2} \text{Ex}[\{E'(t_1)\}\{E'(\tau)\}^T] \{\gamma_k\} h_k(t_2-\tau) d\tau \end{aligned} \quad (\text{B.3})$$

Substituting for  $\text{Ex}[\{E'(t_1)\}\{E'(\tau)\}^T]$  from Eq. 3.23, and considering the stationary response at  $t_2 \rightarrow \infty$ , the above equation can be written as:

$$\begin{aligned}
& \{\chi_j\}^T \text{Ex}[\{E'(t_1)\}\dot{V}_k(t_2)] = \\
& \sum_{\ell=1}^{NE} \left\{ \frac{-a}{\partial t_2} \int_{-\infty}^{+\infty} [ \{\chi_j\}^T [G_1]^T \{d_\ell\} \{d_\ell\}^T [G_1] \{\chi_k\} \right. \\
& \quad + \frac{\omega^2}{4c^2} \{\chi_j\}^T [G_2]^T \{d_\ell\} \{d_\ell\}^T [G_2] \{\chi_k\} \\
& \quad + \frac{i\omega}{2c} ( \{\chi_j\}^T [G_1]^T \{d_\ell\} \{d_\ell\}^T [G_2] \{\chi_k\} \\
& \quad \quad \left. - \{\chi_j\}^T [G_2]^T \{d_\ell\} \{d_\ell\}^T [G_1] \{\chi_k\} ) \right] \\
& \quad \quad \quad \phi_\ell(\omega) H_k^*(\omega) e^{i\omega(t_1-t_2)} d\omega \} \quad (B.4)
\end{aligned}$$

Since the products term like  $\{\chi_j\}^T [G_1]^T \{d_\ell\}$  are scalars, they can also be written as  $\{d_\ell\}^T [G_1] \{\chi_j\}$  in Eq. B.4. Also carrying out differentiation with respect to  $t_2$  and substituting for the vector and matrix products as in Eqs. 3.30, the above equation reduces to:

$$\begin{aligned}
& \{\chi_j\}^T \text{Ex}[\{E'(t_1)\}\dot{V}_k(t_2)] = \\
& \sum_{\ell=1}^{NE} \{d_\ell\}^T [ [\Gamma_{1jk}] \int_{-\infty}^{+\infty} i\omega \phi_\ell(\omega) H_k^*(\omega) e^{i\omega(t_1-t_2)} d\omega \\
& \quad + [\Gamma_{2jk}] \int_{-\infty}^{+\infty} i\omega^3 \phi_\ell(\omega) H_k^*(\omega) e^{i\omega(t_1-t_2)} d\omega \\
& \quad + [\Gamma_{3jk}] \int_{-\infty}^{+\infty} \omega^2 \phi_\ell(\omega) H_k^*(\omega) e^{i\omega(t_1-t_2)} d\omega ] \{d_\ell\} \\
& \hspace{20em} (B.5)
\end{aligned}$$

Similarly, the stationary values of other related cross-correlation terms are obtained as:

$$\begin{aligned}
 \{\gamma_j\}^T \text{Ex}[\{E'(t_1)\}\dot{V}_k(t_2)] = & \\
 \sum_{\ell=1}^{NE} \{d_\ell\}^T [[\Gamma_{1jk}]] \int_{-\infty}^{+\infty} \omega^2 \phi_\ell(\omega) H_k^*(\omega) e^{i\omega(t_1-t_2)} d\omega & \\
 + [\Gamma_{2jk}] \int_{-\infty}^{+\infty} \omega^4 \phi_\ell(\omega) H_k^*(\omega) e^{i\omega(t_1-t_2)} d\omega & \\
 + [\Gamma_{3jk}] \int_{-\infty}^{+\infty} (-i\omega^3) \phi_\ell(\omega) H_k^*(\omega) e^{i\omega(t_1-t_2)} d\omega \{d_\ell\} &
 \end{aligned} \tag{B.6}$$

$$\begin{aligned}
 \{\gamma_k\}^T \text{Ex}[\{E'(t_2)\}\dot{V}_j(t_1)] = & \\
 - \sum_{\ell=1}^{NE} \{d_\ell\}^T [[\Gamma_{1jk}]] \int_{-\infty}^{+\infty} i\omega \phi_\ell(\omega) H_j(\omega) e^{i\omega(t_1-t_2)} d\omega & \\
 + [\Gamma_{2jk}] \int_{-\infty}^{+\infty} i\omega^3 \phi_\ell(\omega) H_j(\omega) e^{i\omega(t_1-t_2)} d\omega & \\
 + [\Gamma_{3jk}] \int_{-\infty}^{+\infty} \omega^2 \phi_\ell(\omega) H_j(\omega) e^{i\omega(t_1-t_2)} d\omega \{d_\ell\} &
 \end{aligned} \tag{B.7}$$

$$\begin{aligned}
 \{\gamma_k\}^T \text{Ex}[\{E'(t_2)\}\dot{V}_j(t_1)] = & \\
 \sum_{\ell=1}^{NE} \{d_\ell\}^T [[\Gamma_{1jk}]] \int_{-\infty}^{+\infty} \omega^2 \phi_\ell(\omega) H_j(\omega) e^{i\omega(t_1-t_2)} d\omega &
 \end{aligned}$$

$$\begin{aligned}
& + [\Gamma_{2jk}] \int_{-\infty}^{+\infty} \omega^4 \phi_{\ell}(\omega) H_j(\omega) e^{i\omega(t_1-t_2)} d\omega \\
& + [\Gamma_{3jk}] \int_{-\infty}^{+\infty} (-i\omega^3) \phi_{\ell}(\omega) H_j(\omega) e^{i\omega(t_1-t_2)} d\omega \{d_{\ell}\}
\end{aligned} \tag{B.8}$$

B.2

$$\underline{\text{Term: } \text{Ex}[V_j(t_1) V_k(t_2)]}$$

Substituting for  $V_j(t_1)$  and  $V_k(t_2)$ , we obtain:

$$\begin{aligned}
\text{Ex}[V_j(t_1) V_k(t_2)] = & \int_0^{t_1} \int_0^{t_2} \{\gamma_j\}^T [ \text{Ex}[\{E'(t_1)\} \{E'(t_2)\}^T] \\
& h_j(t_1-\tau_1) h_k(t_2-\tau_2) d\tau_1 d\tau_2 ] \{\gamma_k\}
\end{aligned} \tag{B.9}$$

Substituting for the correlation matrix of the ground acceleration terms from Eq. 3.23, and letting  $t_1 \rightarrow \infty$  and  $t_2 \rightarrow \infty$ , we get

$$\begin{aligned}
\text{Ex}[V_j(t_1) V_k(t_2)] = & \sum_{\ell=1}^{NE} \{d_{\ell}\}^T [ [\Gamma_{1jk}] \int_{-\infty}^{+\infty} \phi_{\ell}(\omega) H_j(\omega) H_k^*(\omega) e^{i\omega(t_1-t_2)} d\omega \\
& + [\Gamma_{2jk}] \int_{-\infty}^{+\infty} \phi_{\ell}(\omega) \omega^2 H_j(\omega) H_k^*(\omega) e^{i\omega(t_1-t_2)} d\omega \\
& + [\Gamma_{3jk}] \int_{-\infty}^{+\infty} \phi_{\ell}(\omega) (-i\omega) H_j(\omega) H_k^*(\omega) e^{i\omega(t_1-t_2)} d\omega ] \{d_{\ell}\}
\end{aligned} \tag{B.10}$$

Using Eq. B.10, other related autocorrelation functions involving the derivatives of  $V_j$  and  $V_k$  can be obtained as follows:

$$\frac{\partial^{n+m}}{(\partial t_1)^n (\partial t_2)^m} \text{Ex}[V_j(t_1) V_k(t_2)] =$$

$$\text{Ex}\left[\frac{\partial^n}{(\partial t_1)^n} V_j(t_1) \frac{\partial^m}{(\partial t_2)^m} V_k(t_2)\right] \quad n \text{ and } m=1,2$$
(B.11)

$$\sum_{\ell=1}^{NE} \{d_\ell\}^T \left[ [\Gamma_{1jk}] \int_{-\infty}^{+\infty} \omega^{n+m} \bar{\phi}_\ell(\omega) H_j(\omega) H_k^*(\omega) e^{i\omega(t_1-t_2)} d\omega + \right.$$

$$[\Gamma_{2jk}] \int_{-\infty}^{+\infty} \omega^{n+m+2} \bar{\phi}_\ell(\omega) H_j(\omega) H_k^*(\omega) e^{i\omega(t_1-t_2)} d\omega +$$

$$\left. [\Gamma_{3jk}] \int_{-\infty}^{+\infty} (-i\omega^{n+m+1}) \bar{\phi}_\ell(\omega) H_j(\omega) H_k^*(\omega) e^{i\omega(t_1-t_2)} d\omega \right] \{d_\ell\}$$
(B.12)

Thus  $\text{Ex}[\dot{V}_j(t_1) \ddot{V}_k(t_2)]$  can be obtained from Eq. B.12 in which  $n=1$  and  $m=2$ . And

$$\text{Ex}[\dot{V}_j(t_1) \ddot{V}_k(t_2)] = - \text{Ex}[\ddot{V}_j(t_1) \dot{V}_k(t_2)]$$
(B.13)

Also  $\text{Ex}[\dot{V}_j(t_1) \dot{V}_k(t_2)]$  can be obtained from Eq. B.12 in which  $n=m=1$ .

## Appendix C

## COEFFICIENTS OF PARTIAL FRACTIONS

C.1 CLASSICAL DAMPED SYSTEMSC.1.1  $A_1, A_2, A_3$  AND  $A_4$ 

Partial fraction coefficients  $A_1, A_2, A_3$  and  $A_4$  used in Eqs. 2.19, 3.31 and 4.6 are obtained from solution of the following simultaneous equations:

$$[Q]\{A\} = \{W\} \quad (C.1)$$

where

$$[Q] = \begin{bmatrix} 0 & 1 & 0 & 1 \\ 1 & u & 1 & s \\ u & v & s & t \\ v & 0 & t & 0 \end{bmatrix} \quad \{A\} = \begin{Bmatrix} A_1 \\ A_2 \\ A_3 \\ A_4 \end{Bmatrix} \quad \{W\} = \begin{Bmatrix} W_1 \\ W_2 \\ W_3 \\ W_4 \end{Bmatrix} \quad (C.2)$$

in which

$$\begin{aligned} u &= -2\omega_k^2 (1 - 2\beta_k^2) & v &= \omega_k^4 \\ s &= -2\omega_j^2 (1 - 2\beta_j^2) & t &= \omega_j^4 \end{aligned} \quad (C.3)$$

$$W_1 = 0. \quad W_2 = 1. \quad W_4 = \omega_j^2 \omega_k^2$$

$$W_3 = -(\omega_j^2 + \omega_k^2 - 4\beta_j \beta_k \omega_j \omega_k) \quad (C.4)$$

C.1.2 B<sub>1</sub>, B<sub>2</sub>, B<sub>3</sub> AND B<sub>4</sub>

Coefficients of partial fractions B<sub>1</sub>, B<sub>2</sub>, B<sub>3</sub> and B<sub>4</sub>, used in Eqs. 3.31 and 4.6, are obtained from solution of the following set of simultaneous equations:

$$[Q]\{B\} = \{W'\} \quad (C.5)$$

in which [Q] remains the same, and

$$\{B\} = \begin{Bmatrix} B_1 \\ B_2 \\ B_3 \\ B_4 \end{Bmatrix} \quad \{W'\} = \begin{Bmatrix} 1. \\ \omega_j^2 \omega_k^2 \\ -(\omega_j^2 + \omega_k^2 - 4\beta_j \beta_k \omega_j \omega_k) \\ 0. \end{Bmatrix} \quad (C.6)$$

C.1.3 C<sub>1</sub>, C<sub>2</sub>, C<sub>3</sub> AND C<sub>4</sub>

Coefficients of partial fractions C<sub>1</sub>, C<sub>2</sub>, C<sub>3</sub> and C<sub>4</sub>, used in Eqs. 3.31 and 4.6, are obtained from the solution of the following set of simultaneous equations:

$$[Q]\{C\} = \{W''\} \quad (C.7)$$

in which [Q] remains the same, and

$$\{C\} = \begin{Bmatrix} C_1 \\ C_2 \\ C_3 \\ C_4 \end{Bmatrix} \quad \{W''\} = \begin{Bmatrix} 0. \\ (\beta_j \omega_j - \beta_k \omega_k) \\ (\beta_k \omega_j - \beta_j \omega_k) \omega_j \omega_k \\ 0. \end{Bmatrix} \quad (C.8)$$

C.1.4  $F_1, \dots, F_5, F'_1, \dots, F'_5, F''_1, \dots$  AND  $F''_5$

The partial fraction coefficients  $F_1, F_2, F_3, F_4, F_5$ ;  $F'_1, F'_2, F'_3, F'_4, F'_5$ ; and  $F''_1, F''_2, F''_3, F''_4$  and  $F''_5$ , used in Eq. 4.11, are defined as follows:

$$F_1 = 4\beta_j \beta_k \omega_j \omega_k A_1 - \omega_j^4 A_2 + 4(\beta_j \omega_j - \beta_k \omega_k) C_1 + \omega_j^2 (1 - 4\beta_j^2) \quad (C.9a)$$

$$F_2 = A_1 + 2[2\beta_j \beta_k \omega_j \omega_k + \omega_j^2 (1 - 2\beta_j^2)] A_2 + 4(\beta_j \omega_j - \beta_k \omega_k) C_2 - 1. \quad (C.9b)$$

$$F_3 = 4\beta_j \beta_k \omega_j \omega_k A_3 - \omega_k^4 A_4 + 4(\beta_j \omega_j - \beta_k \omega_k) C_3 + \omega_k^2 (1 - 4\beta_k^2) \quad (C.9c)$$

$$F_4 = A_3 + 2[2\beta_j \beta_k \omega_j \omega_k + \omega_k^2 (1 - 2\beta_k^2)] A_4 + 4(\beta_j \omega_j - \beta_k \omega_k) C_4 - 1. \quad (C.9d)$$

$$F_5 = A_2 + A_4 \quad (C.9e)$$

$$F'_1 = 4\beta_j \beta_k \omega_j \omega_k B_1 - \omega_j^4 [B_2 + 4(\beta_j \omega_j - \beta_k \omega_k) C_2 - 1] \quad (C.10a)$$

$$F'_2 = B_1 + 2[2\beta_j \beta_k \omega_j \omega_k + \omega_j^2 (1 - 2\beta_j^2)] B_2 + 4(\beta_j \omega_j - \beta_k \omega_k) [C_1 + \omega_j^2 (1 - 2\beta_j^2) C_2] - \omega_j^2 \quad (C.10b)$$

$$F'_3 = 4\beta_j \beta_k \omega_j \omega_k B_3 - \omega_k^4 [B_4 + 4(\beta_j \omega_j - \beta_k \omega_k) C_4 - 1] \quad (C.10c)$$

$$F_4' = B_3 + 2[2\beta_j\beta_k\omega_j\omega_k + \omega_k^2(1-2\beta_k^2)]B_4 + 4(\beta_j\omega_j - \beta_k\omega_k)[C_3 + \omega_j^2(1-2\beta_j^2)C_4] - \omega_k^2 \quad (C.10d)$$

$$F_5' = B_2 + B_4 + 4\beta_j\beta_k\omega_j\omega_k (C_2 + C_4) - 2 \quad (C.10e)$$

$$F_1'' = \omega_j^4(\beta_j\omega_j - \beta_k\omega_k)A_2 + 4\beta_j\beta_k\omega_j\omega_k C_1 - \omega_j^4 C_2 - \beta_j\omega_j^3 \quad (C.11a)$$

$$F_2'' = -(\beta_j\omega_j - \beta_k\omega_k) A_1 - 2\omega_j^2(1-2\beta_j^2)(\beta_j\omega_j - \beta_k\omega_k) A_2 + C_1 + 2[2\beta_j\beta_k\omega_j\omega_k + \omega_j^2(1-2\beta_j^2)]C_2 \quad (C.11b)$$

$$F_3'' = \omega_k^4(\beta_j\omega_j - \beta_k\omega_k)A_4 + 4\beta_j\beta_k\omega_j\omega_k C_3 - \omega_k^4 C_4 - \beta_k\omega_k^3 \quad (C.11c)$$

$$F_4'' = -(\beta_j\omega_j - \beta_k\omega_k) A_3 - 2\omega_k^2(1-2\beta_k^2)(\beta_j\omega_j - \beta_k\omega_k) A_4 + C_3 + 2[2\beta_j\beta_k\omega_j\omega_k + \omega_k^2(1-2\beta_k^2)]C_4 \quad (C.11d)$$

$$F_5'' = -(\beta_j\omega_j - \beta_k\omega_k) A_2 + A_4 + C_2 + C_4 \quad (C.11e)$$

where  $A_1, \dots, A_4$ ;  $B_1, \dots, B_4$ ; and  $C_1, \dots, C_4$  are defined by Eqs. C.1, C.5 and C.7.

## C.2 NONCLASSICAL DAMPING SYSTEM

### C.2.1 $A'_{1\ell}$ , $A'_{2\ell}$ , $A'_{3\ell}$ AND $A'_{4\ell}$

The partial fraction coefficients  $A'_{1\ell}$ ,  $A'_{2\ell}$ ,  $A'_{3\ell}$  and  $A'_{4\ell}$ , used in Eq. 2.48, are obtained from solution of the following simultaneous equations:

$$[Q]\{A'_\ell\} = \{W_\ell\} \quad (C.12)$$

where  $[Q]$  remains the same; and elements of  $\{W_\ell\}$  are defined by Eq. 2.46 and  $\{A'_\ell\} = \{A'_{1\ell} \quad A'_{2\ell} \quad A'_{3\ell} \quad A'_{4\ell}\}$

### C.2.2 $A'_{1pq}$ , $A'_{2pq}$ , $A'_{3pq}$ AND $A'_{4pq}$

The partial fraction coefficients  $A'_{1pq}$ ,  $A'_{2pq}$ ,  $A'_{3pq}$  and  $A'_{4pq}$ , used in Eq. 3.44, are obtained from the solution of following simultaneous equations:

$$[Q]\{A'_{pq}\} = \{W_{pq}\} \quad (C.13)$$

where  $[Q]$  remains the same and  $\{A'_{pq}\}$  and  $\{W_{pq}\}$  are defined as:

$$\{A'_{pq}\} = \begin{Bmatrix} A'_{1pq} \\ A'_{2pq} \\ A'_{3pq} \\ A'_{4pq} \end{Bmatrix} \quad \{W'_{pq}\} = \begin{Bmatrix} C_0 \\ C_1 \\ C_2 \\ C_3 \end{Bmatrix} \quad (C.14)$$

in which

$$C_0 = a_{pj} a_{qk} \quad (C.15a)$$

$$C_1 = A_{pj} A_{qk} - a_{pj} a_{qk} (\omega_j^2 + \omega_k^2 - 4\beta_j \beta_k \omega_j \omega_k) - 2(\beta_j \omega_j - \beta_k \omega_k) (a_{pj} A_{qk} - a_{qk} A_{pj}) \quad (C.15b)$$

$$C_2 = a_{pj} a_{qk} \omega_j^2 \omega_k^2 - A_{pj} A_{qk} (\omega_j^2 + \omega_k^2 - 4\beta_j \beta_k \omega_j \omega_k) - 2\omega_j \omega_k (\beta_j \omega_j - \beta_k \omega_k) (a_{pj} A_{qk} - a_{qk} A_{pj}) \quad (C.15c)$$

$$C_3 = A_{pj} A_{qk} \omega_j^2 \omega_k^2 \quad (C.15d)$$

### C.2.3 $B'_{1pq}$ , $B'_{2pq}$ , $B'_{3pq}$ , $B'_{4pq}$ AND $B'_{5pq}$

The partial fraction coefficients  $B'_{1pq}$ ,  $B'_{2pq}$ ,  $B'_{3pq}$ ,  $B'_{4pq}$  and  $B'_{5pq}$ , used in Eq. 3.44, are obtained as follows:

$$B'_{1pq} = -\omega_j^4 A'_{2pq}$$

$$B'_{2pq} = A'_{1pq} + 2\omega_j^2 (1 - 2\beta_j^2) A'_{2pq}$$

$$B'_{3pq} = -\omega_k^4 A'_{4pq}$$

$$\begin{aligned}
 B'_{4pq} &= A'_{3pq} + 2\omega_k^2 (1-2\beta_k^2) A'_{4pq} \\
 B'_{5pq} &= A'_{2pq} + A'_{4pq}
 \end{aligned} \tag{C.16}$$

#### C.2.4 $C'_{1pq}$ , $C'_{2pq}$ , $C'_{3pq}$ AND $C'_{4pq}$

The coefficients of partial fractions  $C'_{1pq}$ ,  $C'_{2pq}$ ,  $C'_{3pq}$  and  $C'_{4pq}$ , used in Eq. 3.44, are obtained from the solution of the following simultaneous equations:

$$[Q]\{C'_{pq}\} = \{W''_{pq}\} \tag{C.17}$$

where

$$\{C'_{pq}\} = \begin{Bmatrix} C'_{1pq} \\ C'_{2pq} \\ C'_{3pq} \\ C'_{4pq} \end{Bmatrix} \quad \{W''_{pq}\} = \begin{Bmatrix} C''_0 \\ C''_1 \\ C''_2 \\ 0. \end{Bmatrix} \tag{C.18}$$

in which

$$C''_0 = (a_{pj}A_{qk} - A_{pj}a_{qk}) + 2(\beta_j\omega_j - \beta_k\omega_k)a_{pj}a_{qk} \tag{C.19a}$$

$$\begin{aligned}
 C''_1 &= - (a_{pj}A_{qk} - A_{pj}a_{qk})(\omega_j^2 + \omega_k^2 - 4\beta_j\beta_k\omega_j\omega_k) \\
 &\quad + 2(\beta_j\omega_j - \beta_k\omega_k)A_{pj}A_{qk} + 2\omega_j\omega_k(\beta_k\omega_j - \beta_j\omega_k)a_{pj}a_{qk}
 \end{aligned} \tag{C.19b}$$

$$C''_2 = (a_{pj}A_{qk} - A_{pj}a_{qk})\omega_j^2\omega_k^2 + 2\omega_j\omega_k(\beta_k\omega_j - \beta_j\omega_k)A_{pj}A_{qk} \tag{C.19c}$$

## Appendix D

## RESPONSE COMBINATIONS

The eighteen possible response combinations expressed by Eq. 3.60 and 3.61 are enumerated here.

D.1 EXCITATION-1

$$S_{11} = \lambda_{11} + \{d_2^{(1)}\}^T [R_2] \{d_2^{(1)}\} + \{d_3^{(1)}\}^T [R_2] \{d_3^{(1)}\} \quad (D.1)$$

$$S'_{11} = \lambda_{11} + \{d_2^{(1)}\}^T [R_3] \{d_2^{(1)}\} + \{d_3^{(1)}\}^T [R_2] \{d_3^{(1)}\} \quad (D.2)$$

$$S_{12} = \lambda_{12} + \{d_1^{(1)}\}^T [R_2] \{d_1^{(1)}\} + \{d_3^{(1)}\}^T [R_3] \{d_3^{(1)}\} \quad (D.3)$$

$$S'_{12} = \lambda_{12} + \{d_1^{(1)}\}^T [R_3] \{d_1^{(1)}\} + \{d_3^{(1)}\}^T [R_2] \{d_3^{(1)}\} \quad (D.4)$$

$$S_{13} = \lambda_{13} + \{d_1^{(1)}\}^T [R_2] \{d_1^{(1)}\} + \{d_2^{(1)}\}^T [R_3] \{d_2^{(1)}\} \quad (D.5)$$

$$S'_{13} = \lambda_{13} + \{d_1^{(1)}\}^T [R_3] \{d_1^{(1)}\} + \{d_2^{(1)}\}^T [R_2] \{d_2^{(1)}\} \quad (D.5)$$

D.2 EXCITATION-2

$$S_{21} = \lambda_{21} + \{d_2^{(2)}\}^T [R_1] \{d_2^{(2)}\} + \{d_3^{(2)}\}^T [R_3] \{d_3^{(2)}\} \quad (D.7)$$

$$S_{21}' = \lambda_{21} + \{d_2^{(2)}\}^T [R_3] \{d_2^{(2)}\} + \{d_3^{(2)}\}^T [R_1] \{d_3^{(2)}\} \quad (D.8)$$

$$S_{22}' = \lambda_{22} + \{d_1^{(2)}\}^T [R_1] \{d_1^{(2)}\} + \{d_3^{(2)}\}^T [R_3] \{d_3^{(2)}\} \quad (D.9)$$

$$S_{22}' = \lambda_{22} + \{d_1^{(2)}\}^T [R_3] \{d_1^{(2)}\} + \{d_3^{(2)}\}^T [R_1] \{d_3^{(2)}\} \quad (D.10)$$

$$S_{23}' = \lambda_{23} + \{d_1^{(2)}\}^T [R_1] \{d_1^{(2)}\} + \{d_2^{(2)}\}^T [R_3] \{d_2^{(2)}\} \quad (D.11)$$

$$S_{23}' = \lambda_{23} + \{d_1^{(2)}\}^T [R_3] \{d_1^{(2)}\} + \{d_2^{(2)}\}^T [R_1] \{d_2^{(2)}\} \quad (D.12)$$

### D.3 EXCITATION-3

$$S_{31}' = \lambda_{31} + \{d_2^{(3)}\}^T [R_1] \{d_2^{(3)}\} + \{d_3^{(3)}\}^T [R_2] \{d_3^{(3)}\} \quad (D.13)$$

$$S_{31}' = \lambda_{31} + \{d_2^{(3)}\}^T [R_2] \{d_2^{(3)}\} + \{d_3^{(3)}\}^T [R_1] \{d_3^{(3)}\} \quad (D.14)$$

$$S_{32}' = \lambda_{32} + \{d_1^{(3)}\}^T [R_1] \{d_1^{(3)}\} + \{d_3^{(3)}\}^T [R_2] \{d_3^{(3)}\} \quad (D.15)$$

$$S_{32}' = \lambda_{32} + \{d_1^{(3)}\}^T [R_2] \{d_1^{(3)}\} + \{d_3^{(3)}\}^T [R_1] \{d_3^{(3)}\} \quad (D.16)$$

$$S_{33}' = \lambda_{33} + \{d_1^{(3)}\}^T [R_1] \{d_1^{(3)}\} + \{d_2^{(3)}\}^T [R_2] \{d_2^{(3)}\} \quad (D.17)$$

$$S'_{33} = \lambda_{33} + \{d_1^{(3)}\}^T [R_2] \{d_1^{(3)}\} + \{d_2^{(3)}\}^T [R_1] \{d_2^{(3)}\}$$

(D.18)

